1987-03

A Modal Analysis of the Violin Using MSC/NASTRAN and PATRAN

Knott, George Anthony

Monterey, California: Naval Postgraduate School

NAVAL POSTGRADUATE SCHOOL
Monterey, California

THESIS

A MODAL ANALYSIS OF THE VIOLIN
USING MSC/NASTRAN AND PATRAN

by

George A. Knott

March 1987

Thesis Advisor: Young S. Shin

Approved for public release; distribution is unlimited

REPORT DOCUMENTATION PAGE

1a. REPORT SECURITY CLASSIFICATION Unclassified	1b. RESTRICTIVE MARKINGS
2a. SECURITY CLASSIFICATION AUTHORITY	3. DISTRIBUTION / AVAILABILITY OF REPORT Approved for public release; distribution is unlimited
2b. DECLASSIFICATION / DOWNGRADING SCHEDULE	
4. PERFORMING ORGANIZATION REPORT NUMBER(S)	5. MONITORING ORGANIZATION REPORT NUMBER(S)
6a. NAME OF PERFORMING ORGANIZATION Naval Postgraduate School 6b. OFFICE SYMBOL (If applicable) 69	7a. NAME OF MONITORING ORGANIZATION Naval Postgraduate School
6c. ADDRESS (City, State, and ZIP Code) Monterey, California 93943-5000	7b. ADDRESS (City, State, and ZIP Code) Monterey, California 93943-5000
8a. NAME OF FUNDING / SPONSORING ORGANIZATION 8b. OFFICE SYMBOL (If applicable)	9. PROCUREMENT INSTRUMENT IDENTIFICATION NUMBER
8c. ADDRESS (City, State, and ZIP Code)	10. SOURCE OF FUNDING NUMBERS PROGRAM ELEMENT NO. / PROJECT NO. / TASK NO. / WORK UNIT ACCESSION NO.

11. TITLE (Include Security Classification)

A MODAL ANALYSIS OF THE VIOLIN USING MSC/NASTRAN AND PATRAN

12. PERSONAL AUTHOR(S)

Knott, George, A.

13a. TYPE OF REPORT	13b. TIME COVERED	14. DATE OF REPORT (Year, Month, Day)	15. PAGE COUNT
Master's Thesis	FROM ____ TO ____	March 1987	126

16. SUPPLEMENTARY NOTATION

17. COSATI CODES			18. SUBJECT TERMS (Continue on reverse if necessary and identify by block number)
FIELD	GROUP	SUB-GROUP	Finite Elements, Violin, Modal Analysis, NASTRAN, PATRAN.

19. ABSTRACT (Continue on reverse if necessary and identify by block number)

The MSC/NASTRAN finite element computer program and a Cray XMP computer were used to study the modal characteristics of a violin with the Stradivari shape. The violin geometry was modeled using an arcs of circles scheme with PATRAN, a finite element graphics pre/postprocessor program. The violin was modeled in-vacu and with free boundry conditions. Belly, back,sound post, bassbar, neck, bridge, tail-piece, strings, rib linings, end and corner blocks are the components of the model. Mode shapes and frequencies were calculated for free top and back plates, the violin box, and the complete violin system, including the strings. The results obtained from the finite element technique were compared to experimental data from real violins collected by other investigators.

20. DISTRIBUTION / AVAILABILITY OF ABSTRACT ☒ UNCLASSIFIED/UNLIMITED ☐ SAME AS RPT. ☐ DTIC USERS	21. ABSTRACT SECURITY CLASSIFICATION Unclassified
22a. NAME OF RESPONSIBLE INDIVIDUAL Young S. Shin	22b. TELEPHONE (Include Area Code) (408) 646-2568 22c. OFFICE SYMBOL 69SG

DD FORM 1473, 84 MAR 83 APR edition may be used until exhausted
All other editions are obsolete.

SECURITY CLASSIFICATION OF THIS PAGE

Approved for public release; distribution is unlimited

A Modal Analysis of the Violin Using MSC/NASTRAN and PATRAN

by

George Anthony Knott
Lieutenant Commander, United States Navy
B.A., University of California at Berkeley, 1977

Submitted in partial fulfillment of the
requirements for the degree of

MASTER OF SCIENCE IN ENGINEERING ACOUSTICS

from the

NAVAL POSTGRADUATE SCHOOL

March 1987

Author: [redacted]
George A. Knott

Approved by: [redacted]
Young S. Shin, Thesis Advisor

[redacted]
Steven L. Garrett, Second Reader

[redacted]
Steven L. Garrett, Chairman,
Engineering Acoustics Academic Committee

[redacted]
G. Schacher, Dean of Science and Engineering

ABSTRACT

The MSC/NASTRAN finite element computer program and a Cray XMP computer were used to study the modal characteristics of a violin with the Stradivari shape. The violin geometry was modeled using an arcs of circles scheme with PATRAN, a finite element graphics pre/postprocessor program. The violin was modeled in-vacu and with free boundary conditions. Belly, back, sound post, bassbar, neck, bridge, tail-piece, strings, rib linings, end and corner blocks are the components of the model. Mode shapes and frequencies were calculated for free top and back plates, the violin box, and the complete violin system, including the strings. The results obtained from the finite element technique were compared to experimental data from real violins collected by other investigators.

TABLE OF CONTENTS

LIST OF TABLES

LIST OF FIGURES

ACKNOWLEDGMENT

This thesis would not have been possible without the assistance and encouragement of two persons; Dr. Young Shin and Mladin Chargin.

Dr. Shin took on an inexperienced and naive student of acoustics (not even from his own department, mechanical engineering) two years ago. He provided the direction and facilities needed to complete the violin project over the long months. Most of all, he was forgiving of the numerous errors and misjudgements made by his student, always welcoming the prodigal son home.

Mladin Chargin was the powerhouse behind this thesis. His knowledge of the MSC/NASTRAN computer program is unparalleled in the field and he was always willing to share his expertise.

I. INTRODUCTION

A. PAST AND CURRENT USE OF THE FINITE ELEMENT METHOD IN THE ANALYSIS OF STRINGED INSTRUMENTS

In recent years there has been a vast increase in the application of the finite element method to diverse fields of the physical sciences. This explosion first reached the field of stringed instrument acoustics in 1974, with Schwab's finite element description of the modal shapes of a guitar top plate [Ref. 1]. Richardson and Roberts [Ref. 2] continued the work on guitar plates in 1983, and Jenner [Ref. 3] is currently using the finite element method in his guitar research.

In 1984, Richarson and Roberts [Ref. 4] and Rubin and Farrar [Ref. 5] applied the finite element method to the study of violin plate vibrations.

The first descriptions of the mode shapes and frequencies of the violin box using finite elements were obtained in late 1984 by Richarson and Roberts [Ref. 6] and Knott [Ref. 7]. This study is simply a continuation of the previous research and has as its goal the modal description of the entire violin system.

B. THE PLATES STUDIED AS ENTITIES

Before attempting to describe the modal characteristics of the finite element violin as a complete system the constituent parts must be studied as entities; then the physical knowledge of each part can aid in the attempt to explain the physical characteristics of the system as a whole. This study implements the above technique. First, the top plate (see Figure 1.0) and back plate (see Figure 1.1) of the violin were modeled with the finite element graphics pre/postprocessor language PATRAN* . The natural frequencies for each plate were then obtained using MSC/NASTRAN*, a finite element analysis program (All analysis was performed on a CRAY-XMP* computer). Then the baseline dimensions and material properties of the plates were changed to discover how such variations affect the mode shapes and their frequencies. Most of the effects of the variations were quite intuitive and are not reported in this study. For example, increasing the thickness of a plate shifts the natural frequencies up. Or, for another example, increasing the across-grain stiffness raises the frequency of those modes which have predominant

---

*PATRAN is a trademark of PDA Engineering, Santa Ana, CA, 92705.
MSC/NASTRAN is a trademark of the MacNeal-Schwendler Corporation, Los Angeles, CA, 90041.
CRAY-XMP is a trademark of Cray Research Inc., Minneapolis, MN.

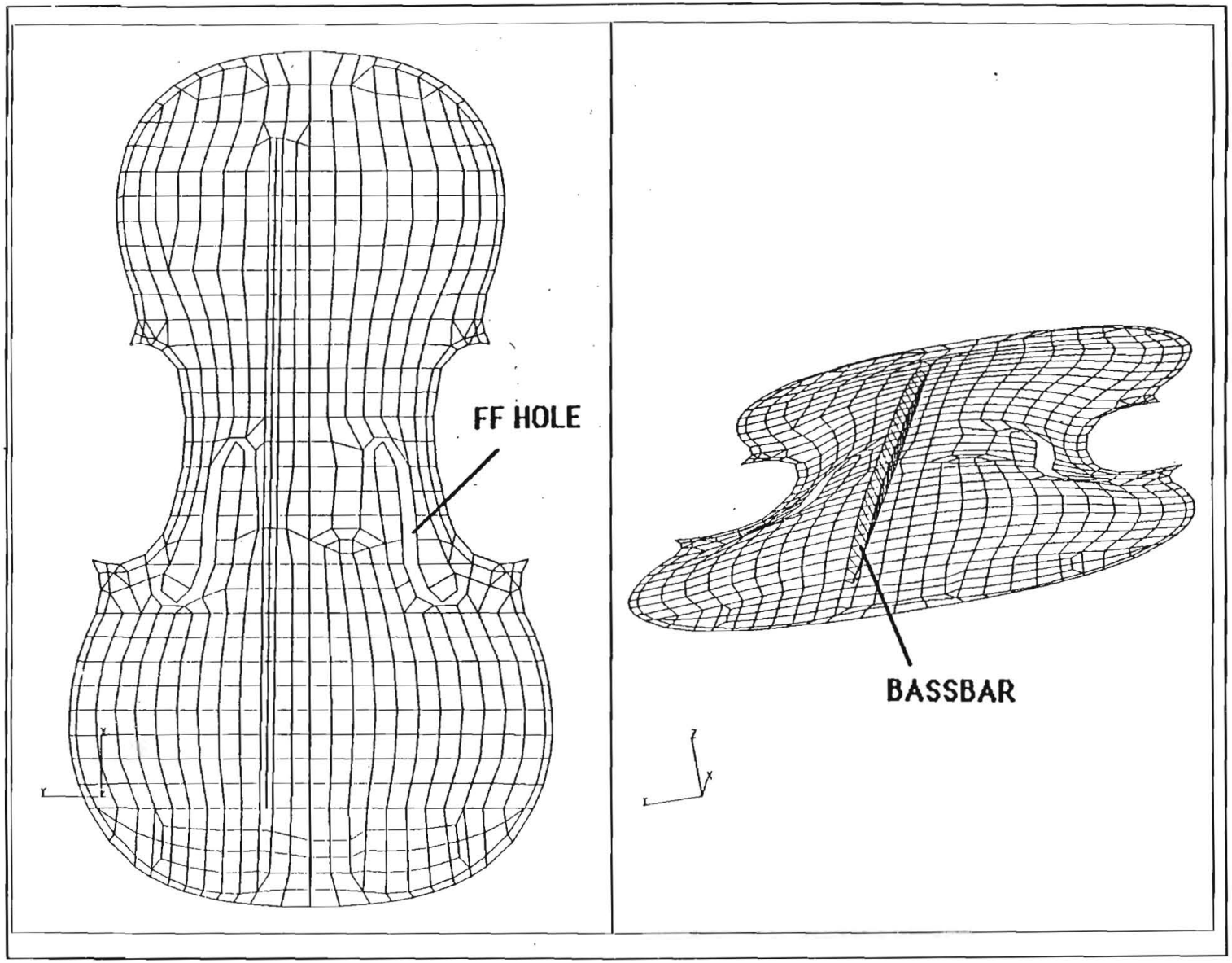

Figure 1.0. Top plate detail

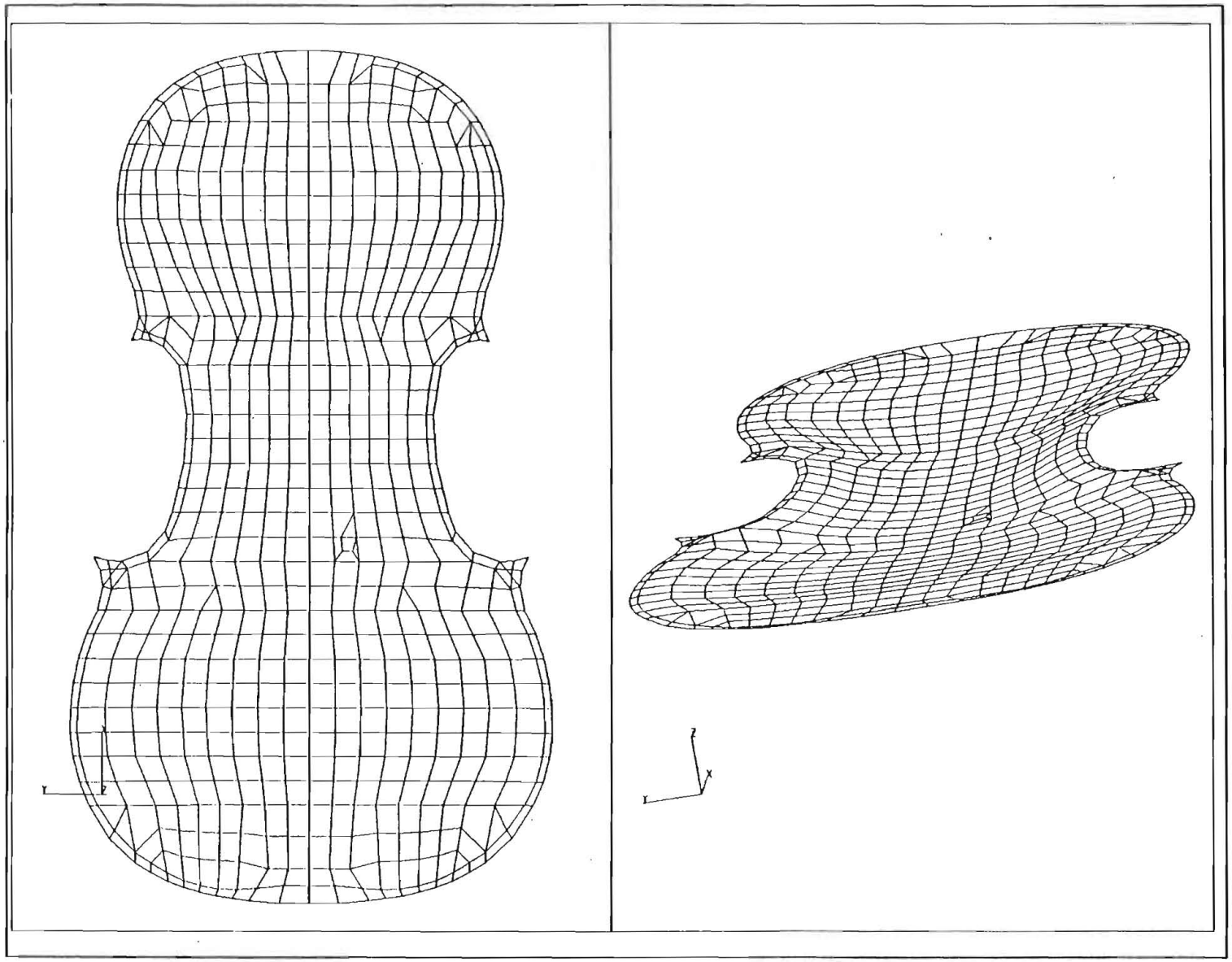

Figure 1.1. Back plate detail

bending action across the grain. Rodgers [Ref. 8] is currently using the finite element method in a sensitivity analysis of the free violin plates to give a detailed description of how the mode shapes and frequencies are affected when various material properties in the plates are varied.

C. THE VIOLIN BOX

1. Modeling the Box

The second stage of the study puts the belly (the top plate) and back together, joined with the ribs, a luthier's term for the side walls of the violin. The decision was made to include eight other components of the violin in this second stage: the soundpost; a dowel of wood attached vertically between the belly and back, the bassbar; a strip of wood attached to the underside of the belly, the two endblocks; blocks of wood attached to the inside ends of the violin box for the purpose of structural rigidity, the four corner blocks; again solid blocks of wood attached to the 'points', or corners of the violin for the same purpose as the end blocks, and the rib linings; wood firring strips which strengthen the bond between the ribs and the belly and back (see Figures 1.2 - 1.5).

2. The Analysis

With the 'box' modeled the second stage analysis could begin. The first nine natural frequencies and mode shapes of the box model were

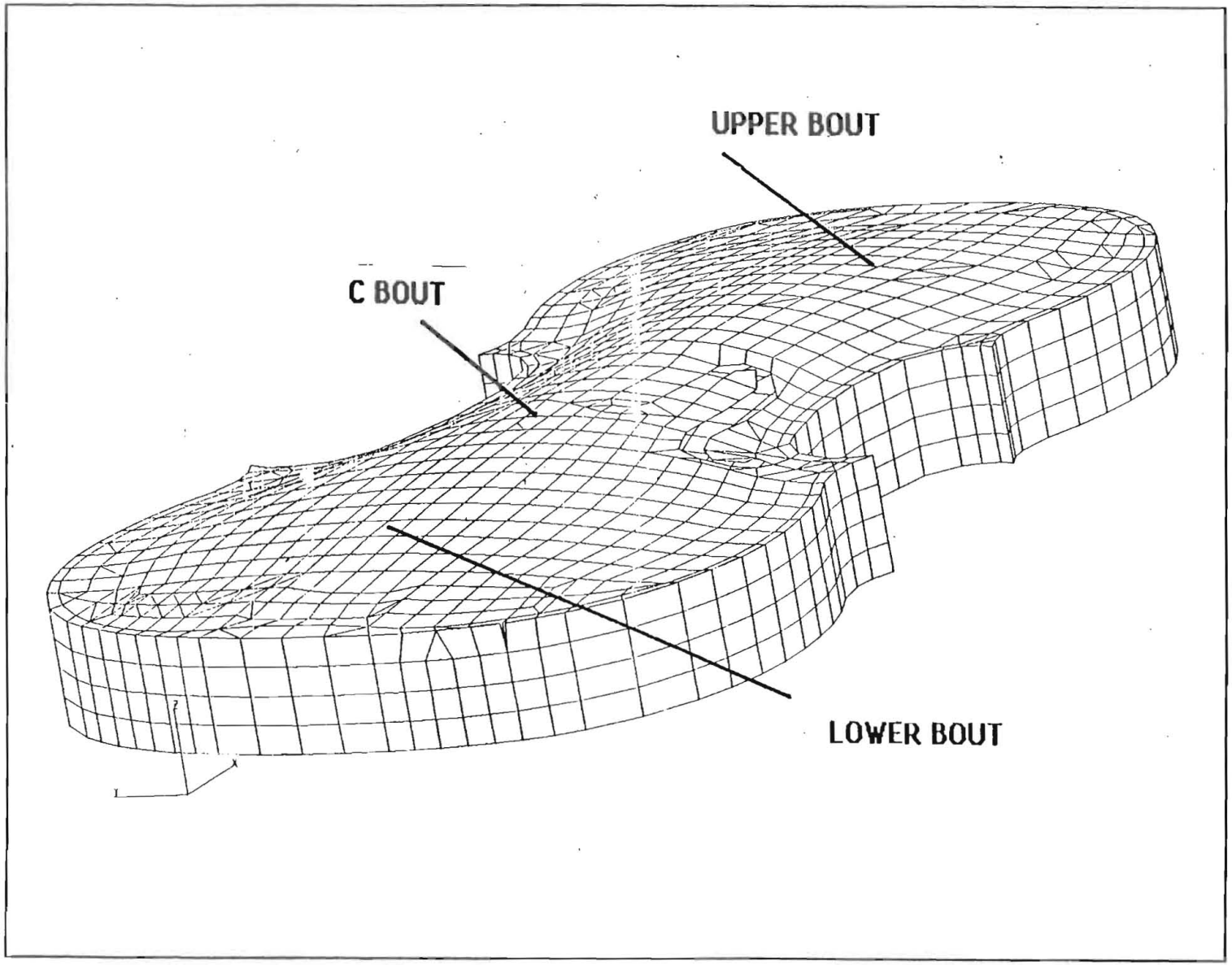

Figure 1.2. Violin corpus

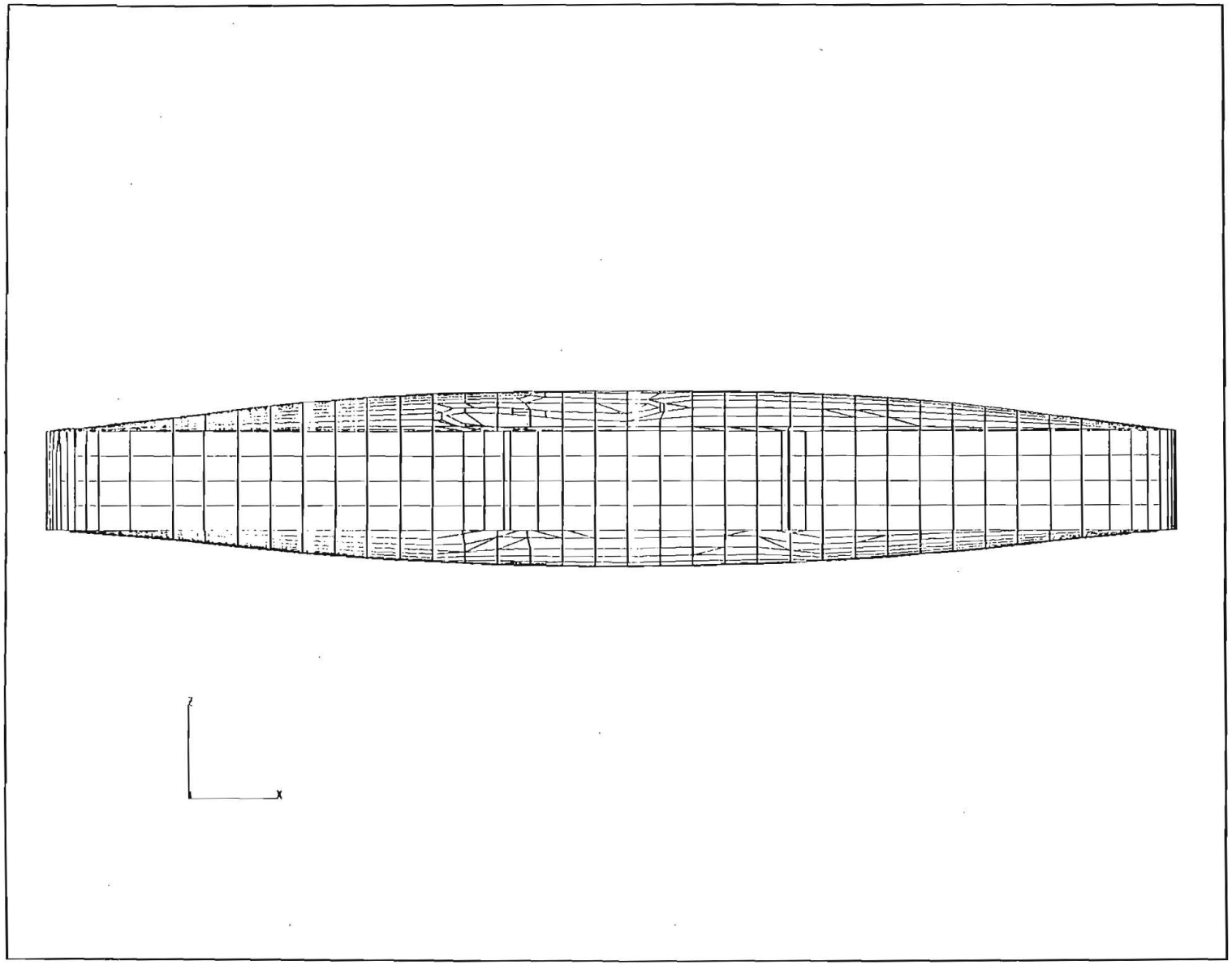

Figure 1.3. Violin corpus - side view

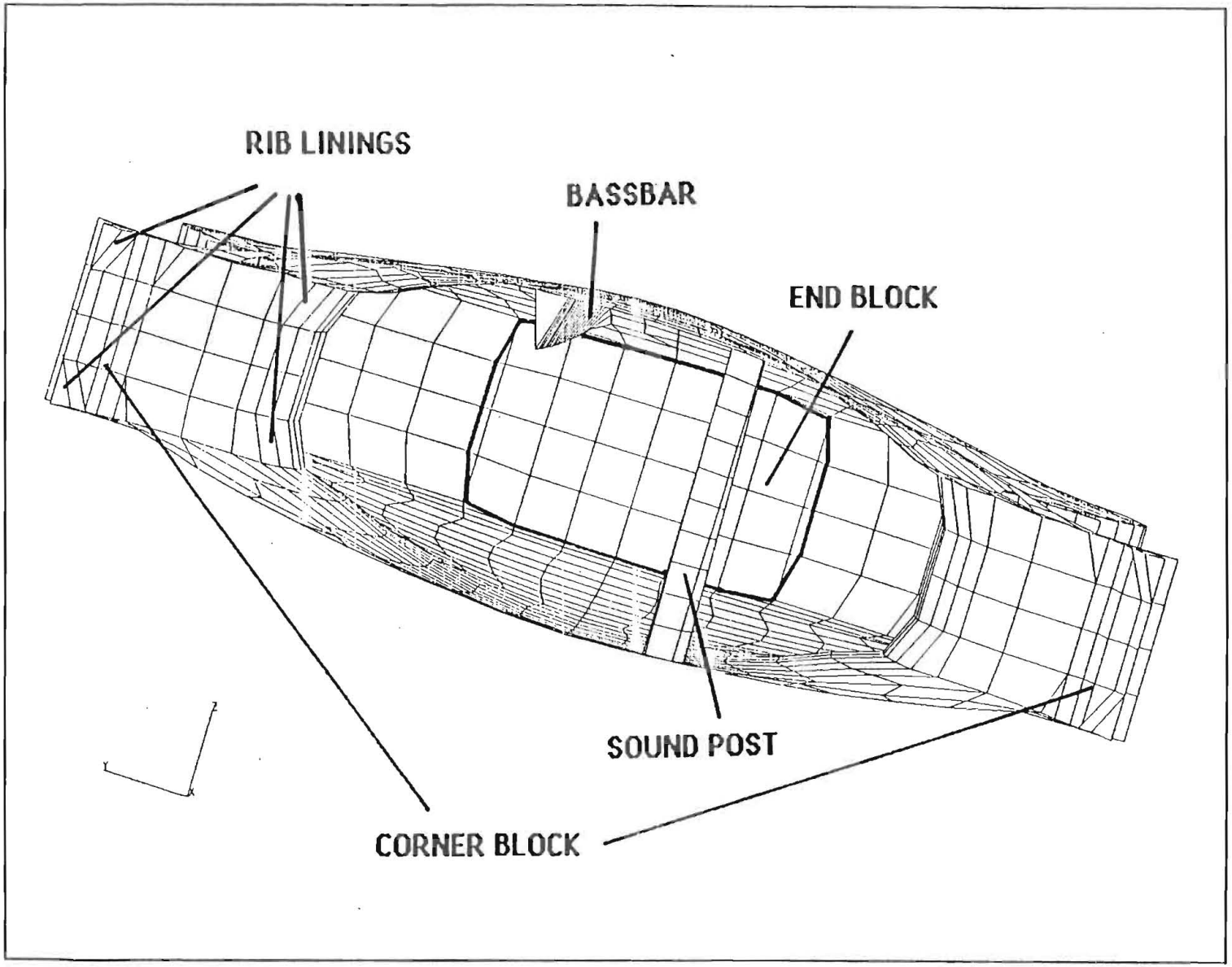

Figure 1.4. Violin corpus - cutaway view

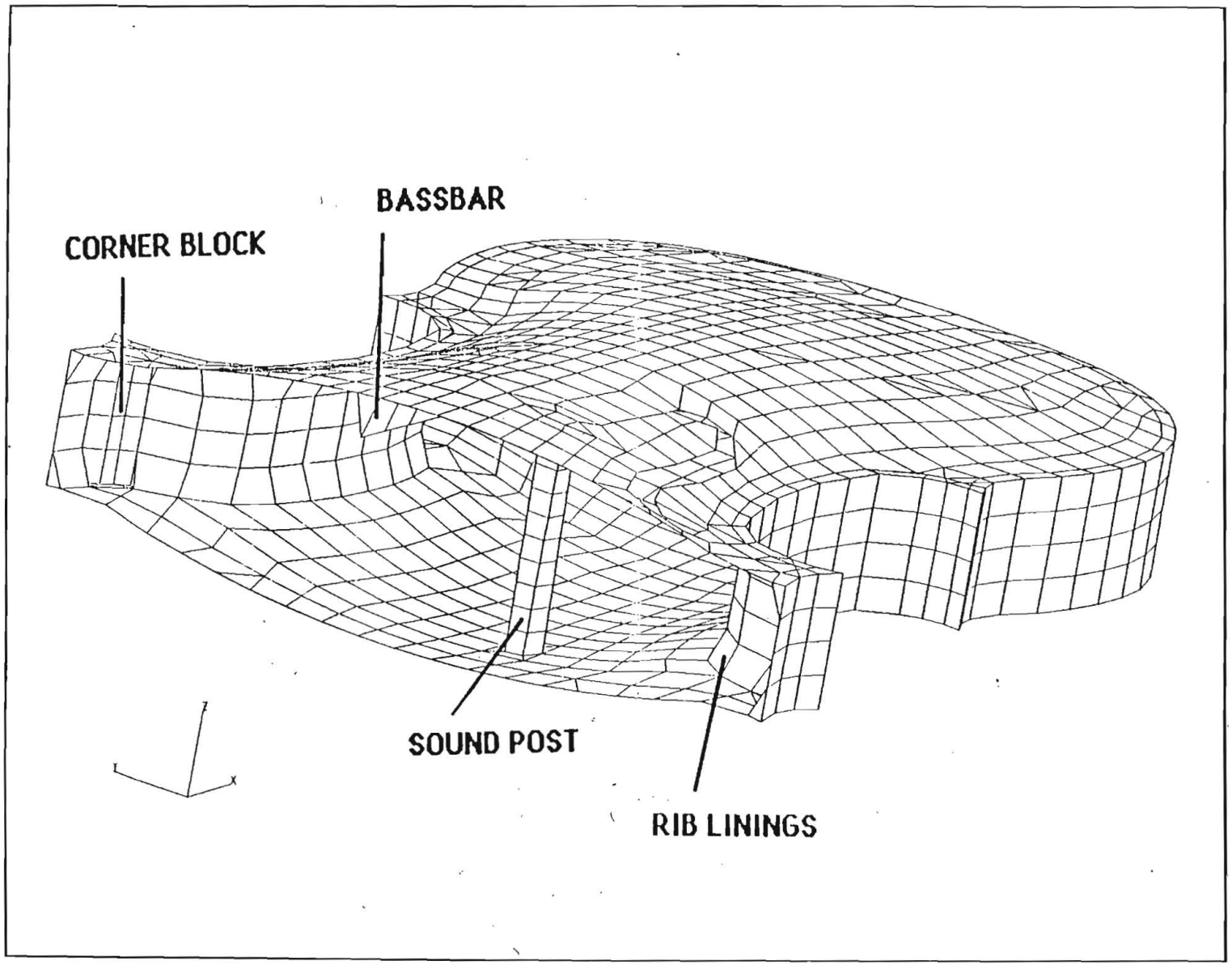

Figure 1.5. Violin corpus - cutaway view

calculated using the MSC/NASTRAN software. The mode shapes and corresponding frequencies were then compared to those obtained from an impact hammer modal test conducted by Marshall [Ref. 9] of a real violin (neck, bridge and strings attached). An experimental modal test of a violin box sans attachments would have been desirable but it was found that Marshall's results confirmed the results of the finite element run in most respects. The mode shapes experimentally obtained were quite similar to those generated by the finite element run for those modes involving the violin box alone. Of course the neck, bridge and string modes were absent. In addition the violin finite element model was in vacu so none of the air modes or their influence on the wood modes was observed. The modal frequencies were also verified to be in the same general order and close to those obtained by Marshall.

D. THE WHOLE VIOLIN

1. Modeling the Remaining Components

The final stage of the study began with the modeling of the remaining components of the violin. With neck, bridge, strings and tail piece models added to the data base a complete violin system was realized (see Figures 1.6 - 1.8).

2. Analysis of the Whole Violin

With the whole violin modeled the final step in the study was to run a normal mode analysis and once again compare the results to those obtained by Marshall's modal test on a real violin. This final analysis proved to be the most difficult portion of the study. All of the previous runs had used canned solution sequences included in the MSC/NASTRAN software. Linear static and dynamic analyses of relatively simple problems can usually be solved using these preprogramed sequences of matrix manipulations. The addition of the strings and the requirement that they be under tension complicated the system to the extent that the rigid format solution sequences were no longer applicable to the structure. Specifically, off-axis deformations of the strings and large relative displacements between the string elements and those in the rest of the violin model introduced geometric non-linearities which must be included in the finite element model.

The NASTRAN finite element analysis package is written entirely in DMAP (Direct Matrix Abstraction Programming), a high-level language for defining matrix operation algorithms. The geometric non-linearities in the violin system under tension were incorporated by using the DMAP language to alter the rigid format solution sequences. A brief discussion

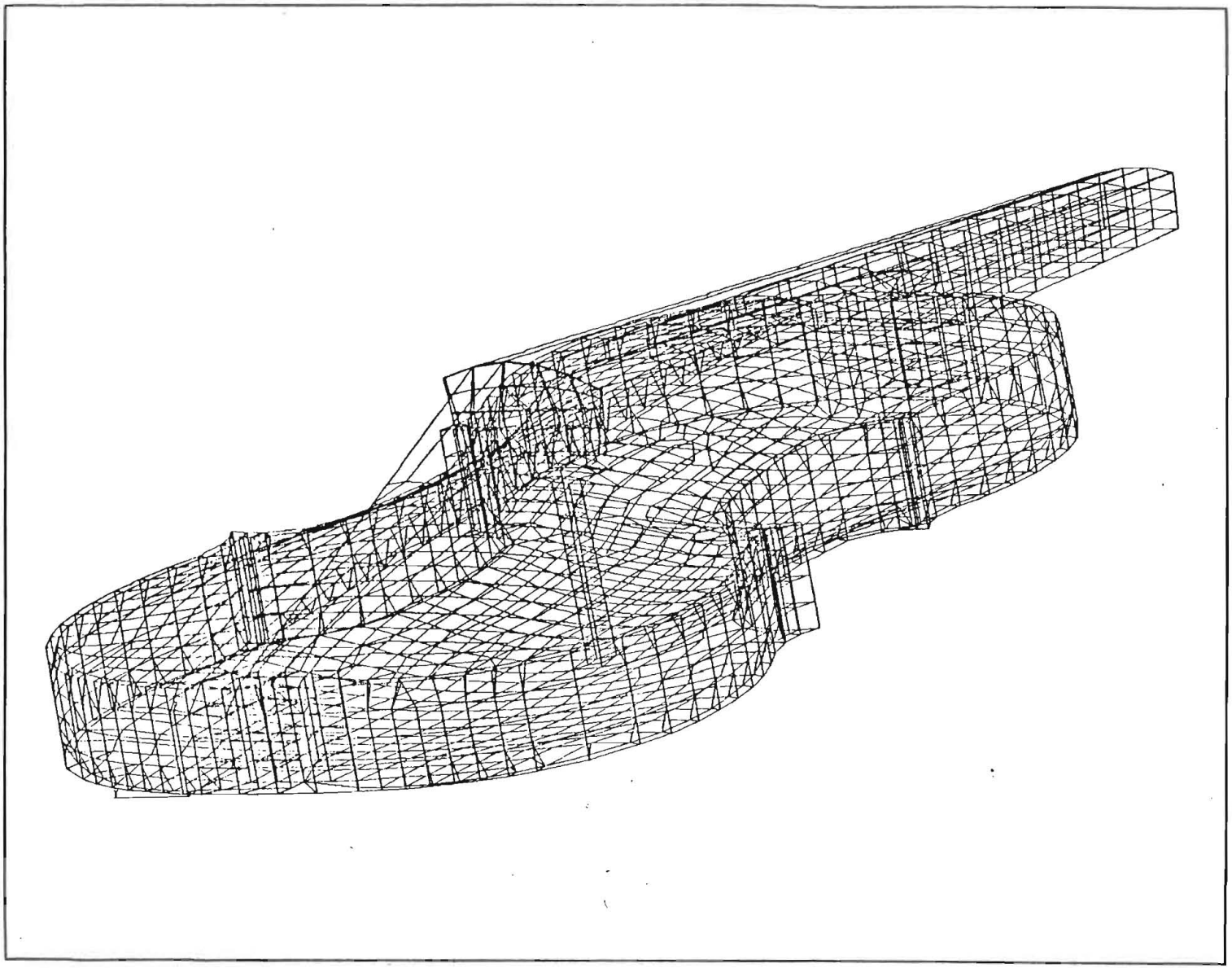

Figure 1.6 Finite Element Model of the Violin

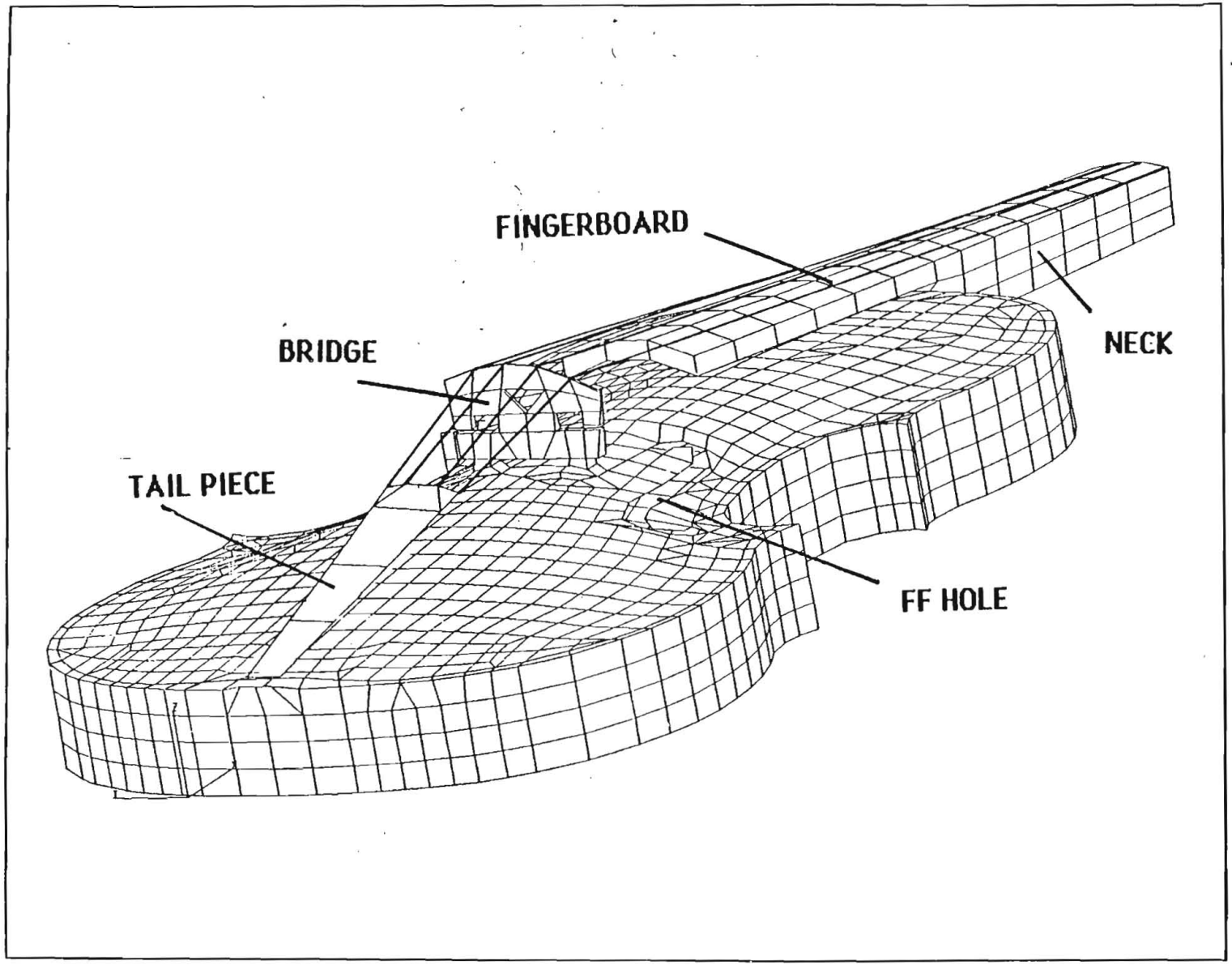

Figure 1.7. Whole violin

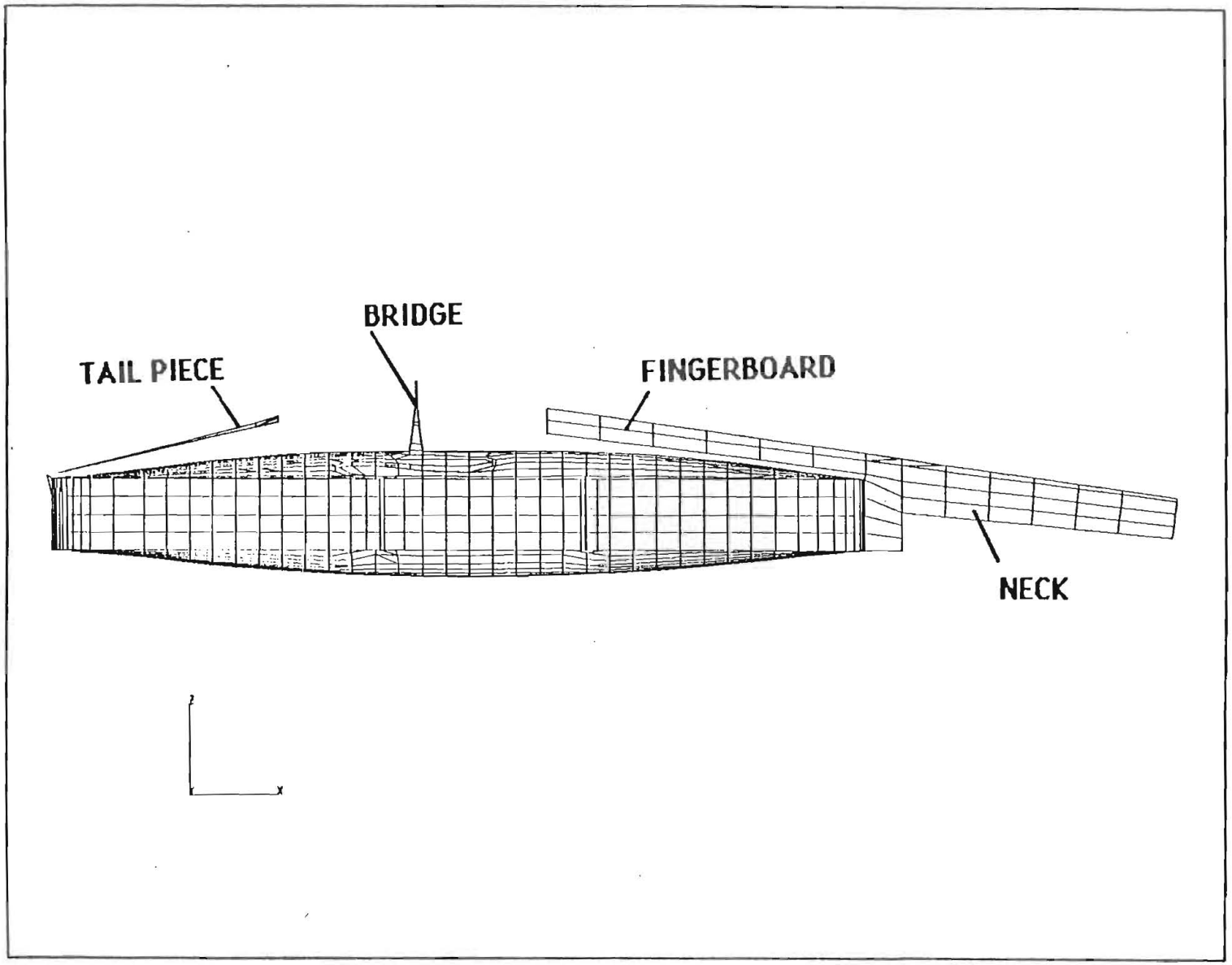

Figure 1.8. Whole violin - side view

of the DMAP language and the details of the alterations are discussed in the analysis portion of this paper.

Once the solution sequence was altered the normal modes of the entire system were computed to 1,200 Hz. Thirty-nine mode shapes and frequencies were obtained and compared to those found by Marshall on a real violin. This time, as was expected, the agreement between experiment and the finite element simulation was even better than in the case of the box alone.

E. SOURCES FOR THE INPUT DATA AND EXPERIMENTAL VERIFICATION

The correct implementation of any numeric method requires that the input data be accurate, the methods be sound, and that the results be experimentally verifiable. As a result this work, like so much research, leans heavily on the efforts of others. Specifically, Eckwall [Ref. 10] and Sacconi [Ref 11] provided the geometry for the violin model. Eckwall's arcs of circles scheme for describing a Stradavari violin saved hundreds of hours in data preparation. Haines [Ref. 12] and the United States Department of Agriculture [Ref. 13] was the source for most of the material properties. Marshall's recent study [Ref. 9], a modal analysis of a real violin, was an extremely valuable source for experimental verification and will be referred to often in this paper. Hutchen's work on

plate tuning [Refs. 14 and 15] provided the experimental basis for comparison of the finite element plate mode shapes with the mode shapes of real violin plates.

II. THE FINITE ELEMENT MODEL OF THE VIOLIN

Ekwall's work describes "Il Cremonese 1715" ex Joachim entirely in arcs of circles [Ref. 10]. These arc lines are ideally suited as inputs to the PATRAN preprocessing graphics software. Once the outlines and archings of the violin box were described with the arcs, adjacent arcs were used to describe surfaces. The components of the box were then attached to the surfaces, resulting in a highly accurate numerical representation of the violin geometry. The finite elements were defined from the surface geometry and consist of triangular and quadrilateral shell elements for the belly, back, and tail piece, beam elements for the strings, and solid elements for the rest of the components.

The material properties used for the analysis runs are listed in Table I. The data listed in Table I can be considered as a good starting point since it represents "average" values obtained from the wood handbook [Ref. 13] and from Haines' study [Ref. 12]. The belly, soundpost, rib linings, bridge, end and corner blocks are modeled as Sitka spruce; the back, neck, and tailpiece are modeled as Norwegian maple; and the bassbar is modeled as Douglas fir.

TABLE I

MATERIAL PROPERTIES

	NECK, BACK, TAILPIECE, RIBS (MAPLE)	BELLY, RIBLININGS, POST, BRIDGE,BLOCKS (SPRUCE)	BASSBAR (FIR)
E1 (Young's Modulus, Pa X 109)	17.000	13.000	12.400
E_2	1.564	0.890	0.621
E_3	0.731	0.649	0.621
G_1 (Sheer Modulus, Pa X 10^9)	1.275	1.015	0.794
G_2	1.173	0.715	0.868
G_3	0.187	0.416	0.967
ν_{12} (Poisson's Ratio)	0.318	0.375	0.292
ν_{13}	0.392	0.436	0.449
ν_{23}	0.703	0.468	0.390
ν_{32}	0.329	0.248	0.287
ν_{21}	0.030	0.034	0.020
ν_{31}	0.019	0.022	0.022
∂ (Density, kg/m^3)	800.000	460.000	506.00

The material orientations for the whole model are defined in Figure 2.0 and are illustrated to avoid confusion when refering to the material properties Table.

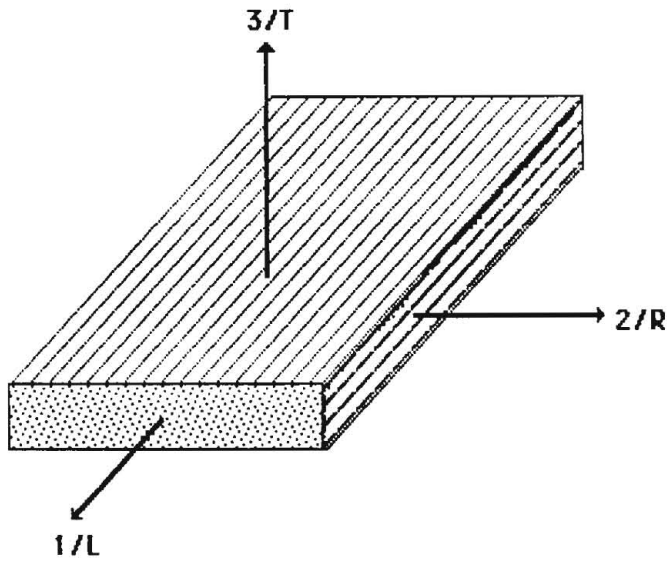

R - Radial direction of wood grain.
T - Tangential direction of wood grain.
L - Longitudinal direction of wood grain.

Figure 2.0. Material orientations

The thickness of the belly was defined in accordance with Sacconi [Ref.11] to be 3 mm except at the edges and area around the two ff holes (these holes can be seen in Figure 1.0), where it was 3.8 mm. In the violin model the top plate was modeled with a uniform thickness of 3.0 mm. The back was defined to the thickness of 4.5mm at the center, descending to 3.8 mm on the first circles, to 3.5 mm on the second, to 2.5 mm in the upper lung and to 2.6 mm in the lower one. Figure 2.1 shows a countour map of the back thicknesses.

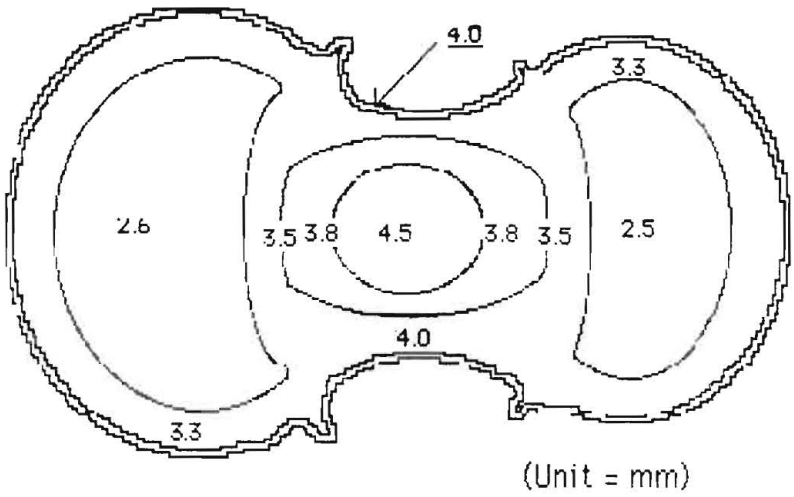

Figure 2.1. Back thicknesses

The neck dimensions were unavailable for the Stradivari violin, so the modeling of the neck was accomplished using neck dimensions from the author's violin. Hexahedral and wedge elements were used for the neck model. Neck details are illustrated in Figure 2.2.

For the tail-piece quadrilateral and triangular shell elements were used. The geometry of the tail-piece was obtained from the author's violin.

The bridge model was created using the classical bridge form found in most violins. The model realization is, of neccessity, a simplification of the true geometry as can be seen in Figure 2.3. However, the obvious design objectives are retained. The thickness of the bridge varies from 5.0 mm at the feet to 0.5 mm at the top.

The strings were modeled as beam elements. Beam elements were chosen instead of rod elements to allow the inclusion of bending stiffness into the string model, which the rod element does not consider. The 'G', 'D',

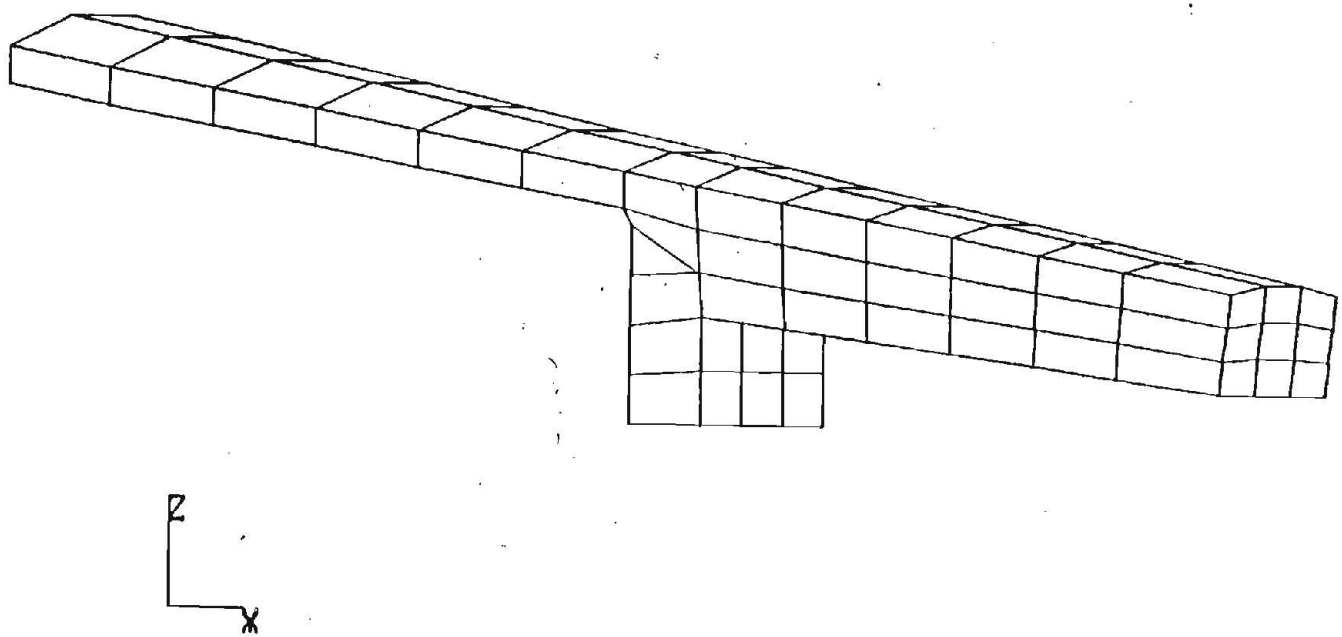

Figure 2.2. Neck detail

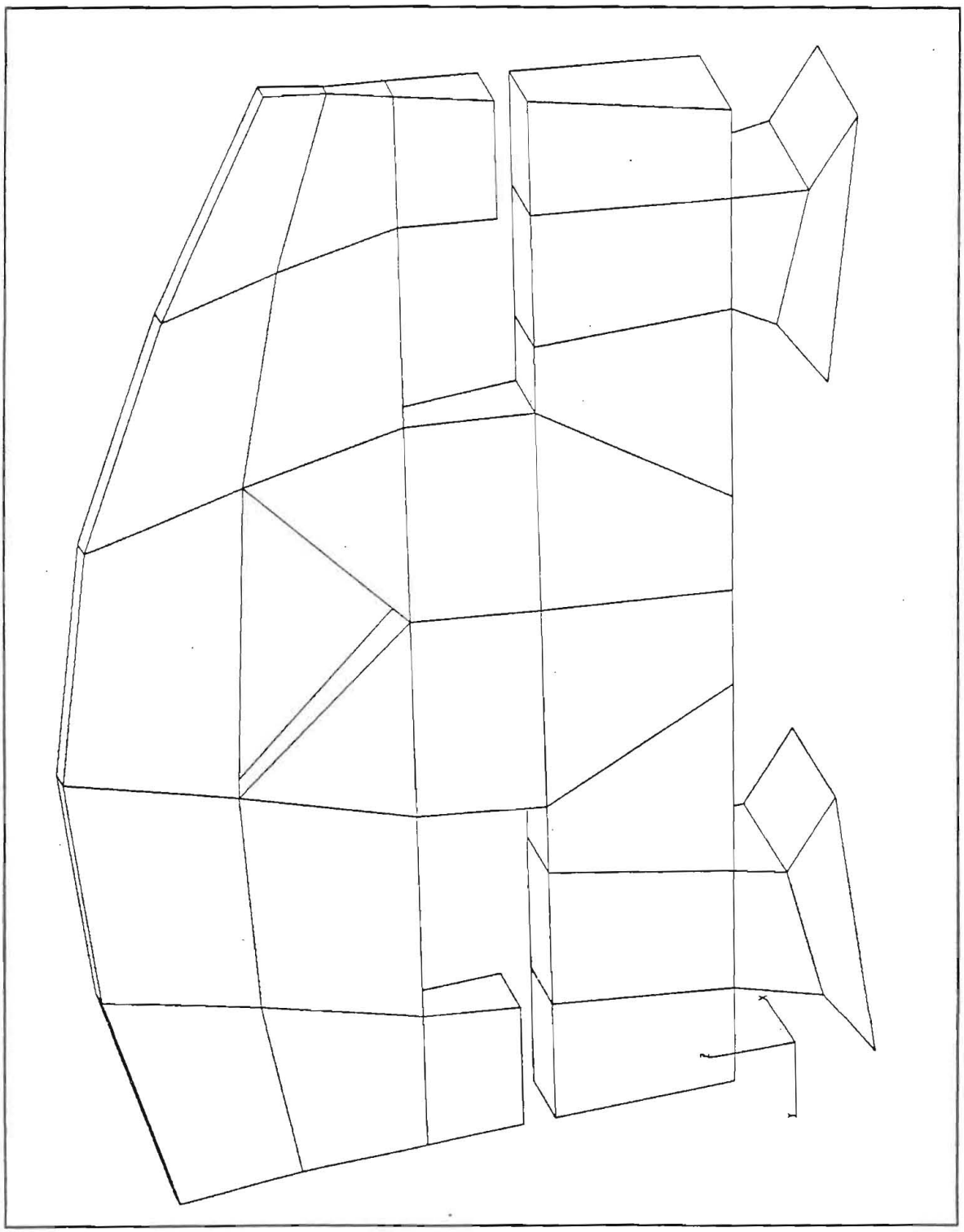

Figure 2.3. Bridge detail

and 'A' string's material properties were modeled as gut cores with steel windings. The windings were modeled as a non-structural mass since their contribution to bending stiffness is assumed to be negligible. Solid steel was used for the 'E' string. Table II lists the dimensions and material properties for the strings. The number of beam elements for each string was determined from the desired frequency response of about 8,000 Hz.

TABLE II

STRING DIMENSIONS AND MATERIAL PROPERTIES

	STRING			
	'G'	'D'	'A'	'E'
CORE MASS(g)	0.110	0.065	0.034	0.130
N.S.M.(g/m)	3.314	1.352	0.557	0.000
TOTAL MASS(g)	1.200	0.750	0.260	0.130
CORE DIAMETER(mm)	0.600	0.460	0.330	0.270
E (Young's Modulus, Pa x 10^9)	30.000	30.000	30.000	195.000
ν (Poisson's Ratio)	0.400	0.400	0.400	0.280
∂ (Density, kg/m^3)	1200.000	1200.000	1200.000	7700.000
No. OF ELEMENTS	110	82	46	33

III. THE ANALYSIS

A. REAL EIGENVALUE EXTRACTION TECHNIQUES

The motion of the violin can be described by a set of equations representing the balance of forces acting on the system. In the eigenvalue problem we are interested in the solution of the undamped and unforced system of equations:

$$\mathbf{M}\ddot{\mathbf{u}} + \mathbf{K}\mathbf{u} = 0 \tag{3.1}$$

assuming a solution:

$$\mathbf{u} = \mathbf{a}e^{i\omega t} \tag{3.2}$$

where $\mathbf{a}$ is a vector of displacement amplitudes, ω is the natural frequency, and t is the time. Rearranging:

$$(\mathbf{K} - \lambda\mathbf{M})\mathbf{a} = 0 \tag{3.3}$$

where $\lambda = \omega^2$.

The solution is nontrivial only if:

$$\det(\mathbf{K} - \lambda\mathbf{M}) = 0 \tag{3.4}$$

A polynomial expansion of (3.4), where the values of λ which satisfy the equation are called the eigenvalues.

Each of the roots satisfies (3.4) so we have:

$$(\mathbf{K} - \lambda_i \mathbf{M})\mathbf{a}_i = 0 \qquad (3.5)$$

where $\mathbf{a}_i$ is the vector of displacement amplitudes, the eigenvector, associated with the eigenvalue λ_i. An eigenvalue is obtained by solving (3.4) and then the eigenvector is determined by solving (3.5) with that value for λ.

In MSC/NASTRAN one of the available methods for extracting eigenvalues is the Givens method [Ref. 16]. For the Givens method the standard form of the eigenvalue problem is used:

$$(\mathbf{J} - \lambda \mathbf{I})\mathbf{w} = 0 \qquad (3.6)$$

Where $\mathbf{J}$ is real and symmetric (as is the stiffness matrix $\mathbf{K}$). Equation (3.6) is formed by decomposing the mass matrix, $\mathbf{M}$, into Choleski factors $\mathbf{C}$ such that:

$$\mathbf{M} = \mathbf{C}\mathbf{C}^T \qquad (3.7)$$

Substituting (3.7) into (3.3) gives:

$$(-\lambda \mathbf{C}\mathbf{C}^T + \mathbf{K})\mathbf{a} = 0 \qquad (3.8)$$

So:

$$\mathbf{w} = \mathbf{C}^T\mathbf{a} \qquad (3.9)$$

Substituting and rearranging gives:

$$\mathbf{J} = \mathbf{C}^{-1}\mathbf{K}\mathbf{C}^{-T} \qquad (3.10)$$

and the standard form, equation (3.6) is realized.

MSC/NASTRAN uses the Givens method to reduce the **J** matrix in (3.6) to tridiagonal form and then uses the Q-R method [Ref. 17] to obtain a diagonal matrix whose elements are the eigenvalues. The eigenvalues are then determined by the tridiagonal form of the eigenvalue problem.

The computer runs used the above technique for eigenvalue and eigenvector extraction. Further explanation of the eigenvalue problem as it applies to MSC/NASTRAN can be found in the MSC/NASTRAN Primer [Ref. 15].

B. TOP AND BACK PLATE ANALYSIS

The eigenvalue extraction techniques covered in section A were used for the top and back plates. Appendix E, Figure E1, shows a simplified example of the data deck used. The initial runs on the top plate were without the bassbar and then with. Then the back plate was run. The analysis runs used free boundary conditions but rigid body modes are not included in the tables. Table III lists the natural frequencies, Figures A1 - A6 illustrate the mode shapes for the top plate with bassbar and Figures B1 - B6, the back plate.

TABLE III

NATURAL FREQUENCIES FOR FREE TOP AND BACK PLATES

Mode	Top (Hz)	Top/w/Bar (Hz)	Back
1	67.0	88.0	97.0
2	115.0	161.0	170.4
3	200.0	255.3	268.2
4	202.3	272.7	268.3
5	274.0	330.4	353.0
6	-	422.0	413.7
7	-	436.0	453.7
8	-	494.1	558.0
9	-	617.4	632.4

C. THE VIOLIN BOX

The violin box used the same executive routine directives as the free plates for its eigenvalue analysis runs. Of course the bulk data deck, which specifies the model geometry and material properties, was much larger in that it included both plates and the additional components making up the violin box model. Table IV lists the nine extracted natural frequencies and their descriptions. Figures C1 - C18 illustrate the corresponding mode shapes. Note that since the displacement amplitudes are mass normalized for each eigenvalue and are therefore meaningless for comparison of amplitudes among distinct modes, absolute displacements are not shown on any of the contour diagrams in this paper.

D. THE WHOLE VIOLIN

As mentioned in the introduction the transition from the violin box model to the model of the violin with all of its components was a difficult one. The greatest difficulty was in the fact that the finite element "strings" had to be streched a large amount relative to other strains in the violin. Large errors in strain energy were experienced when the complete violin system under string loading was programmed for a statics analysis. The rigid formats available in the NASTRAN software had to be modified, and the

TABLE IV

NATURAL FREQUENCIES FOR F.E. CORPUS

Mode	Freq.(Hz)	Description (IP = in phase, OP = out of phase)
1	462.9	Vertical translation of C bouts. Top and back IP. Left and right sides OP.
2	478.9	Vertical bending of corpus. Top plate transverse, back plate longitudinal.
3	573.9	Vertical bending of corpus. Top plate longitudinal, back plate transverse.
4	682.5	Top and back plates OP. Essentially a lengthwise dipole. Back plate upper hump extends through the center area and resembles a ring mode.
5	736.2	Dipole action in lower bout of top plate. Breathing in back plate, strongest in lower bout.
6	749.6	Dipoles in lower bouts of both plates. Strong torsional action of the corpus.
7	810.9	Similar to mode 4, a lengthwise dipole, except that top and back are IP.
8	899.1	Double dipoles in top and back plates. Top and back OP.
9	968.5	Top exhibits three "poles" in lower bout. Back plate shows ill-defined dipoles in upper and lower bouts.

DMAP language used to tailor the solution sequence to the problem. The following is a step by step explanation of the process:

1. Assemble the stiffness matrix for the violin box with the neck included, but without the bridge/tail piece/strings system. A static analysis, SOL 61, was run with an alteration in line 355 of the preprogrammed solution sequence (see Fig. E2 for the data deck listing). The ALTER statement simply provides the capability to extract the stiffness matrix for the follow-on runs (named KGGW in Fig. E2)
2. Perform static condensation of the above stiffness matrix "eliminating" all degrees of freedom except at those 14 locations where: the strings attach to the neck (4), where the bridge feet attach to the top plate (8), and where the two gut cords from the tail piece attach to the body (2). MSC/NASTRAN's substructuring capability was utilized for the condensation. The SESET cards in the data deck (see Fig. E2) define the substructure, in this case all of the nodes in the violin box/neck that are to be omitted from the KGGW matrix. In other words, the stiffness of the entire box/neck structure is defined for each unit stiffness of each of one of the 14 points, effectively "eliminating" all degrees of freedom except at those 14 points.
3. Run an iterative, non-linear static solution sequence for the bridge/tail piece/strings system (see Fig. E3) using the 84 X 84 KGGW matrix (14 nodes times 6 degrees of freedom per node) matrix obtained in step 2 as the boundary conditions. The stiffness matrix KGGW is essentially the stiffness of the neck and body that the string

ends and bridge feet would experience. Problems of large relative strains are avoided since the box/neck system is present only as a boundary condition (strains are not calculated for the box/neck). The first iteration uses the rigid format for a static analysis in which the strings are subjected to differing amounts of thermal stress. In essence, the strings were "cooled down" to shrink them and bring them to the required tensions. The desired tensions were those that would place the natural frequencies of the strings as close as possible to the tones found on a real violin, that is, G, D, A, and E. The following subcases (or iterations) of the run successively add the geometric non-linear terms and compute the stiffness matrix for each added term until an equilibrium of forces exists:

$$\mathbf{F} = \mathbf{P} + \mathbf{Q} \qquad (3.11)$$

where **F** is the vector of element forces, **P** is the vector of applied thermal loads, and **Q** is the vector of forces of constraint. The string/bridge system stiffness matrix is now modified for the stress of the thermal loads on the strings and is saved for the next step.

4. The final run puts the violin system back together (see Fig. E4). The string/bridge system, now in equilibrium, is added to the box/neck system. Then the rigid format solution sequence computes the normal modes of the entire violin model.

Table V lists the natural frequencies obtained and a description of each mode. Figures D1 - D74 illustrate the mode shapes with contour diagrams and wire mesh deformed plots. Listings of the executive and case control decks for the analysis runs are included in Appendix E.

TABLE V

VIOLIN SYSTEM NATURAL FREQUENCIES

Mode number	Frequency (Hz)	Description (OP = out of phase, IP = in phase)
1	191	Fingerboard bending and tailpiece deflection.
2	201	Fingerboard bending and tailpiece deflection.
3/4	212/213	G1
5/6	312/313	D1
7	363	Maximum motion in C bouts. Top and back OP. Left and right sides OP.
8/9	421/423	G2
10	439	First bending of corpus. Top plate transverse, back plate longitudinal.
11	458	Same as mode 7 except top and back IP.
12/13	486/487	A1
14	494	First fingerboard torsion.

TABLE V (CONT)

Mode number	Frequency (Hz)	Description
15	536	First bending of corpus. Top plate longitudinal, back plate transverse. Strong relative displacement on top plate in the thickest area of the bassbar inhibits the longitudinal bending somewhat.
16	568	Fingerboard torsion.
17	618	A combination of G3,D2, and E1.
18/19	629/632	D2
20	640	G3
21/22	648/652	E1
23	656	Another combination string mode.
24	683	Relatively strong breathing action in upper bouts of both plates. First mode where bridge moves vertically rather than rocking back and forth. Top and back plates are OP.

TABLE V (CONT)

Mode number	Frequency (Hz)	Description
25	693	Tailpiece 'twisting'.
26	727	Dipole in lower bout of top plate. Relatively small breathing action of OP in lower bout of back plate.
27	771	First torsional mode of corpus supported by a strong dipole in lower bout of back plate. The top plate lower bout shows a relatively low amplitude dipole.
28	812	Strong IP breathing of lower bouts in top and back plates. Essentially a lengthwise dipole.
29	856	G4
30	885	Double dipoles. Top and back plates OP.
31	902	G4, D3, and A2 combined string modes.
32	908	Top plate exhibits three 'poles' in lower bout. Back plates shows dipoles in upper and lower bouts.

TABLE V (CONT)

Mode number	Frequency (Hz)	Description
33	961	D3
34	971	Similar to mode 32 in that it is of opposite phase except in the lower bout of the top plate.
35	1000	A2
36	1083	Three poles in lower bouts of both plates. Top and back OP.
37	1092	Second bending mode of fingerboard/neck. Three poles in upper and lower bouts of both plates. Top and back IP.
38	1121	Similar to mode 37 except no fingerboard action.
39	1155	Back plate; three poles in lower bout, two in C bout, and two in upper bout. Top plate; similar except C bout area translates vertically.

IV. COMPARISON TO EXPERIMENT

A. GENERAL COMMENTS

The finite element method is a numerical technique that cannot stand alone; this is especially so when applied to a complex structure such as the violin. Ideally, as each subsystem is simulated using finite elements, a parallel verification of the model is accomplished using experimental methods. For the violin, an exhaustive verification would involve:

1. Top and back plate.
2. Bassbar.
3. Top plate with bassbar.
4. Violin box without sound post.
5. Violin box with sound post.
6. Neck.
7. Violin box with neck.
8. Bridge.
9. Tail piece.
10. Strings with rigid mounts.
11. Whole violin.

In the ideal case the material properties and precise geometry of each component used for experimental verification would be known and would constitute the data base for the finite element modeling process.

In the present study steps 1, 3, 5, and 11 were the only ones which were compared to experimental results. The experimental data was obtained

from Marshall [Ref. 9] and Hutchens [Refs. 14 and 15]. There exists no geometry or material property data for Marshall's violin SUS #295 or Hutchen's violin plates so the examination of the results in the present study must be done with the realization that natural frequencies and mode shapes were not expected to match exactly. A basic assumption to be tested in this study is that there exists a fundamental commonality of mode shapes among all but the most poorly constructed violins. This assumption has been shown to hold in the case of free violin plates, at least among the lower modes of vibration [Ref. 14]. That is, even plates with differing geometries and material properties show a clear similarity in the ordering and shape of their vibration patterns. That all violins sound like a violin (some sound better than others!), is the intuitive and rather obvious basis for the mode shape similarity assumption.

B. TOP AND BACK PLATES

The free top and back plate mode shapes of the finite element analysis were found to compare well with experiments done using Chladni patterns and holographic interferometry. Figure 4.0 is an example of holographic pictures of a back plate [Ref. 15] (see Figures B1 - B5 for the corresponding mode shapes obtained using the finite element method).

Figure 4.0. Holographic fringe patterns of a violin back plate (freq = Hz)

C. THE VIOLIN BOX

Experimental data on a violin box was not available but the author thought it wise to attempt a comparison of the finite element box to that of a complete violin modal test. Then the transition to the complete finite element model would possibly be less confusing. Table VI compares the finite element box to the violin modal test results conducted by Marshall [Ref.9]. SUS*295 refers to the particular violin used by Marshall. Bear in mind that the finite element model does not include the neck, bridge, tail piece or strings, so the mode density of the computer model is much less than that of the real violin.

TABLE VI

MODE COMPARISON BETWEEN F.E. CORPUS AND SUS #295

MODE # F.E./SUS#295	FREQ (Hz) F.E./SUS#295	COMPARISON OF MODE SHAPES
1/10	462.9/410.5	Similar.
2/12	478.9/466.1	Similar.
3/16	573.9/574.1	Similar.
4/19	682.5/656.1	That the two modes are related is suggested by the presence of similar motions in the back plates. The top plates would not be expected to have the same motion since the one has the bridge as a major factor in the mode (it translates vertically) and the other has no bridge at all.
5/22	736.2/690.8	No difference except breathing action is weaker in back plate of the finite element model.
6/24	749.6/760.3	Similar.
7/28	810.9/882.0	Similar.
8/29	899.1/930.1	Similar except that in the finite element model the lower bouts are OP.
9/31	968.5/1087.0	Similar.

D. THE WHOLE VIOLIN

Table VII details the comparison between the finite element model, complete with strings, etc., and SUS#295 used by Marshall for his modal test. The complete violin model compared reasonably well with the real violin in mode shapes, frequencies and relative order of the modes as can been seen by studying Table VII. The source of the discrepancies could be due to a number of factors, the most obvious being that the degree to which the material properties and geometries of the finite element violin and the real violin match is unknown. Any firm conclusions about the origins of the discrepancy between the finite element model and the real violin would require the actual dimensions and material properties of violin SUS#295. The following are other causes of disagreement between mode shapes and frequencies between the finite element model and SUS #295:

- In the finite element model the strings were not tuned to the exact frequencies used on a real violin. For the G string the model was off by +16 Hz; the D string, +18 Hz; the A string, + 46 Hz; and the E string, - 7 Hz. The differences in tuning could have caused some of the discrepancies in mode shapes and ordering of the modes. Fixing the tuning problem will merely require an adjustment of the thermal

loads applied to the string model but, unfortunately, this was not possible prior to publication.

- The air modes of the real violin can be expected to couple to varying degrees with the structural modes of the violin. The model does not contain "air" elements. The air modes are absent from the finite element model and any effect they may have had on the structural modes is a matter for future research.
- A real violin is glued together in most places. In the finite element model there is no attempt to model the glue joints.
- Pressure from the plates and strings hold the soundpost and bridge to the real violin body. In the finite element model most of these forces exist (not the stress mounting of the soundpost in the violin box), but the components are "attached" to the plates and the bridge. In other words, there is no provision for slipping in the case of the strings or decoupling from the plates in the case of the soundpost.

TABLE VII

COMPARISON BETWEEN FINITE ELEMENT MODEL AND SUS *295

Mode number F. E./SUS*295	Frequency (Hz) F.E./SUS*295	Comparison
1,2/1,7	191,201 /119,303	In the F.E. model, the vertical deflection of the tailpiece found in mode 1 of SUS*295 and the first vertical bending of the neck fingerboard found in mode 7 of SUS*295, are both combined in mode 1. Modes 1 and 2 in the F.E. model are dual modes
7,11/10	363,458/410	F.E. mode 7 is coupled with a sideways deflection of the tailpiece. F.E. mode 11 matches SUS*295 mode10 in phase.
10/12	439/466	Similar.
15/16	536/574	Similar.
16/11	568/435	Similar.
17/13	618/471	Similar.
24/19	683/656	An interesting point here is that in the F.E. model the sound post is not stress mounted to the box. The difference in mode shapes between the F.E. model and SUS*295 seems to originate from this difference between the model and reality.

TABLE VII (CONT)

26/22	727/691	Similar.
27/24	771/760	Similar.
28/28	812/882	Similar.
30/29	885/930	Similar except that in the F.E. model the lower bouts are OP.
32/31	908/1187	Similar.

* For higher mode numbers the F.E. model and SUS#295 do not compare well. For example, all higher modes in the F.E. model have a larger number of poles.

V. CONCLUSION AND FUTURE WORK

Since this paper is little more than a catalogue of a finite element violin's mode shapes more questions are raised than answered. The purpose of the study was to provide this preliminary catalogue and to lend support to the idea that the mode shapes of a violin, complete with the string system, can be described using the finite element method. It should be kept in mind that the method's real utility lies not in mere reproduction and description of physical reality but in sensitivity analyses and design optimization. However, before research can progress to violin design optimization still more will be required in the effort to accurately describe the violin. Further work will first concentrate on gaining a more complete data base of real violins and components, with known geometries and material properties. A coincident finite element analysis can then be expected to agree with experimental modal tests of the real violins and components. Different violins can be tested and modeled and the mode shapes compared, perhaps leading to an understanding of what differentiates a "good" sounding violin from a "poor" one.

The incorporation of air elements into the model is a long-term but necessary goal for further research. The extent of the air mode's coupling effects with the structural modes could be easily determined through the study of simple finite element models. Radiation and string exitation studies using finite element models are also promising areas for further work.

After developing the finite element model of the violin the author found the model to be nearly as full of mystery as a real violin! A more methodical, step-by-step analysis should clear up many of the grey areas. The finite element method is an extremely powerful descriptor of physical reality and this author believes that much of the violin "puzzle" will be solved as research continues.

APPENDIX A

TOP PLATE MODES OF VIBRATION

The contour figures are drawn to show motion as it would appear if viewed from above the plate, with plus signs representing motion up, or towards the viewer, and minus signs representing downward motion.

The darker contour lines represent lines of near zero motion.

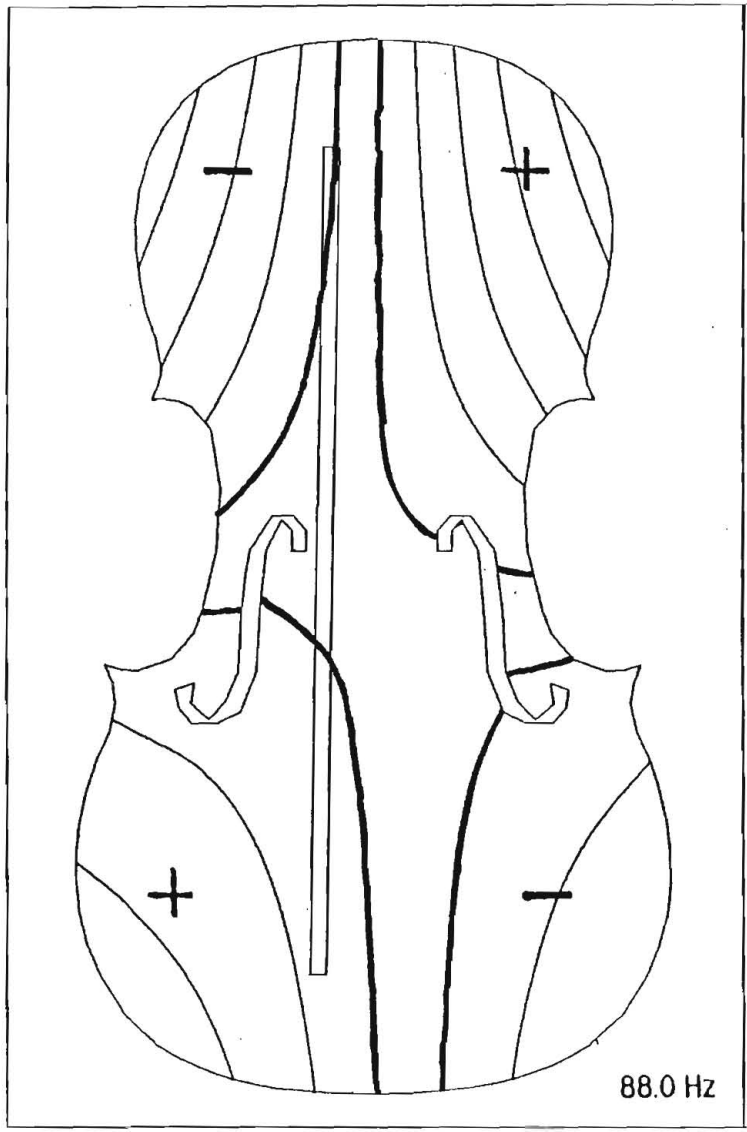

Figure A1. Mode 1

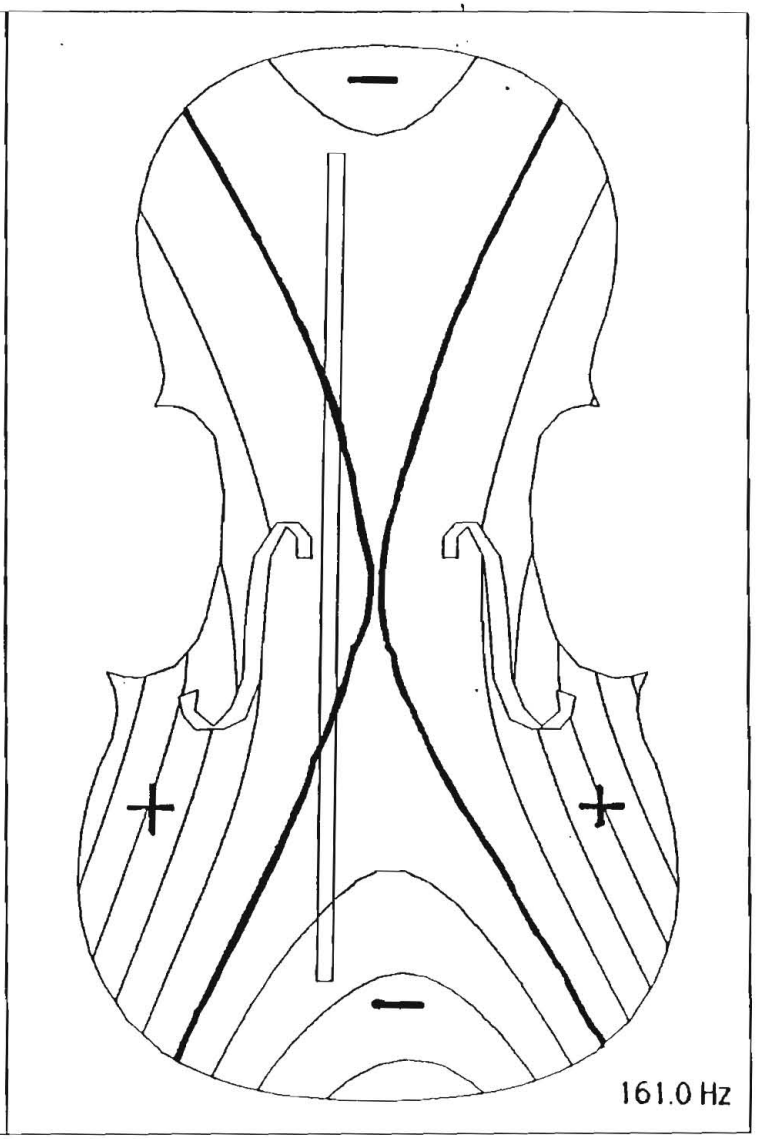

Figure A2. Mode 2

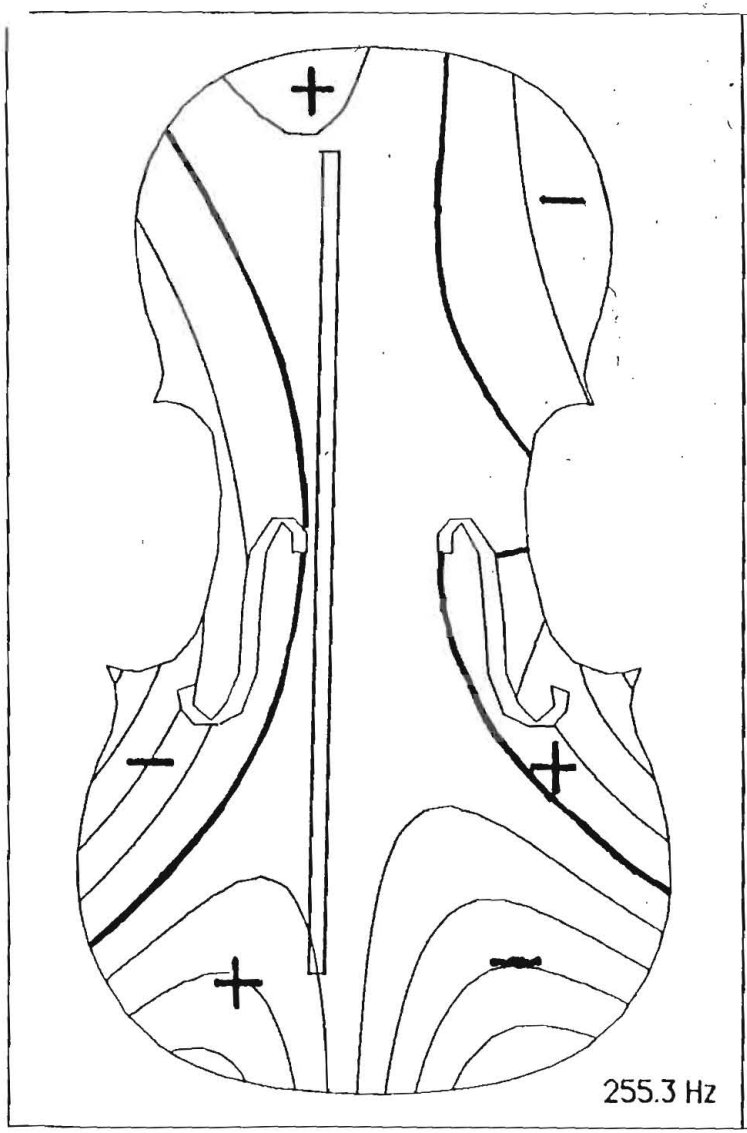

Figure A3. Mode 3

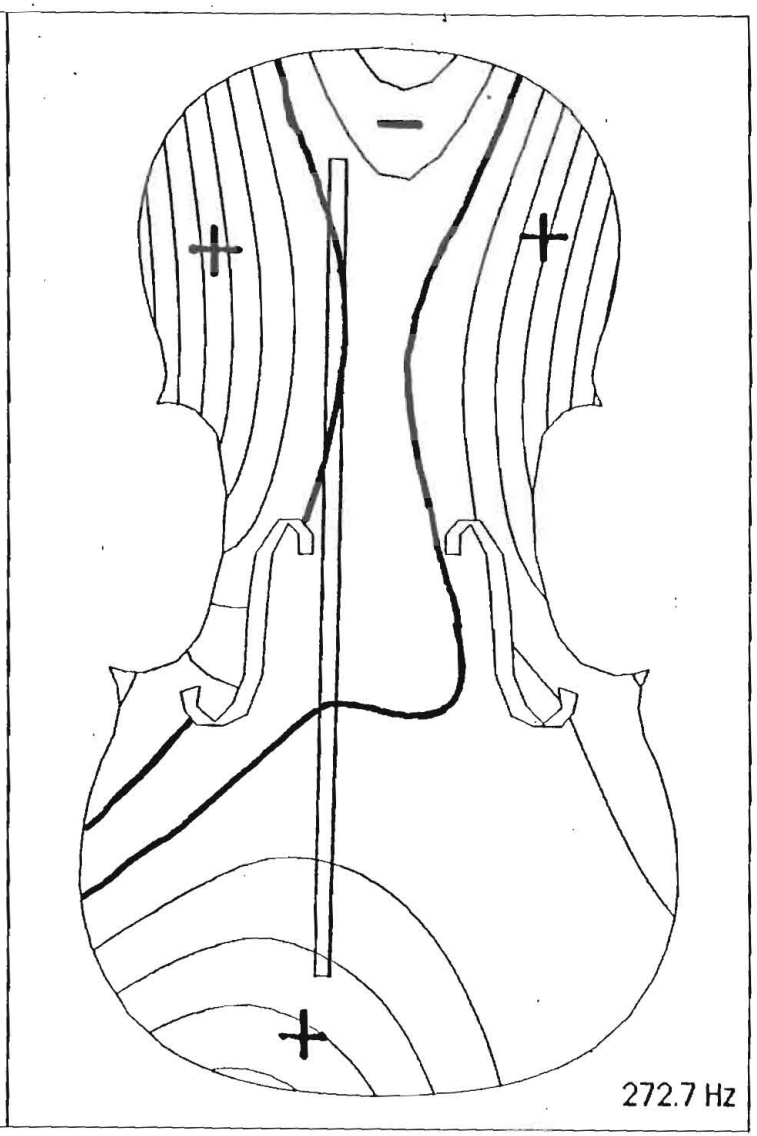

Figure A4. Mode 4

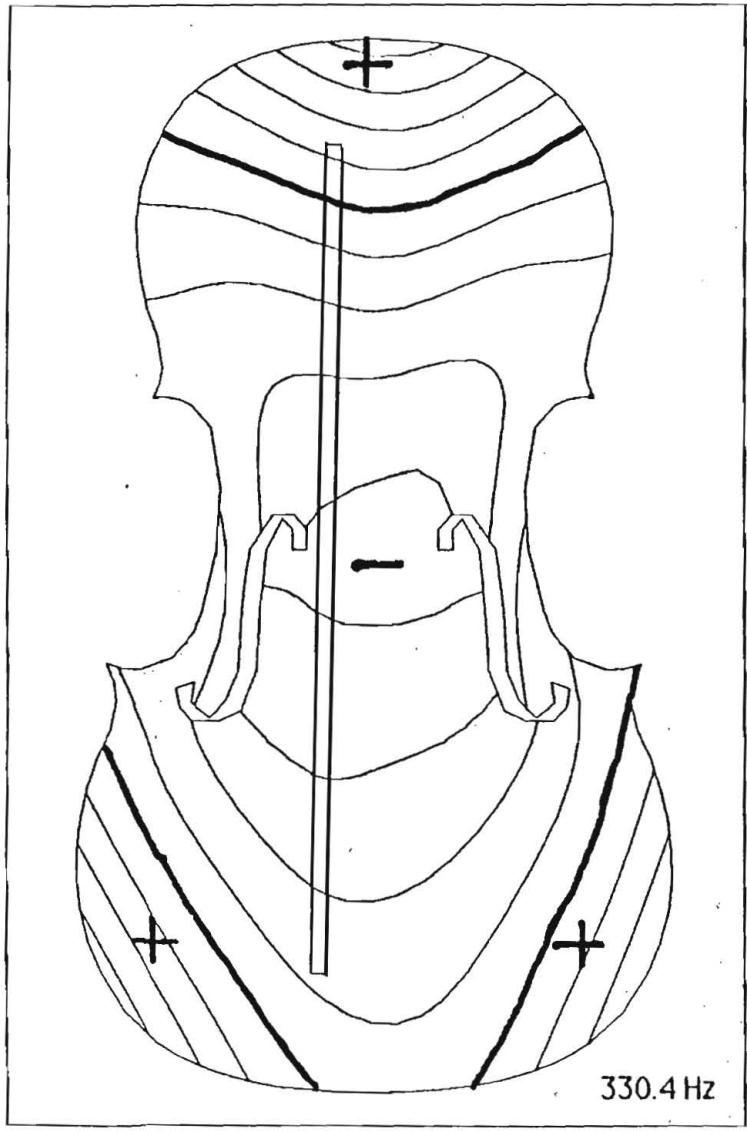

Figure A5. Mode 5

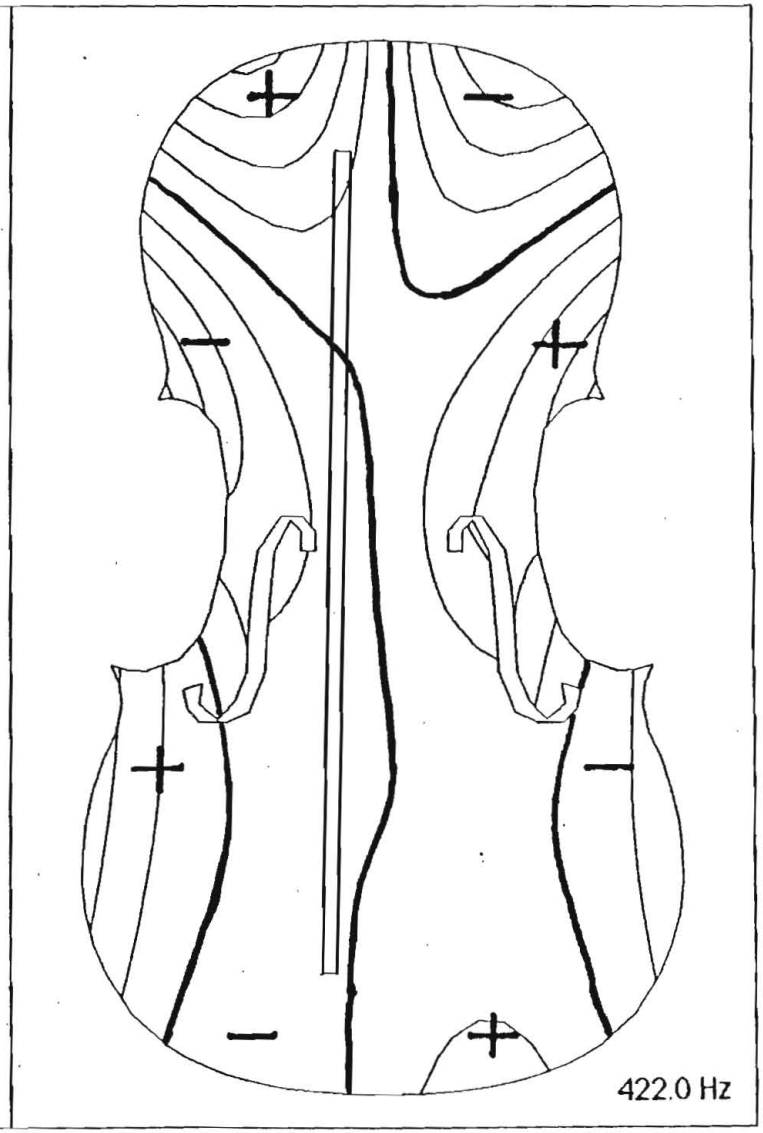

Figure A6. Mode 6

APPENDIX B

BACK PLATE MODES OF VIBRATION

The contour figures are drawn to show motion as it would appear if viewed from above the plate, with plus signs representing motion up, or towards the viewer, and minus signs representing downward motion.

The darker contour lines represent lines of near zero motion.

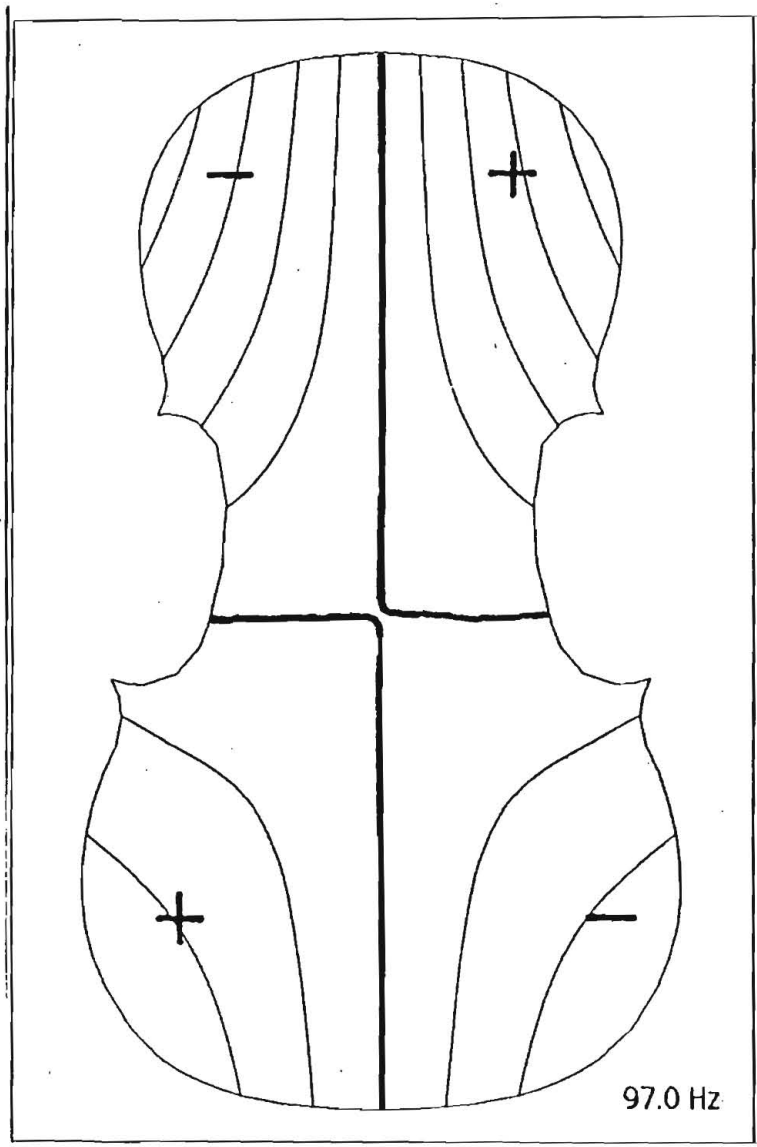

Figure B1. Mode 1

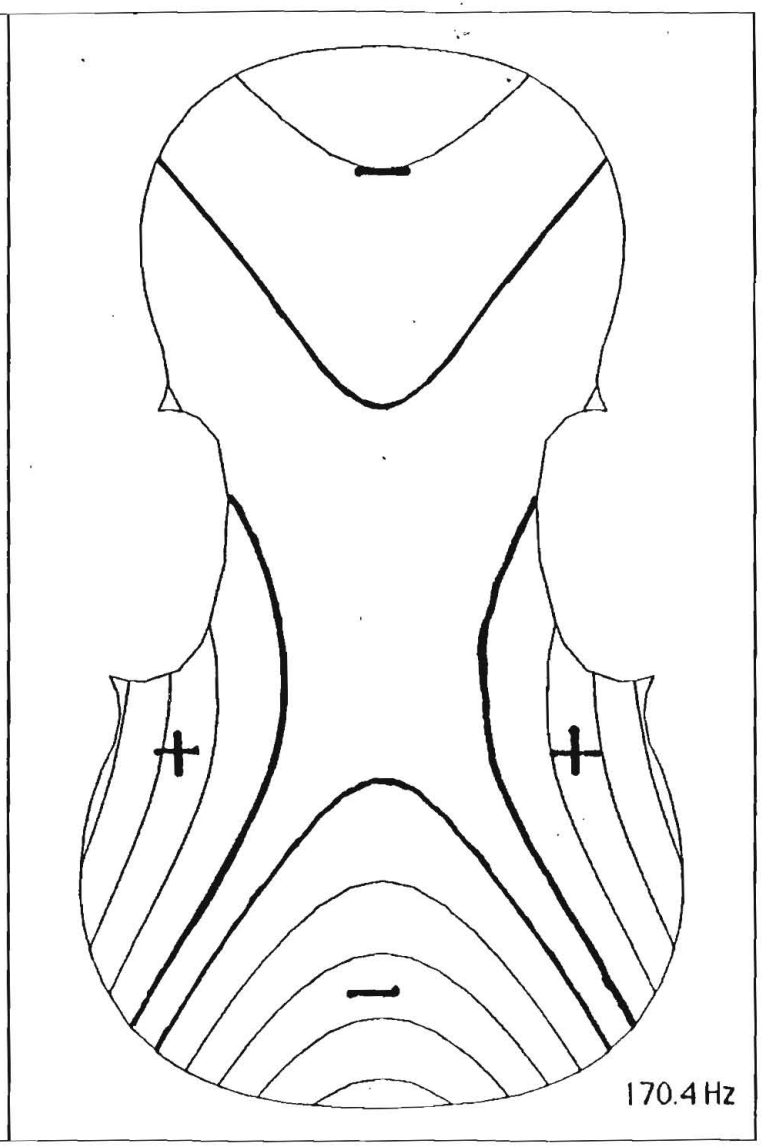

Figure B2. Mode 2

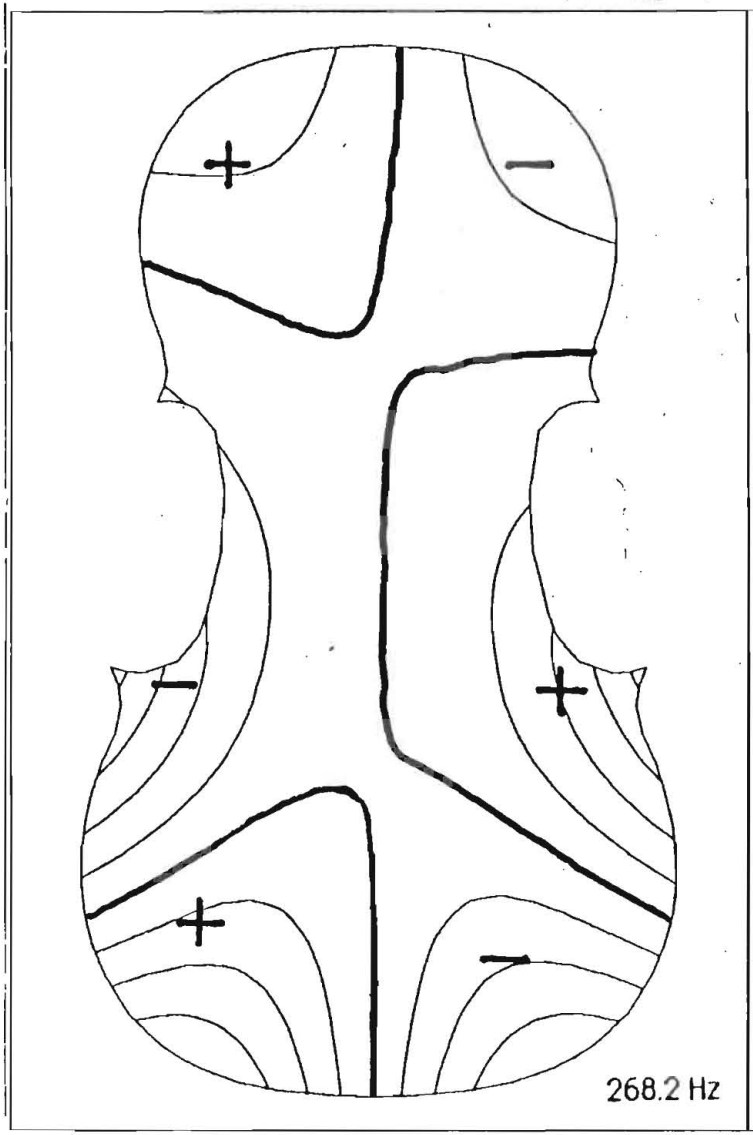

Figure B3. Mode 3

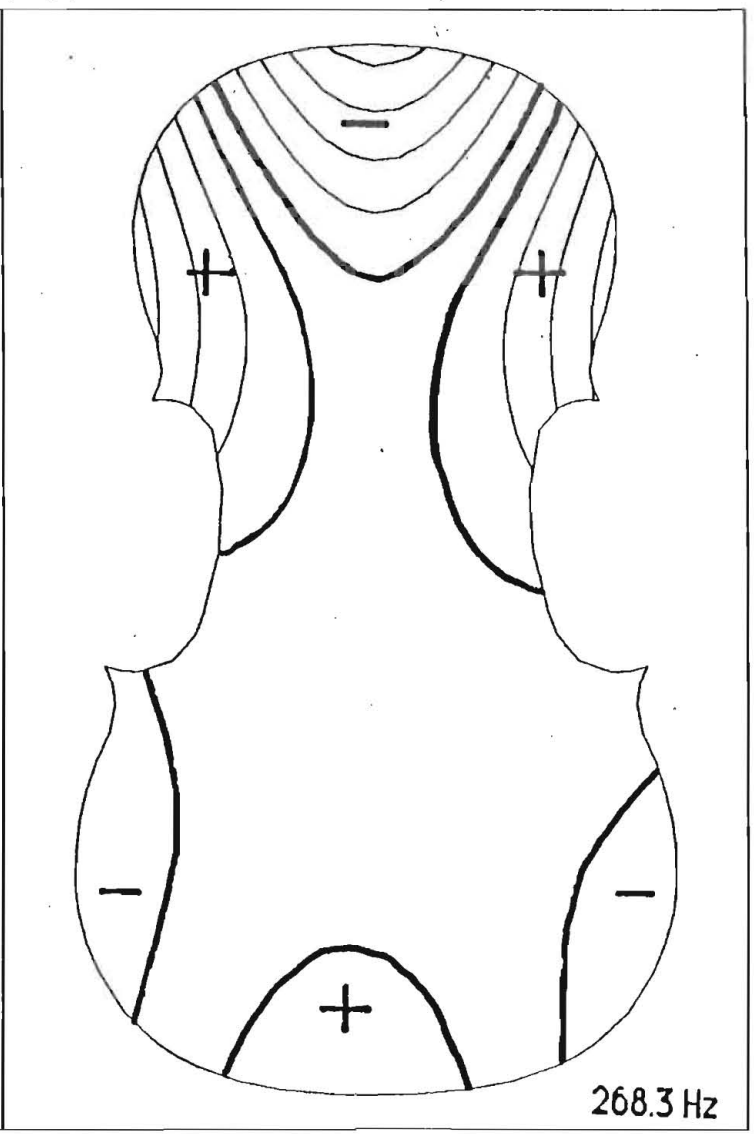

Figure B4. Mode 4

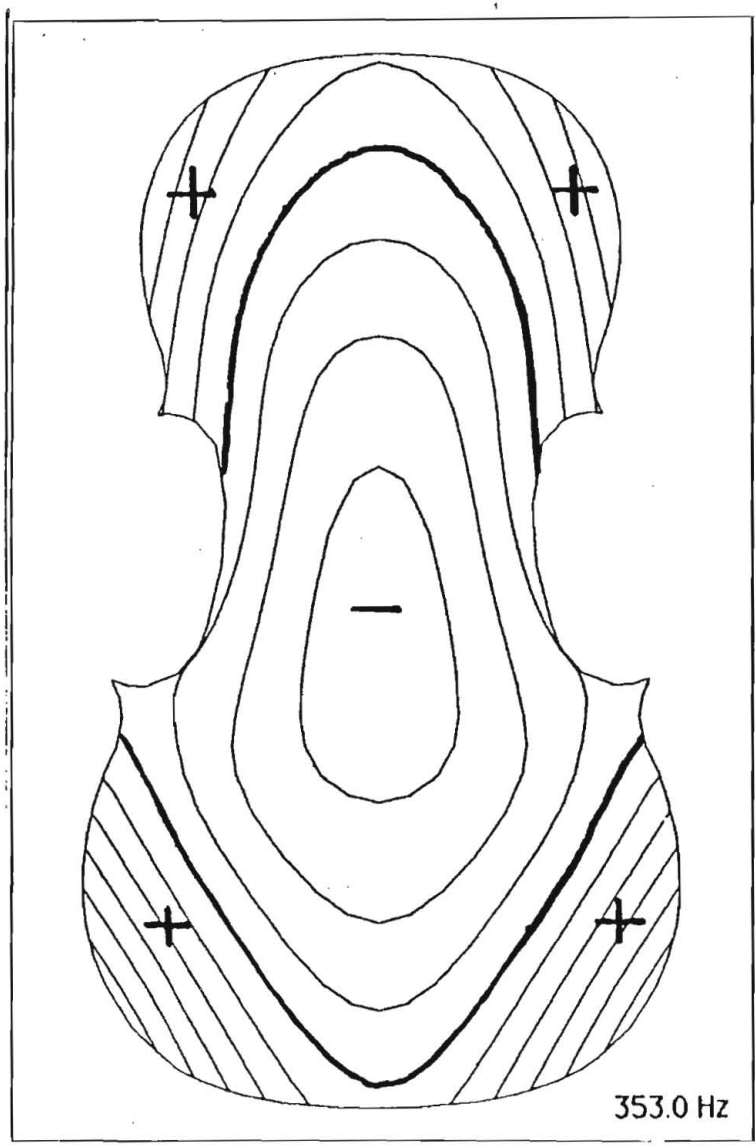

Figure B5. Mode 5

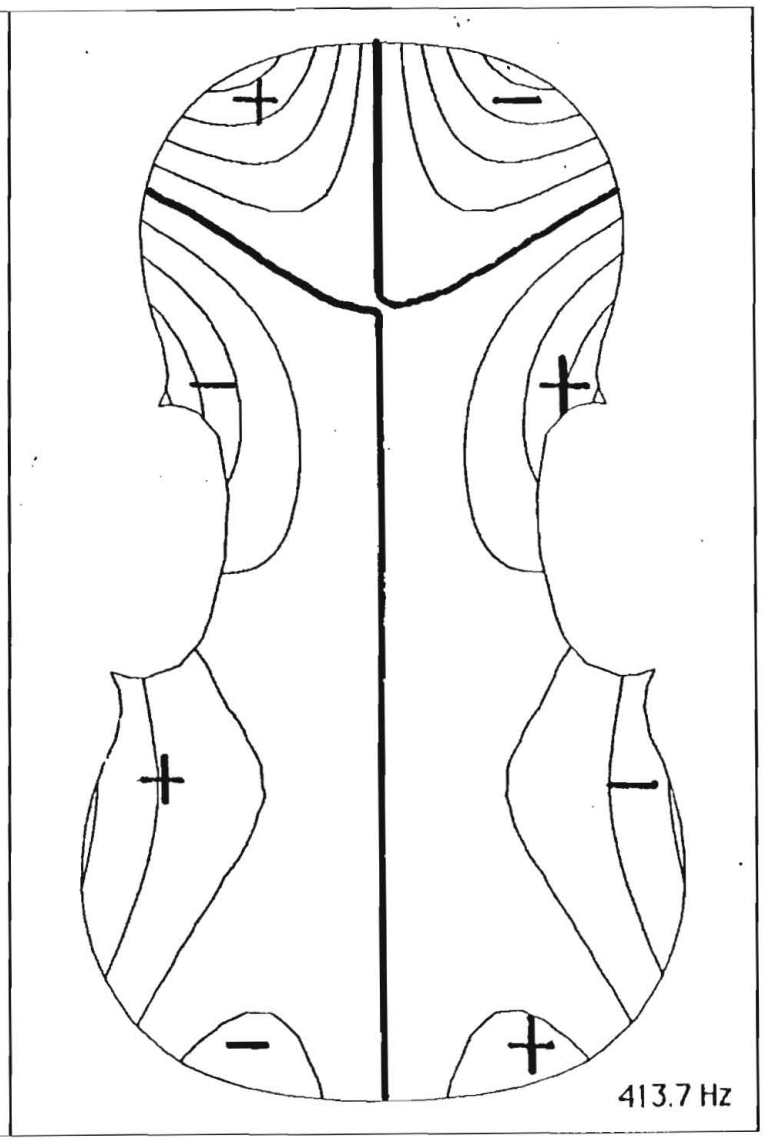

Figure B6. Mode 6

APPENDIX C

VIOLIN CORPUS MODES OF VIBRATION

The contour figures are drawn to show motion as it would appear if viewed from above the plate, with plus signs representing motion up, or towards the viewer, and minus signs representing downward motion. The back plate is seen as if the top plate was transparent.

The darker contour lines represent lines of near zero motion.

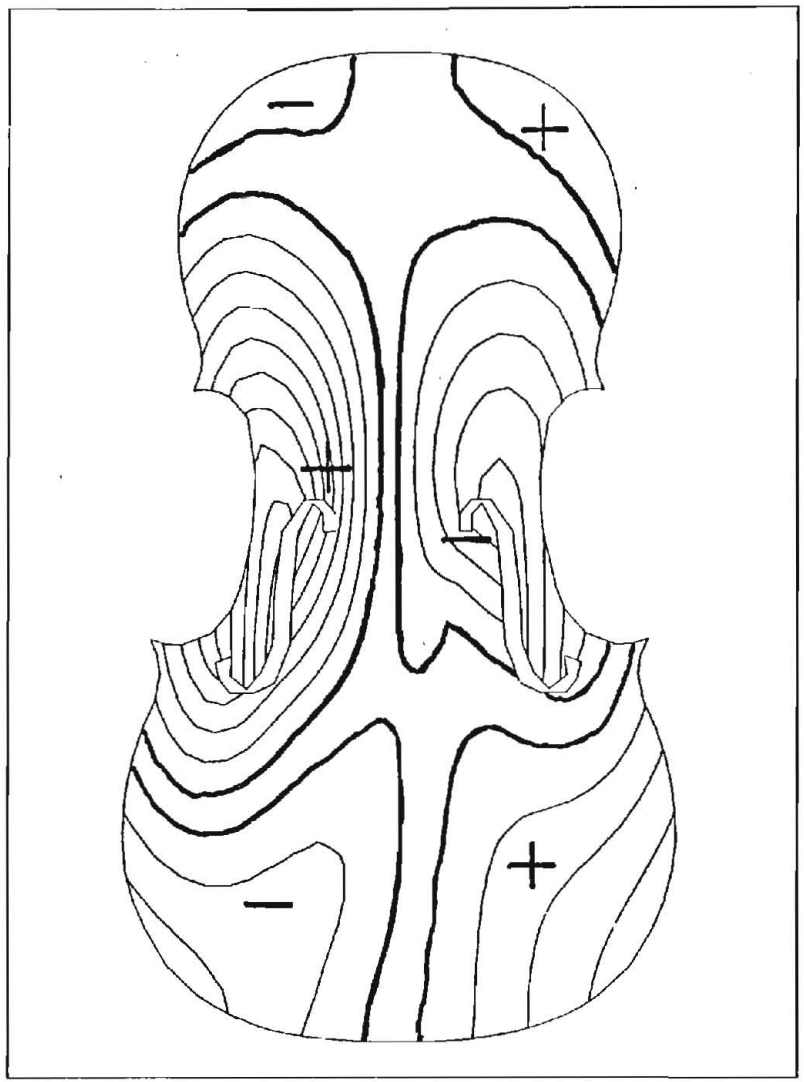

Figure C1. Mode 1 - top

462.9 Hz

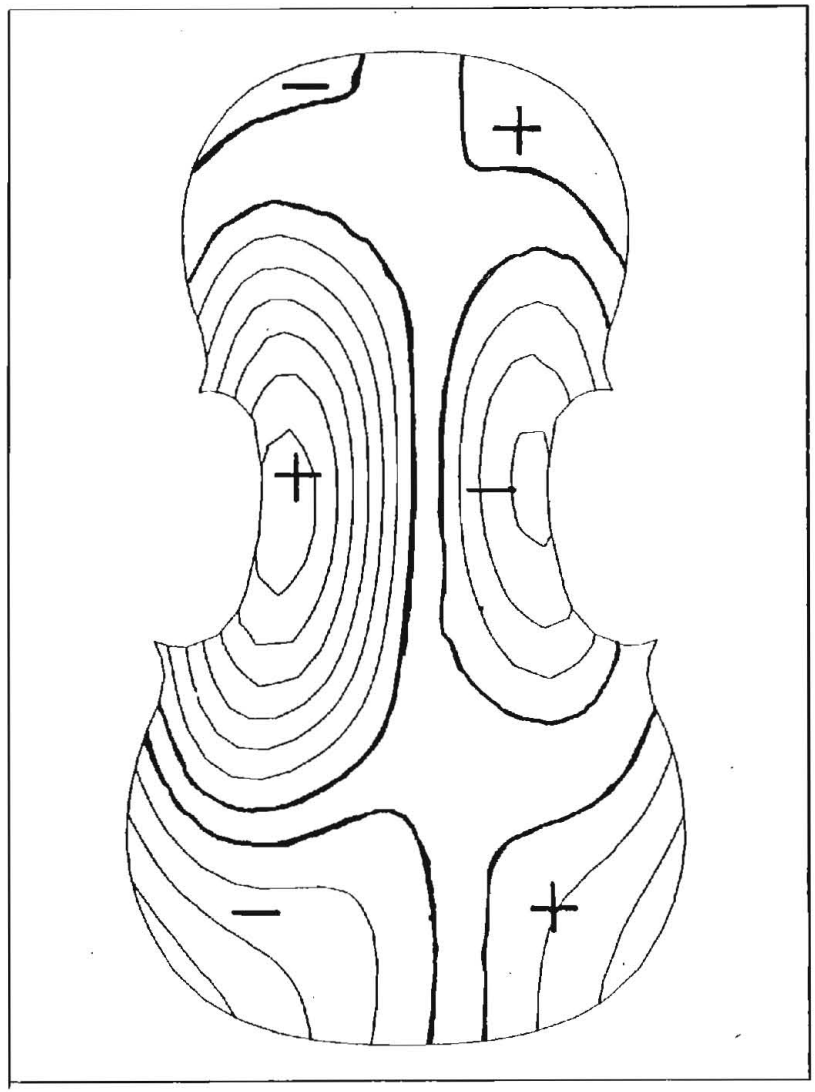

Figure C2. Mode 1 - back

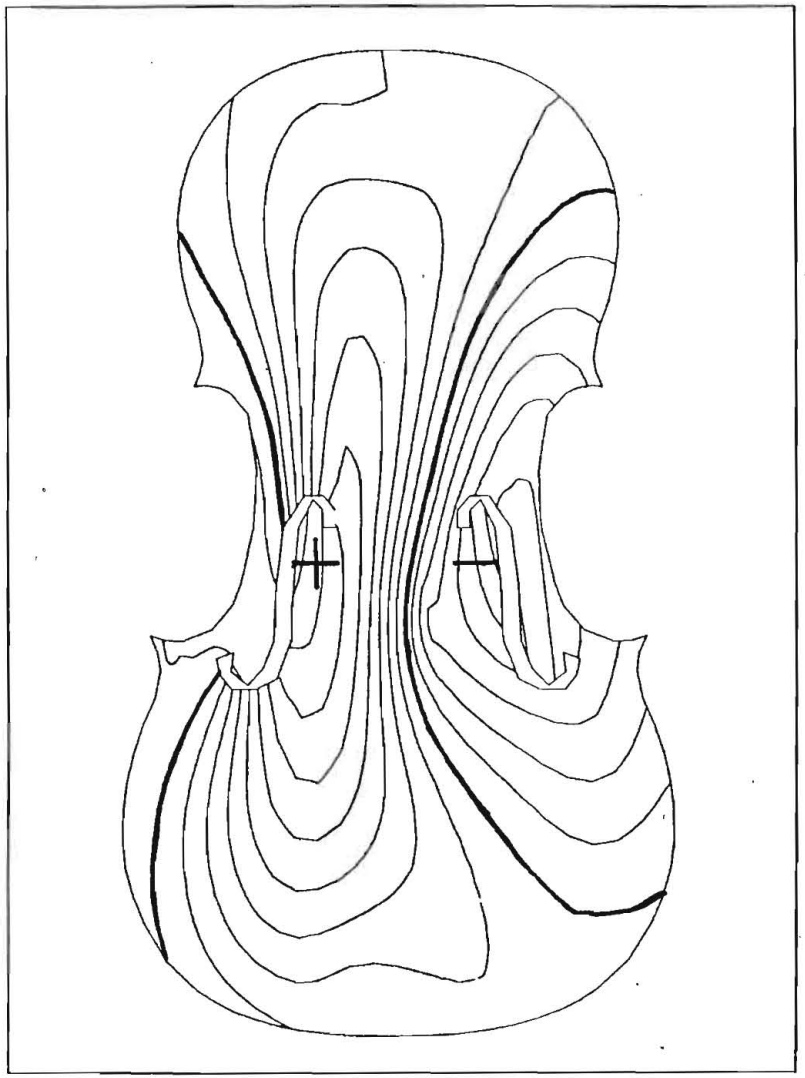

Figure C3. Mode 2 - top

478.9 Hz

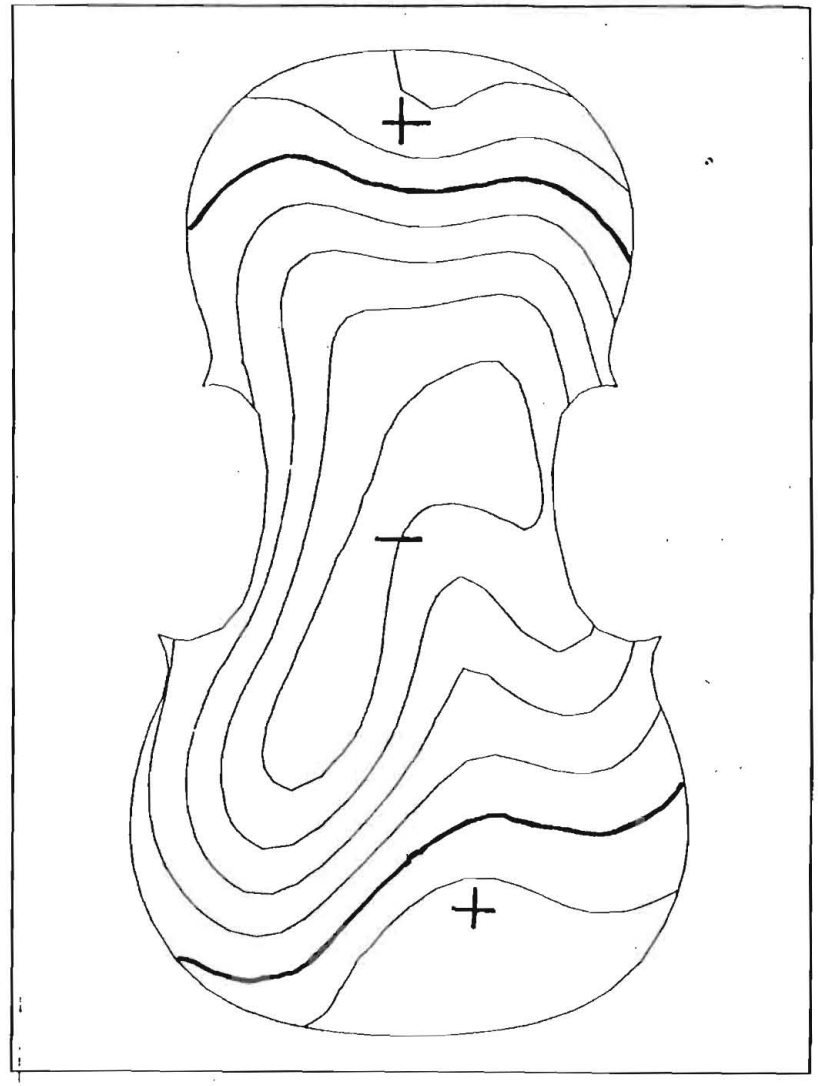

Figure C4. Mode 2 - back

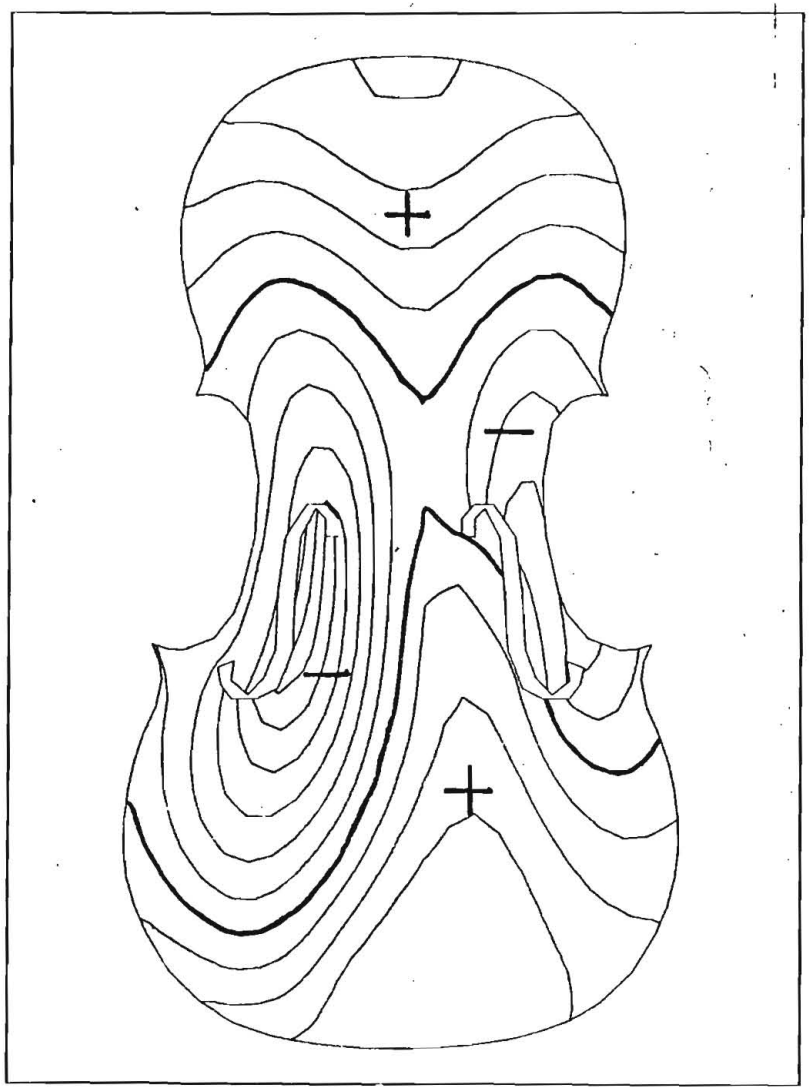

Figure C5. Mode 3 - top

573.9 Hz

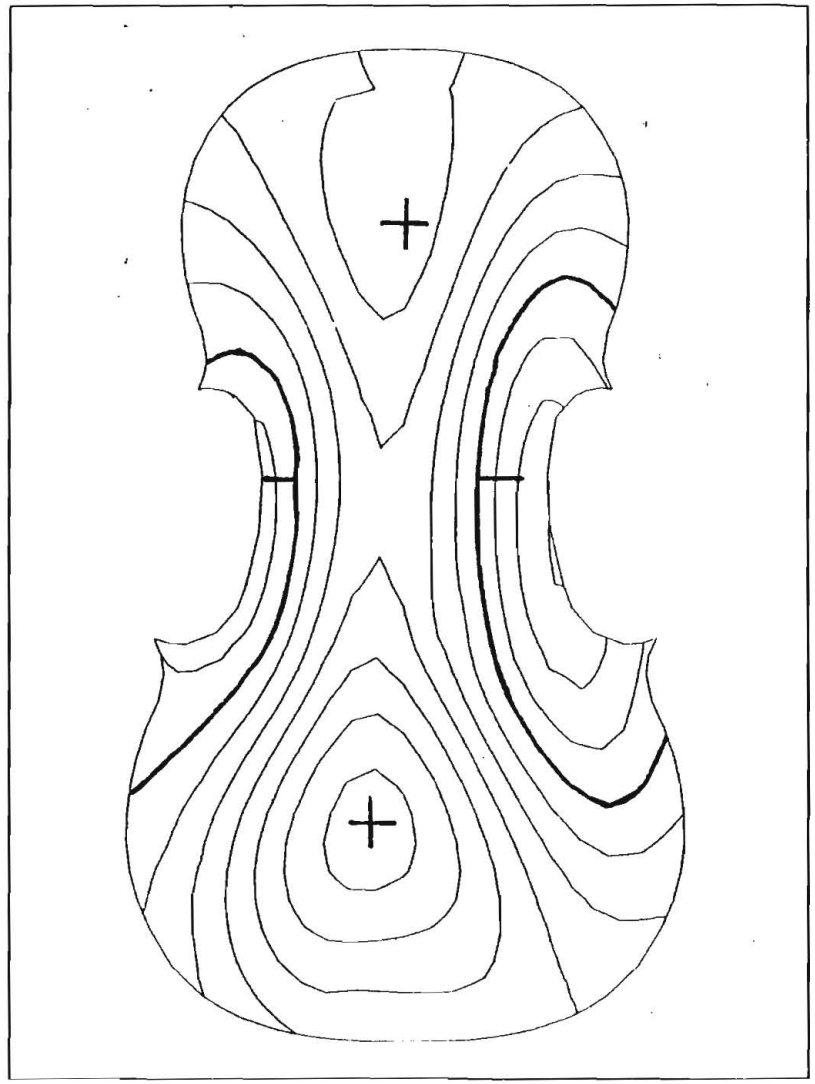

Figure C6. Mode 3 - back

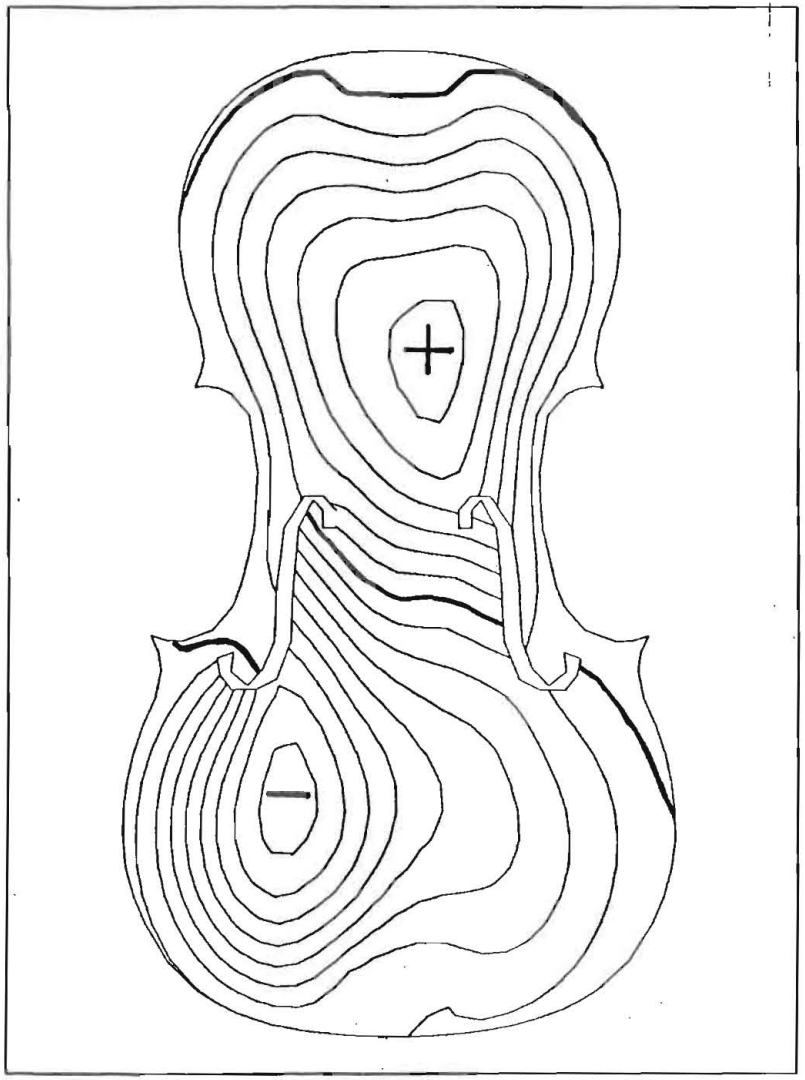

Figure C7. Mode 4 - top

682.5 Hz

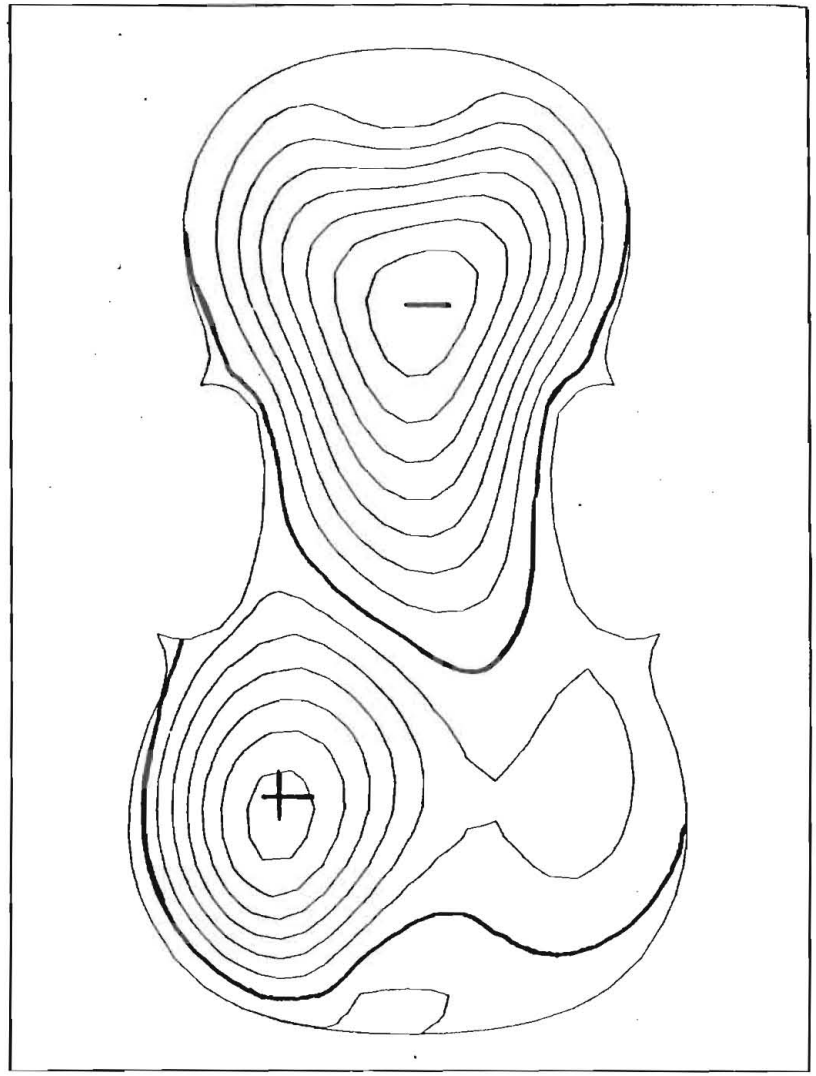

Figure C8. Mode 4 - back

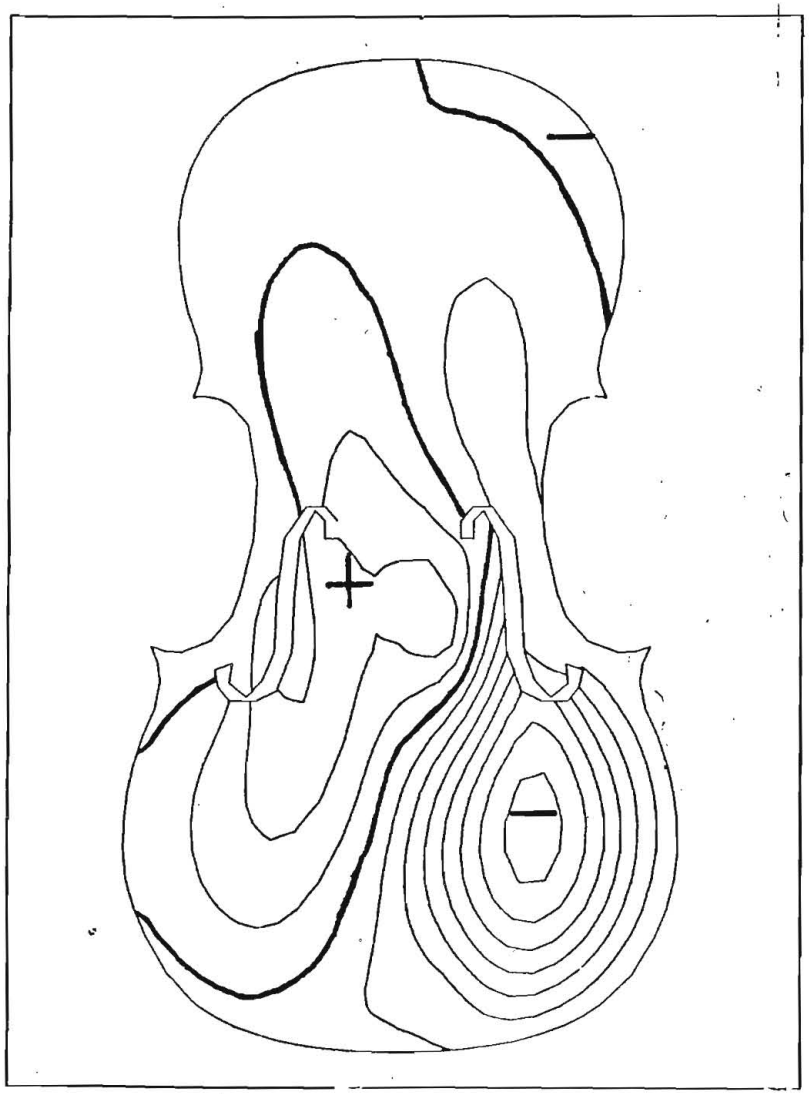

Figure C9. Mode 5 - top

736.2 Hz

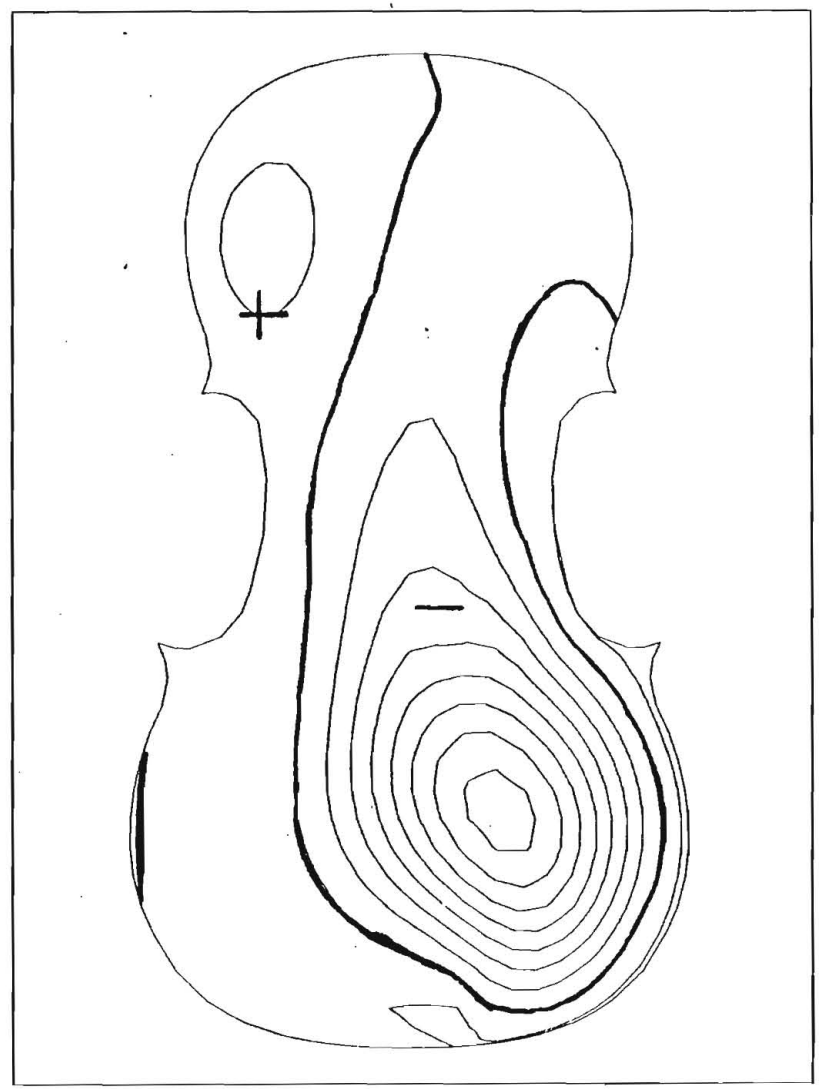

Figure C10. Mode 5 - back

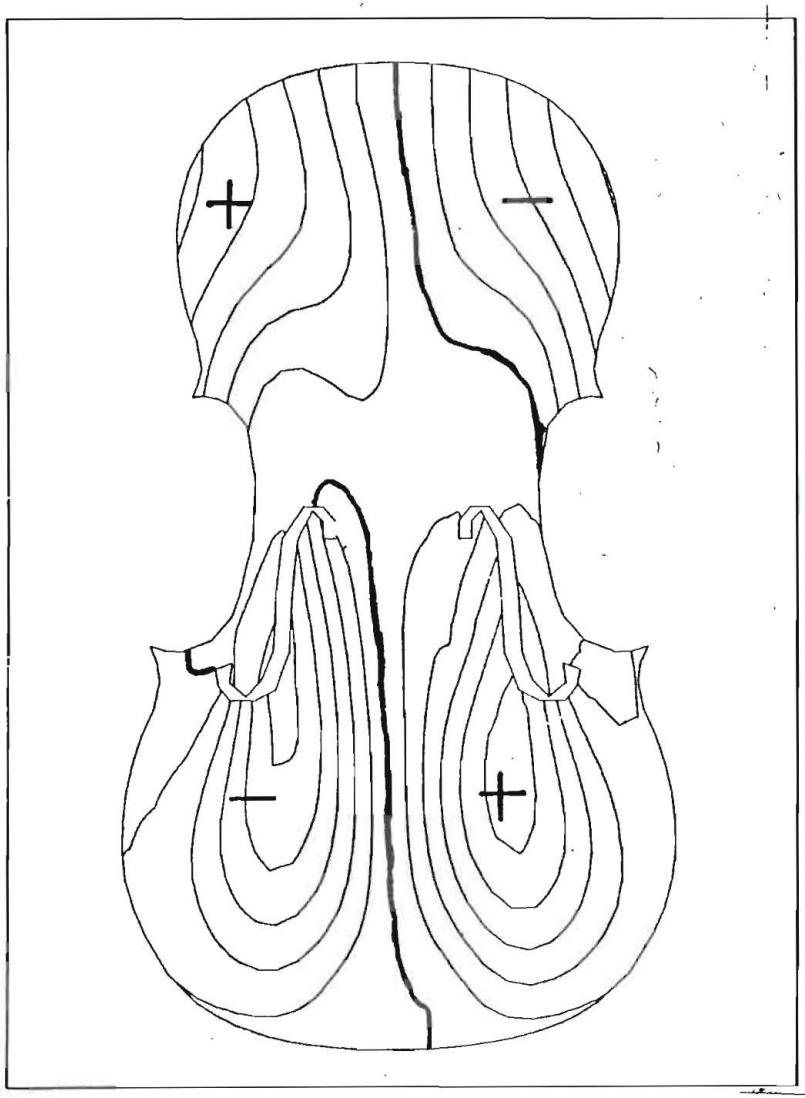

Figure C11. Mode 6 - top

749.6 Hz

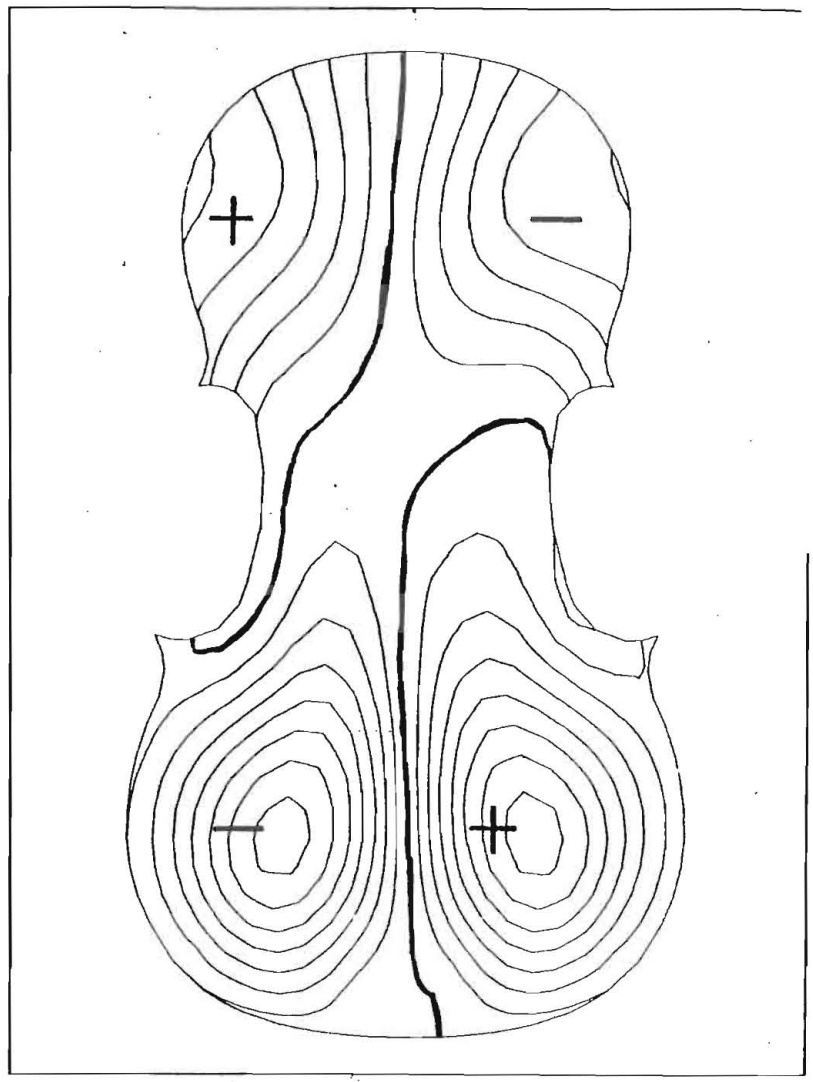

Figure C12. Mode 6 - back

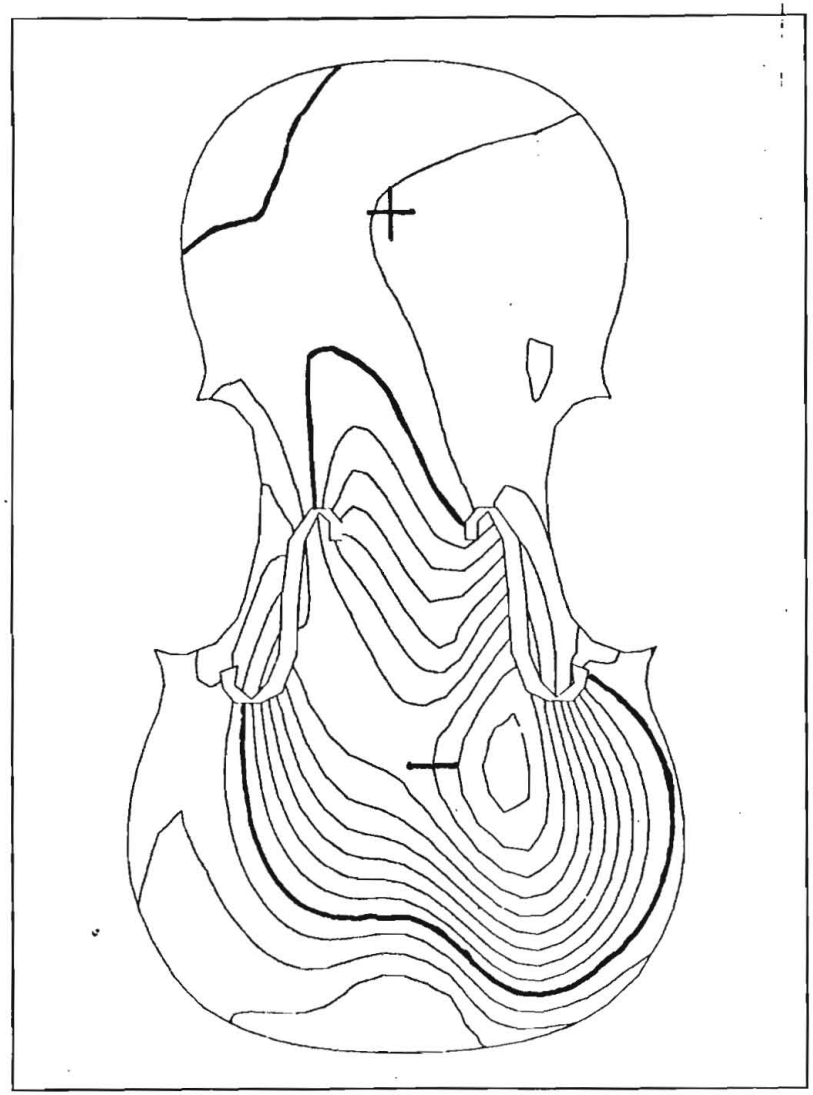

Figure C13. Mode 7 - top

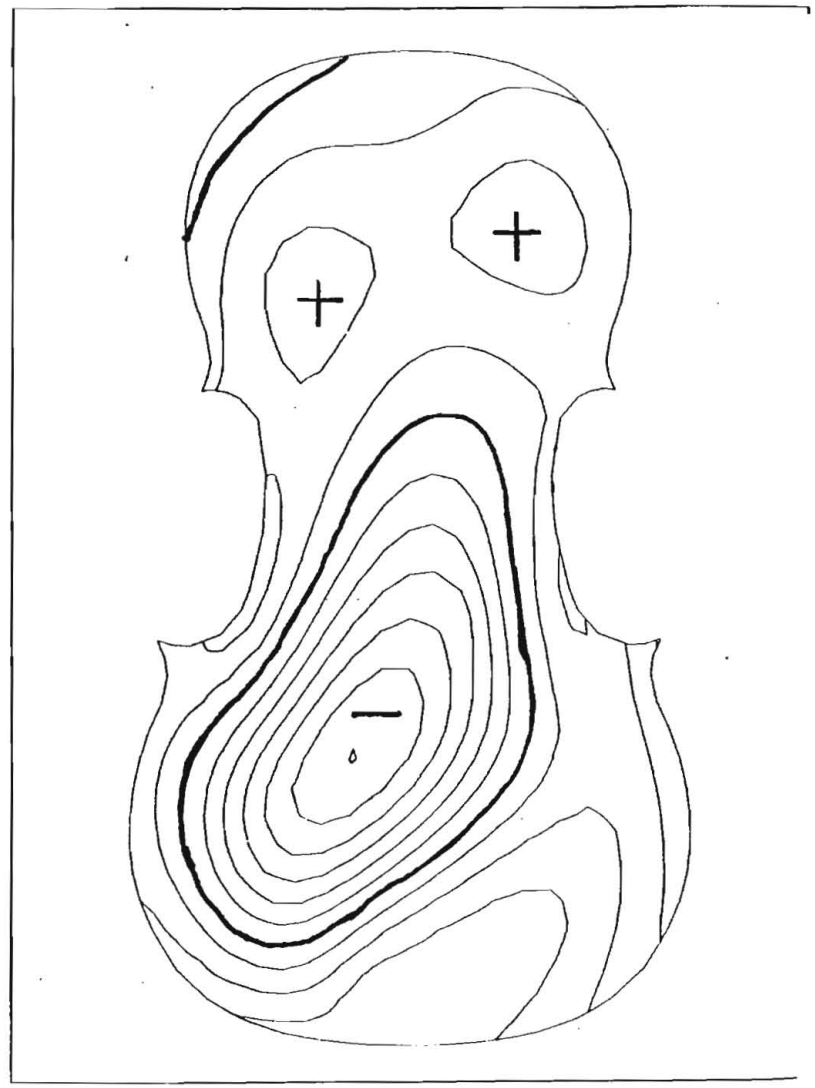

Figure C14. Mode 7 - back

810.9 Hz

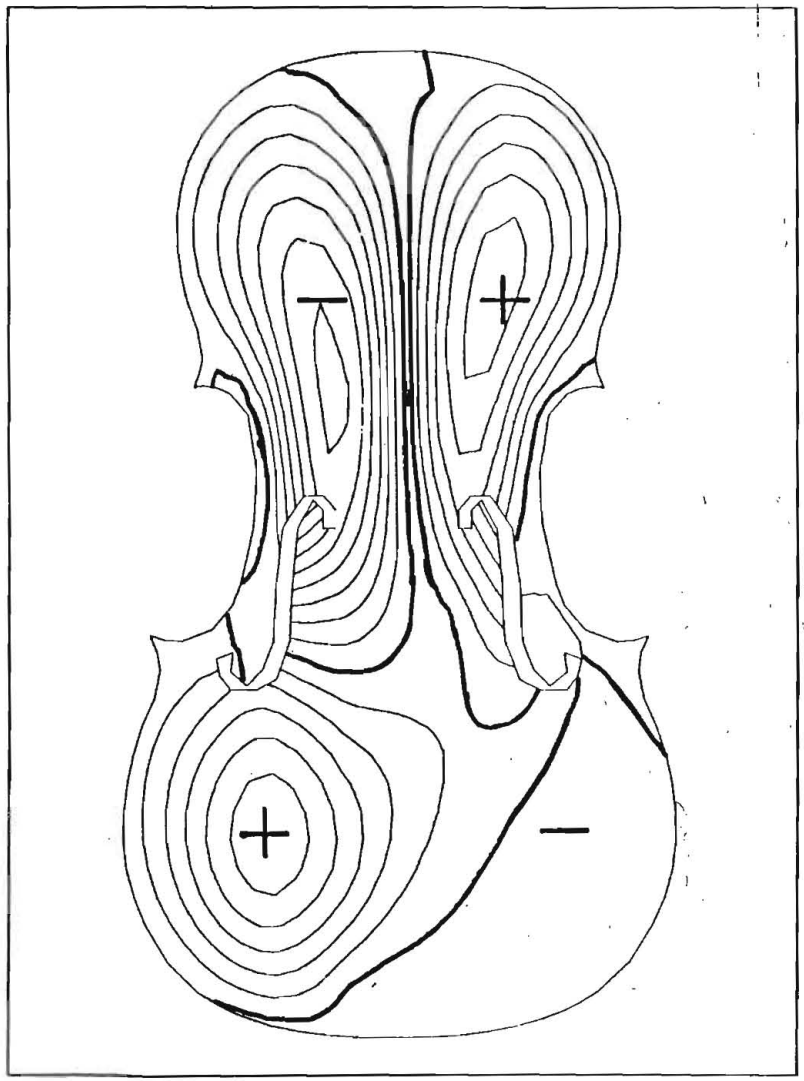

Figure C15. Mode 8 - top

899.1 Hz

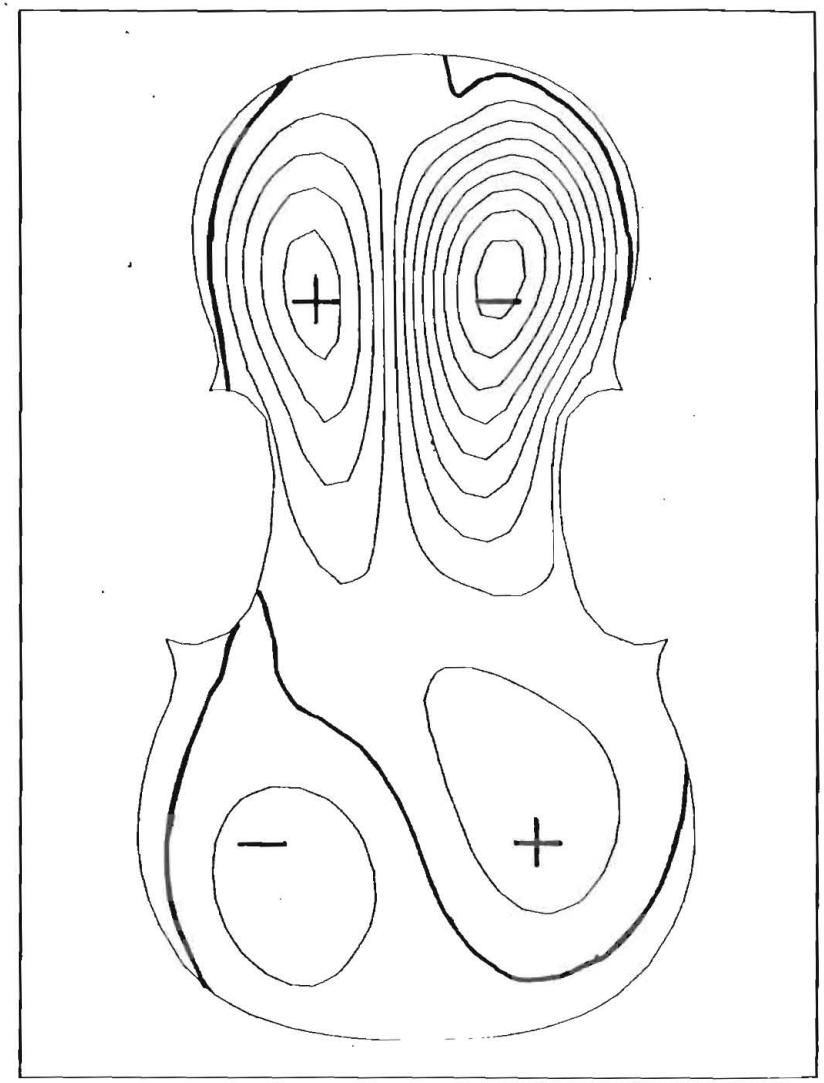

Figure C16. Mode 8 - back

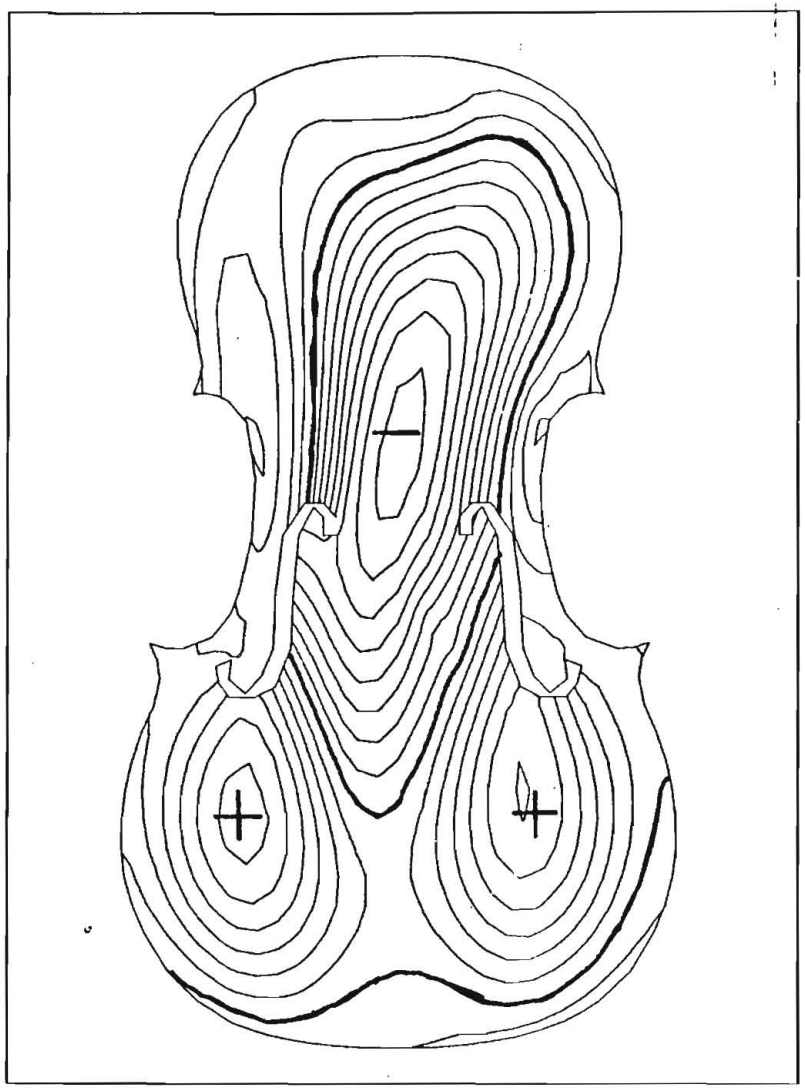

Figure C17. Mode 9 - top

968.5 Hz

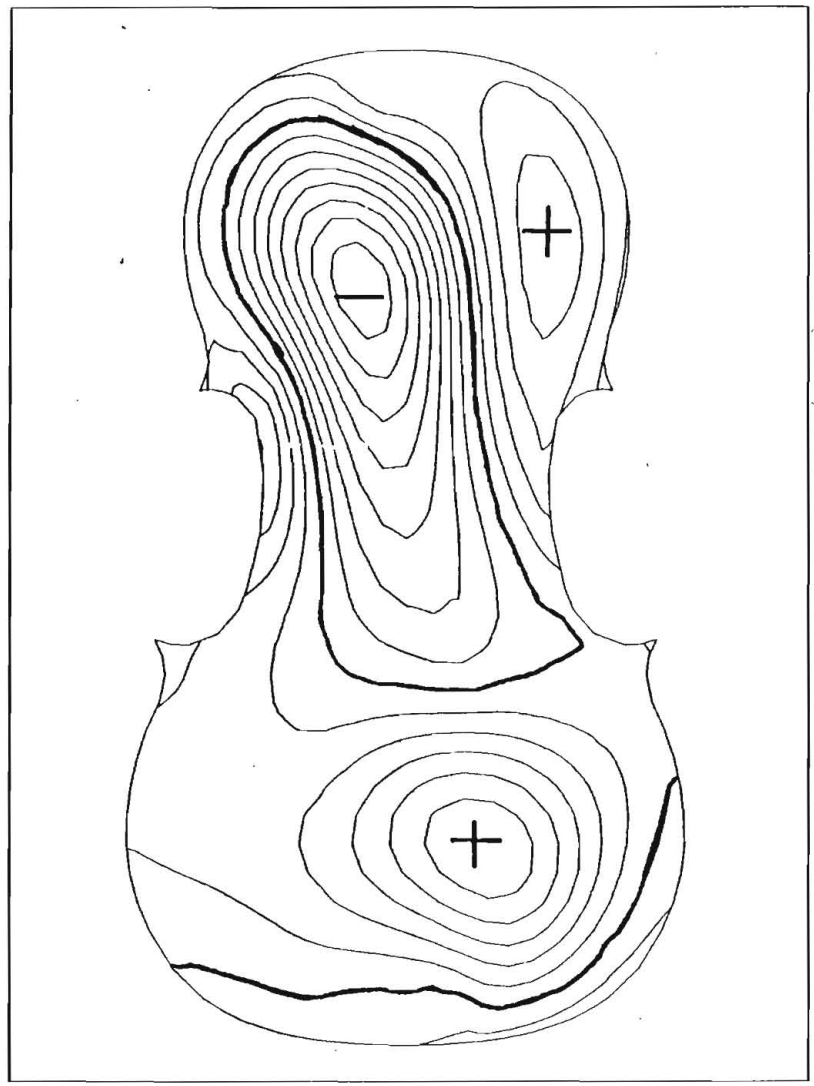

Figure C18. Mode 9 - back

APPENDIX D

COMPLETE VIOLIN MODES OF VIBRATION

Most of the figures in this appendix are in groups of four figures per mode. The first plot is of the deformed mesh as it would appear to the viewer looking at the top, or belly of the violin. The second plot is a contour diagram of the top plate viewed from above the instrument. The third plot is of the deformed mesh as it would appear to the viewer looking towards the back of the instrument, from below the violin. The fourth plot is a contour diagram of the back plate viewed from above the instrument as if the top plate was transparent.

For the contour figures plus signs represent motion up, or towards the viewer, and minus signs represent downward motion.

The neck, bridge and strings are not shown in the contour figures for purposes of clarity.

The darker contour lines represent lines of near zero motion.

The strings are not shown in the deformed mesh plots for purposes of clarity.

For the string mode deformed plots, the rest of the finite element model is not shown.

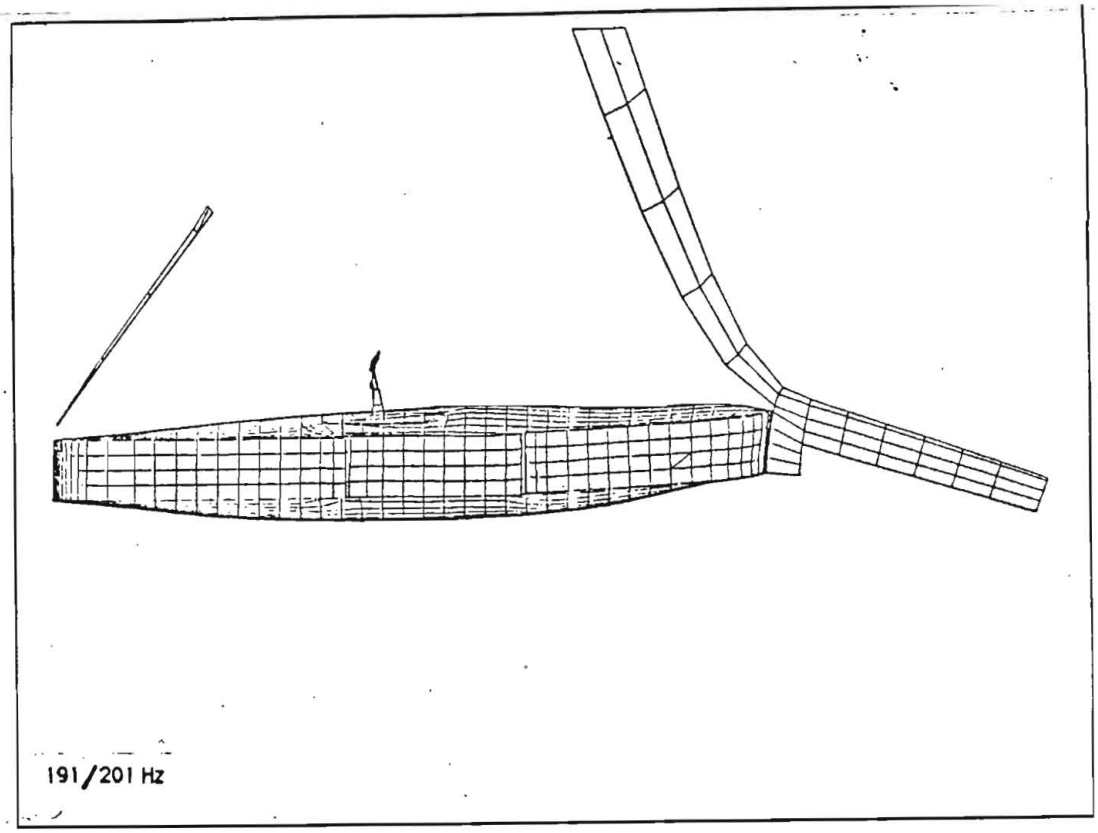

Figure D1. Modes 1/2

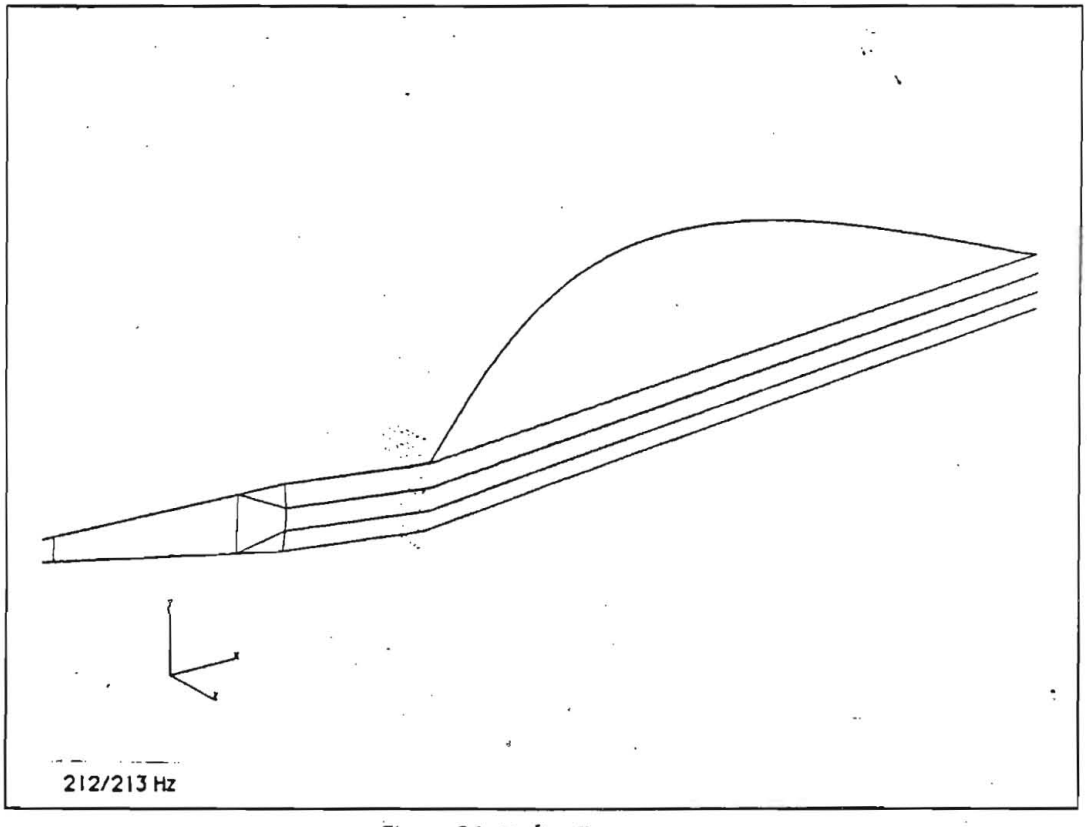

Figure D2. Modes 3/4

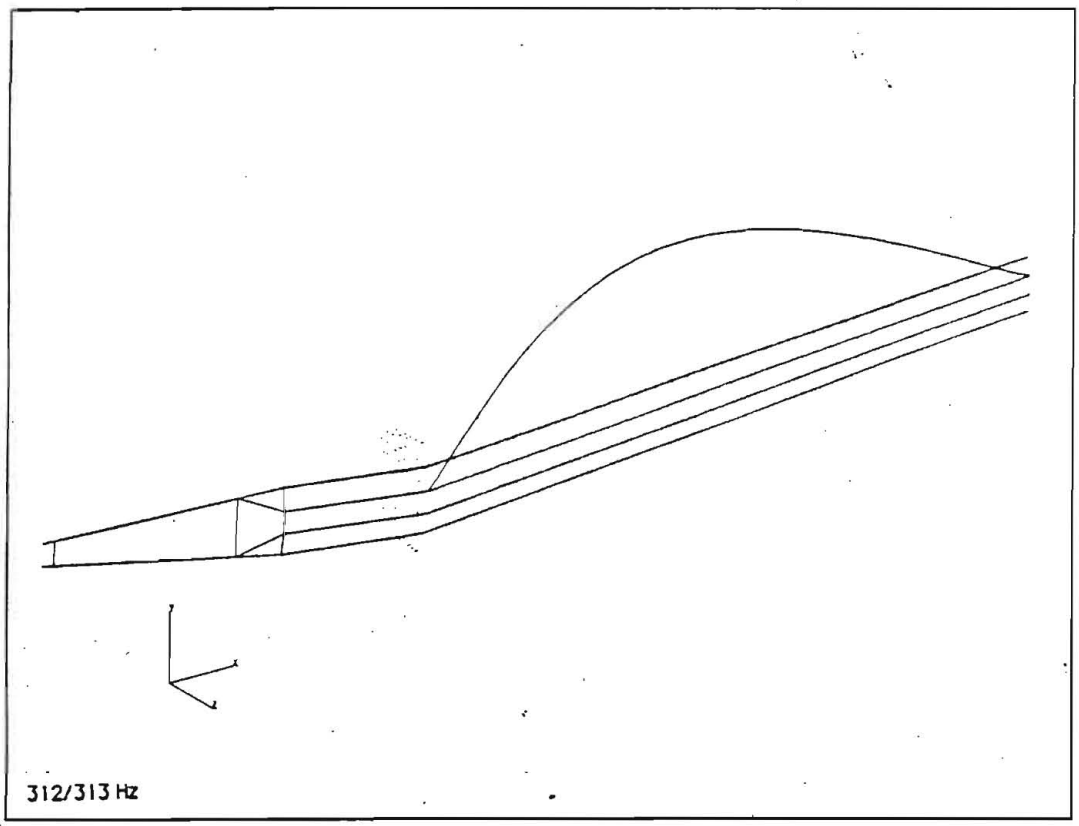

Figure D3. Modes 5/6

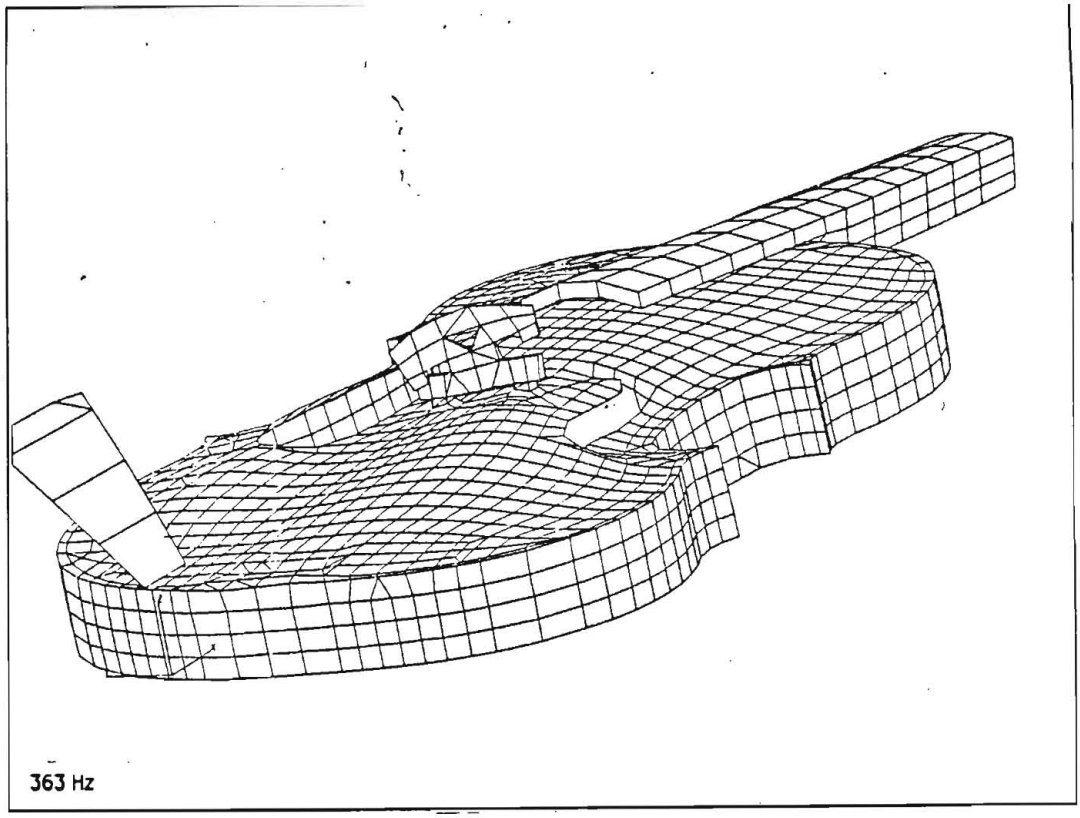

Figure D4. Mode 7

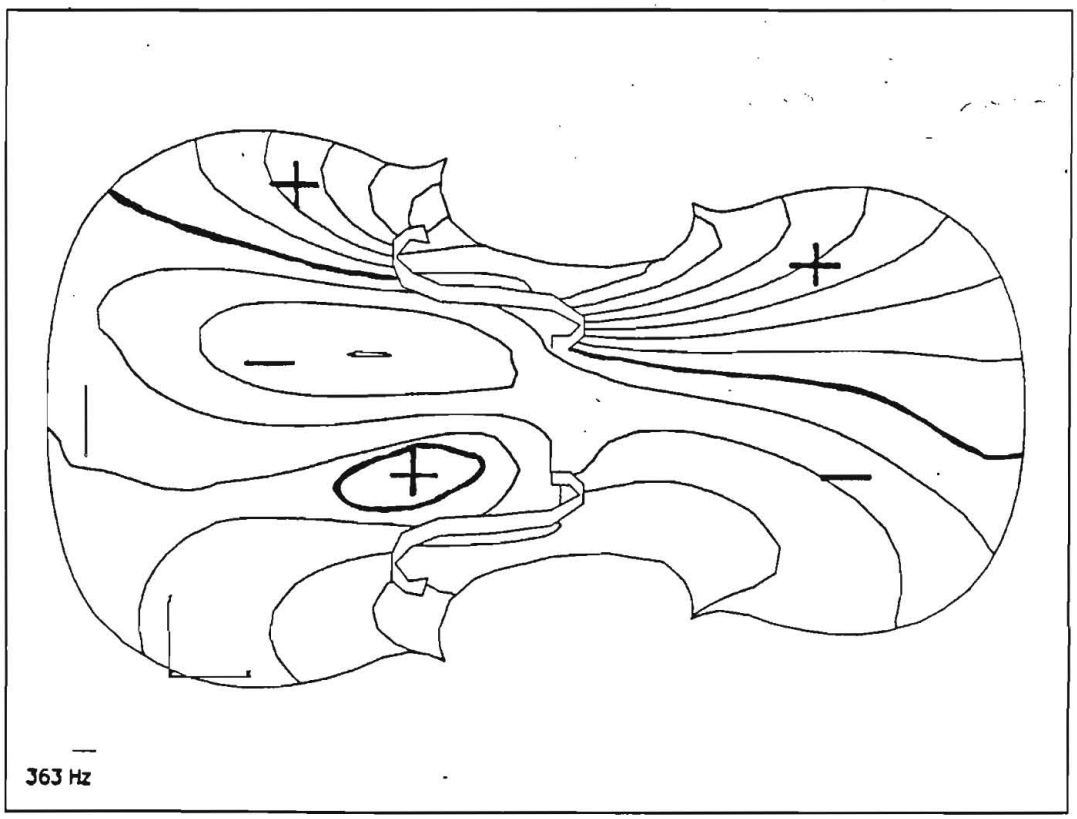

Figure D5. Mode 7 - top

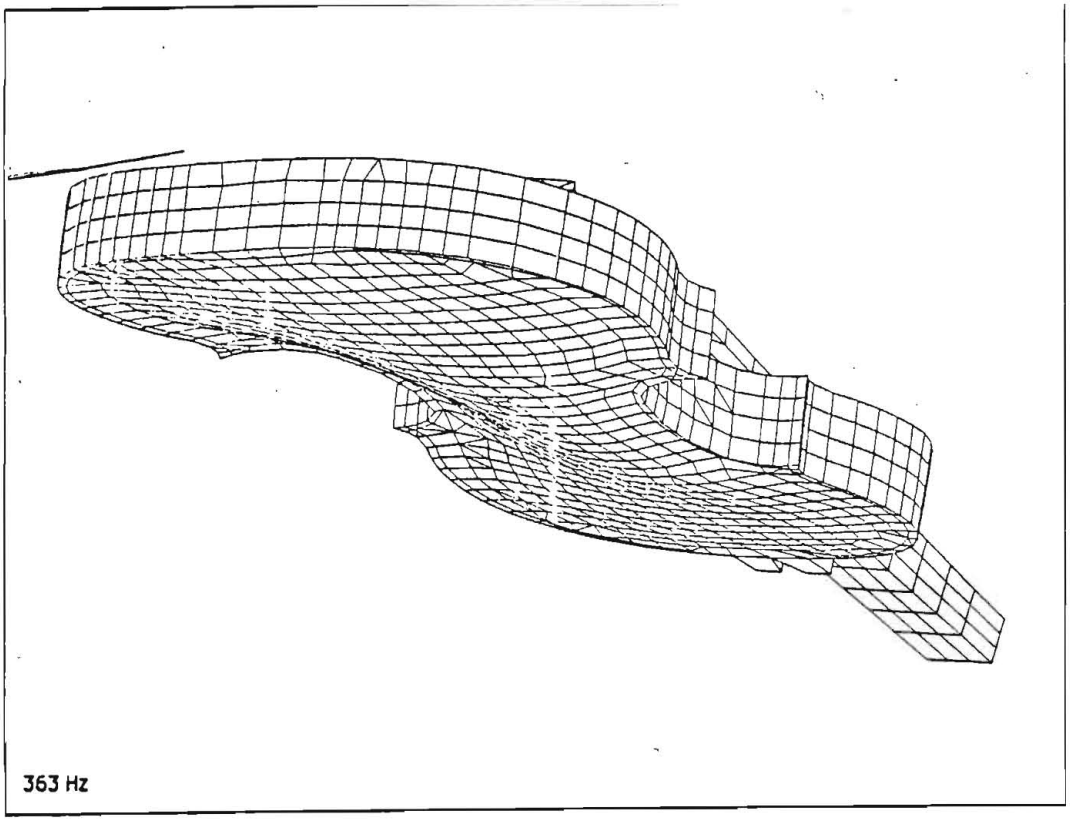

Figure D6. Mode 7

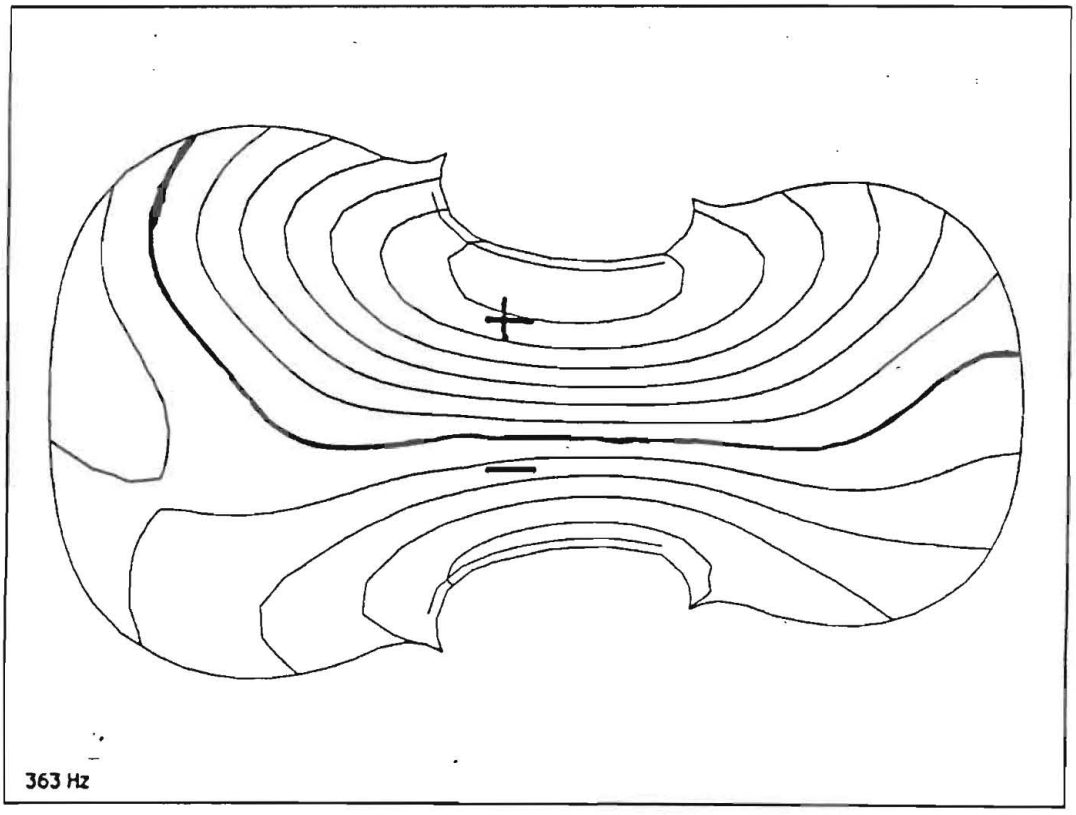

Figure D7. Mode 7 - back

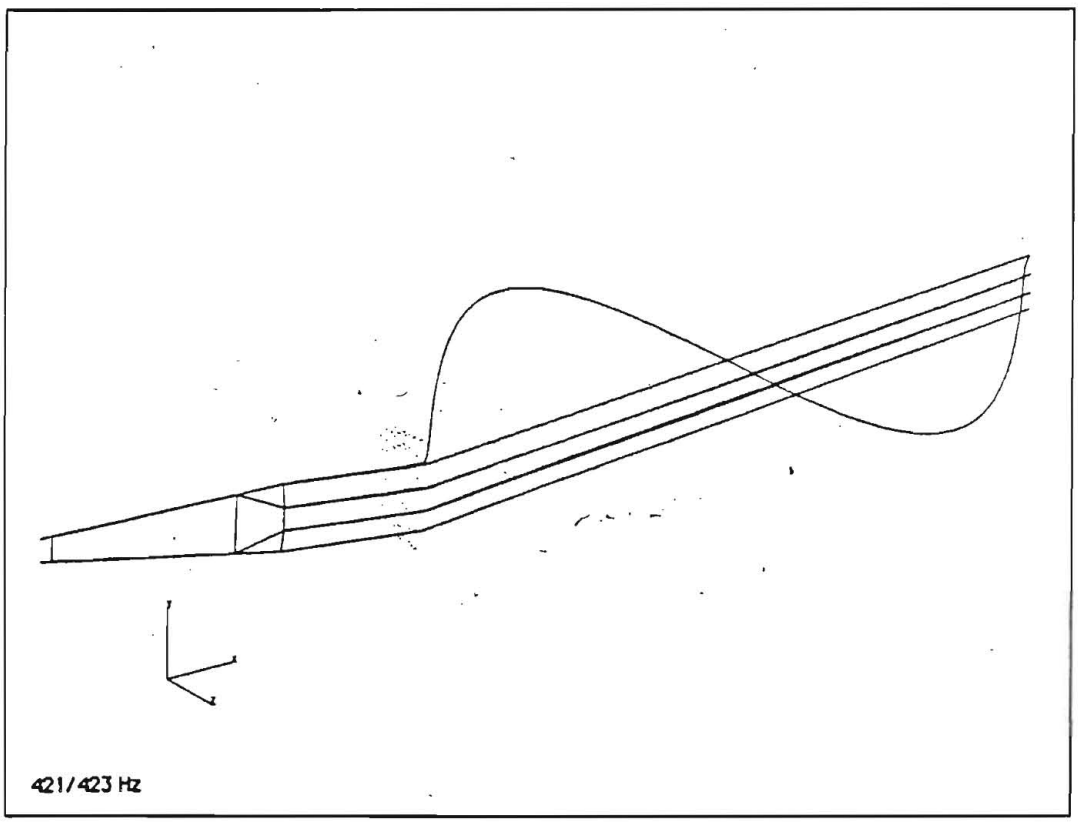

Figure D8. Modes 8/9

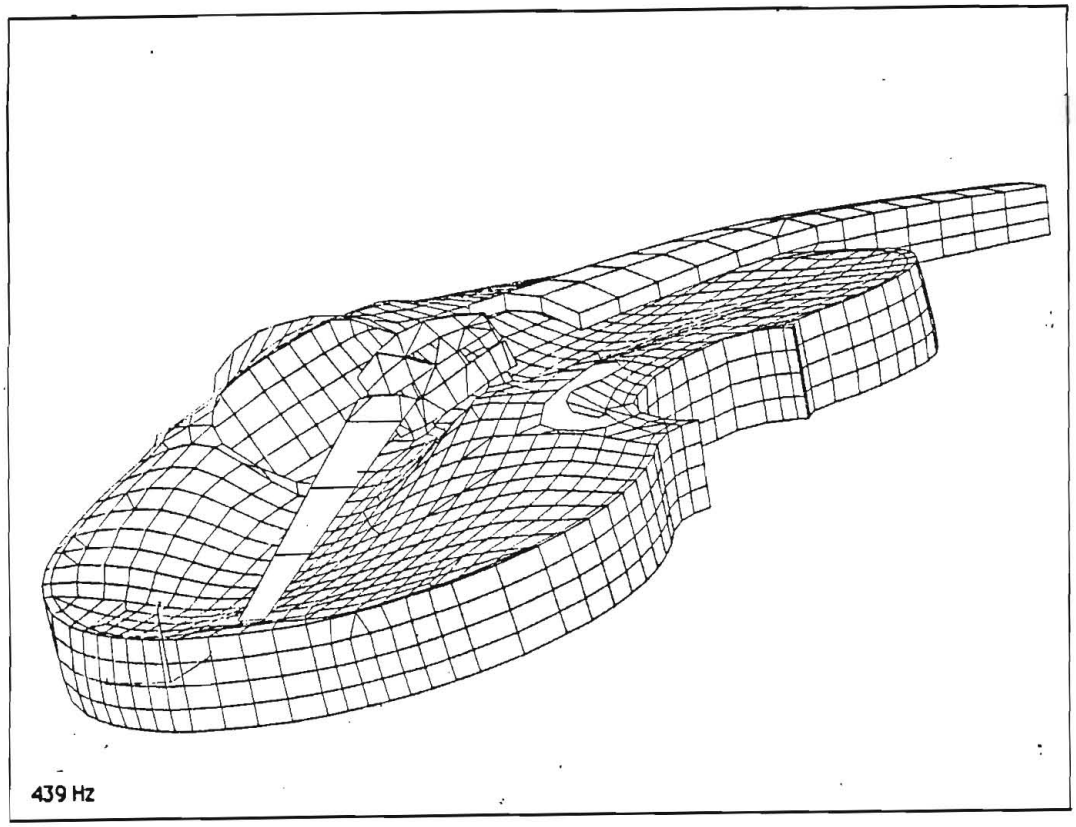

Figure D9. Mode 10

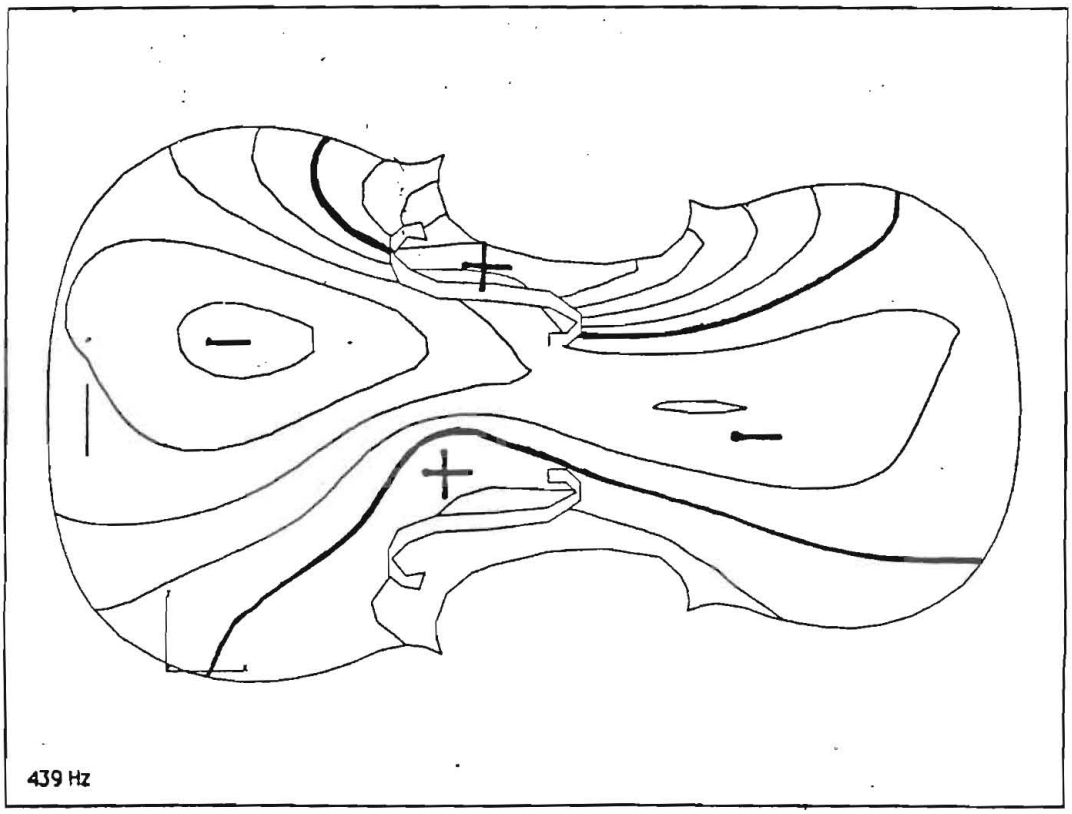

Figure D10. Mode 10 -top

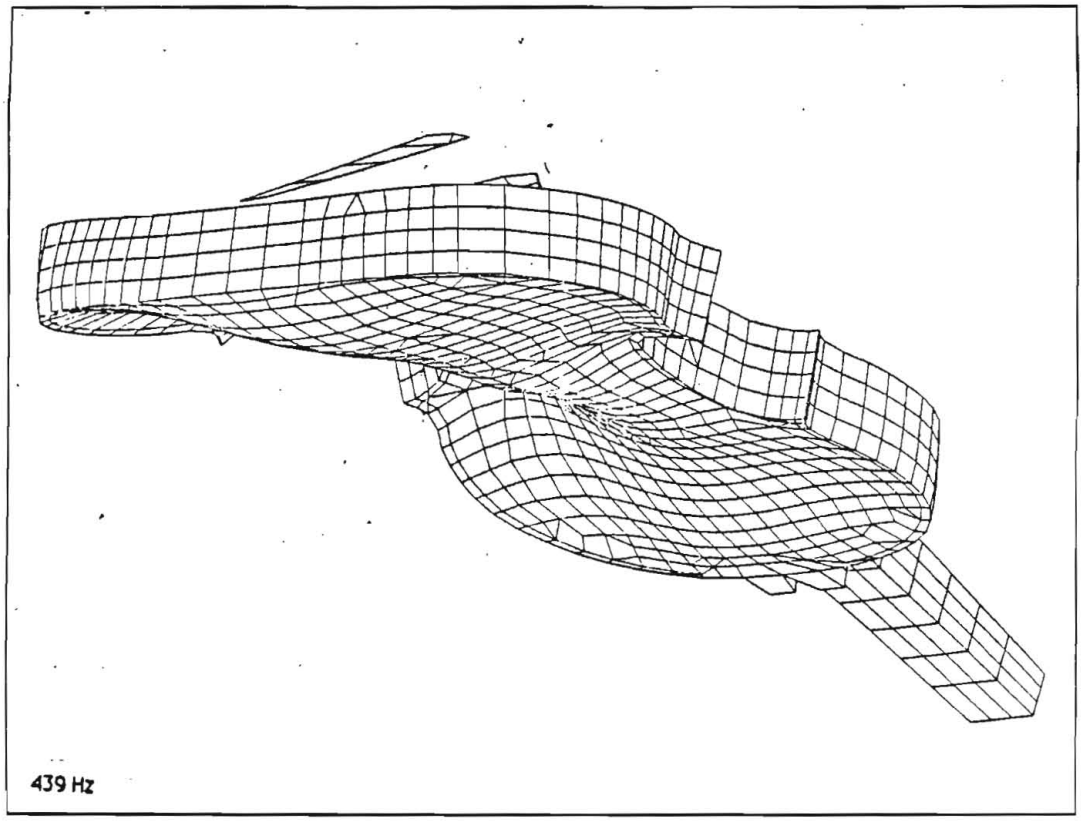

Figure D11. Mode 10

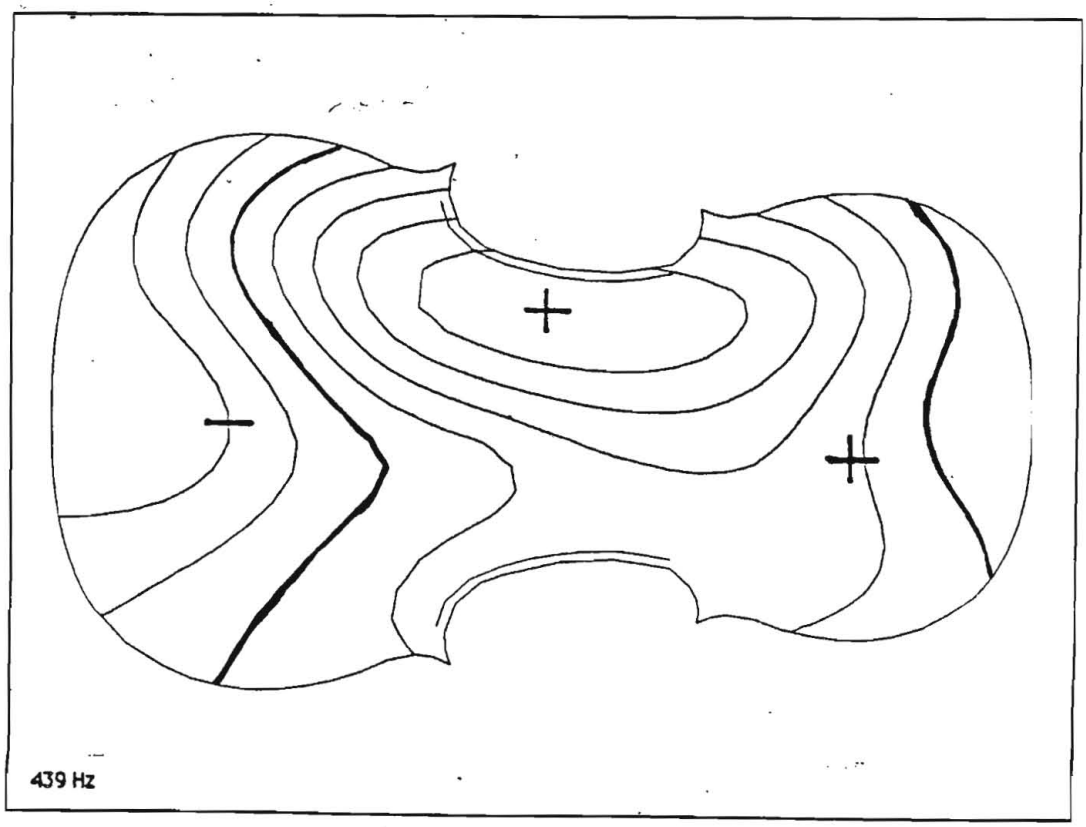

Figure D12. Mode 10 - back

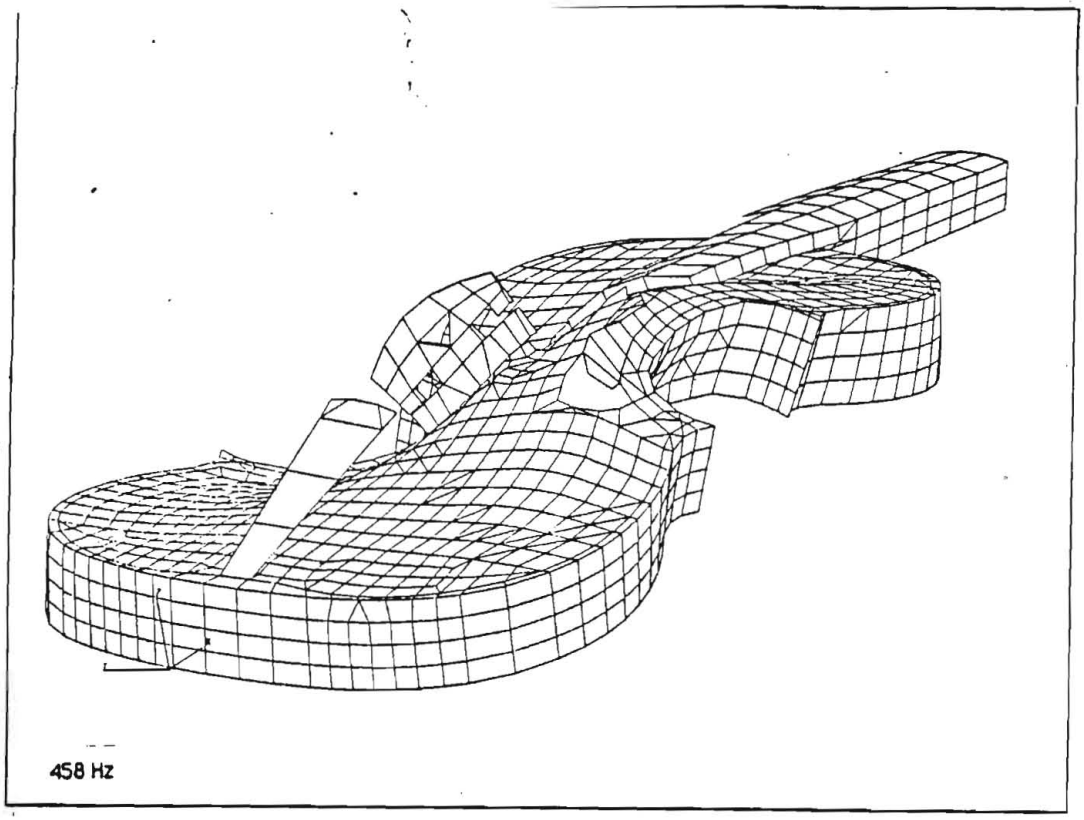

Figure D13. Mode 11

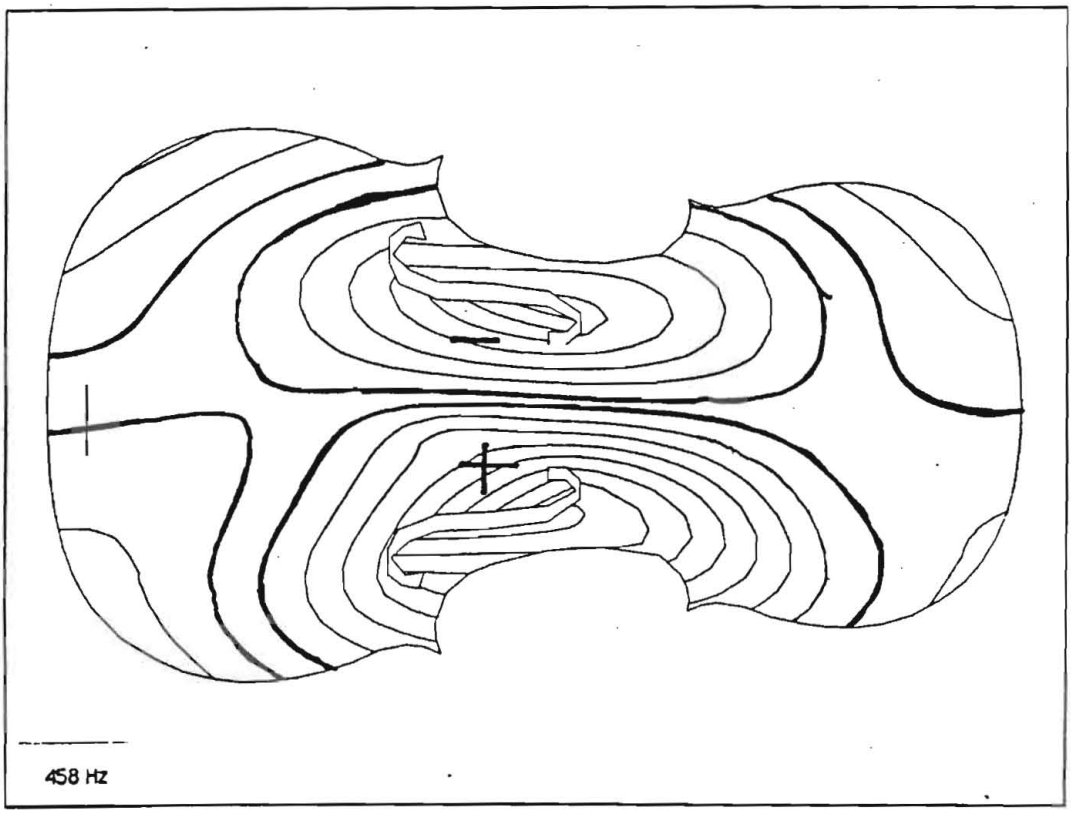

Figure D14. Mode 11 - top

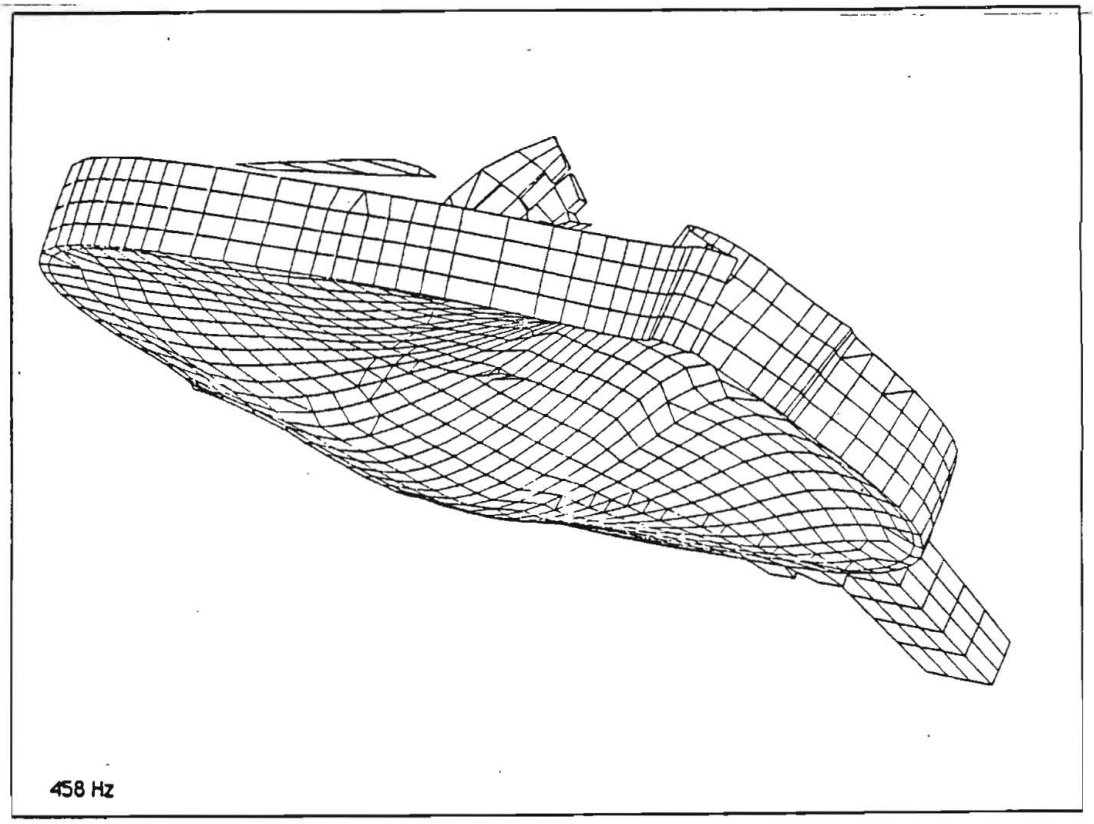

Figure D15. Mode 11

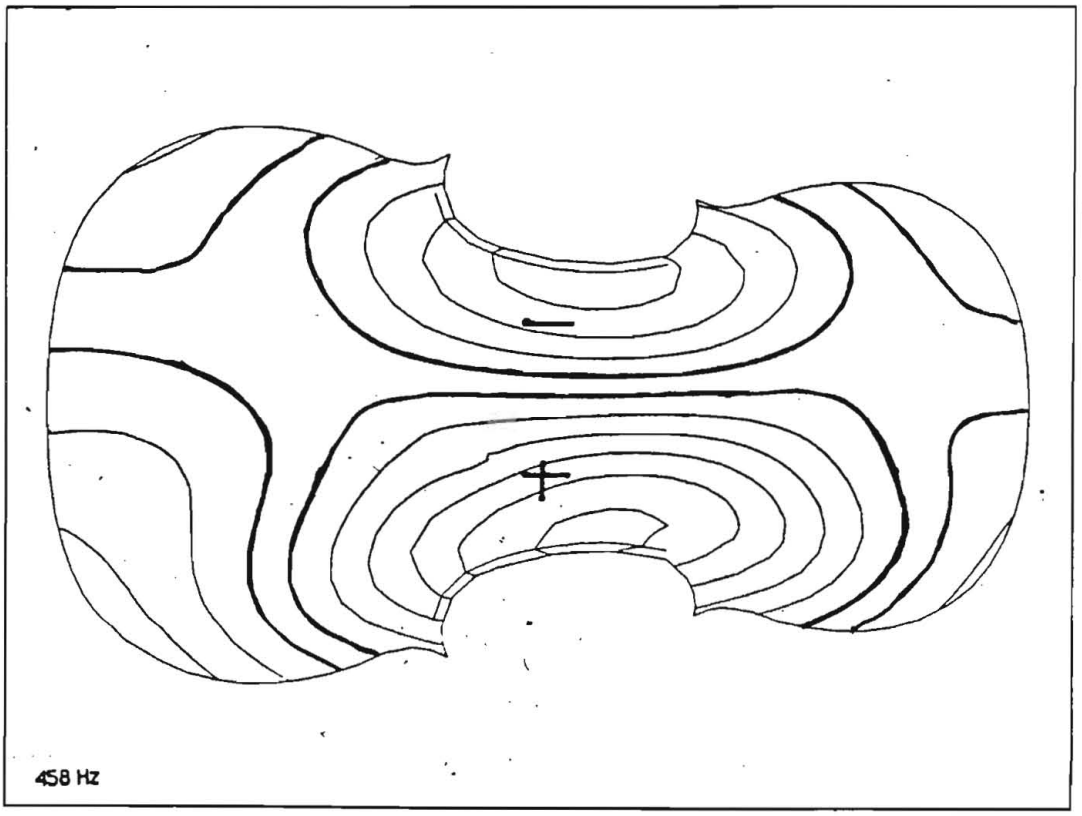

Figure D16. Mode 11 - back

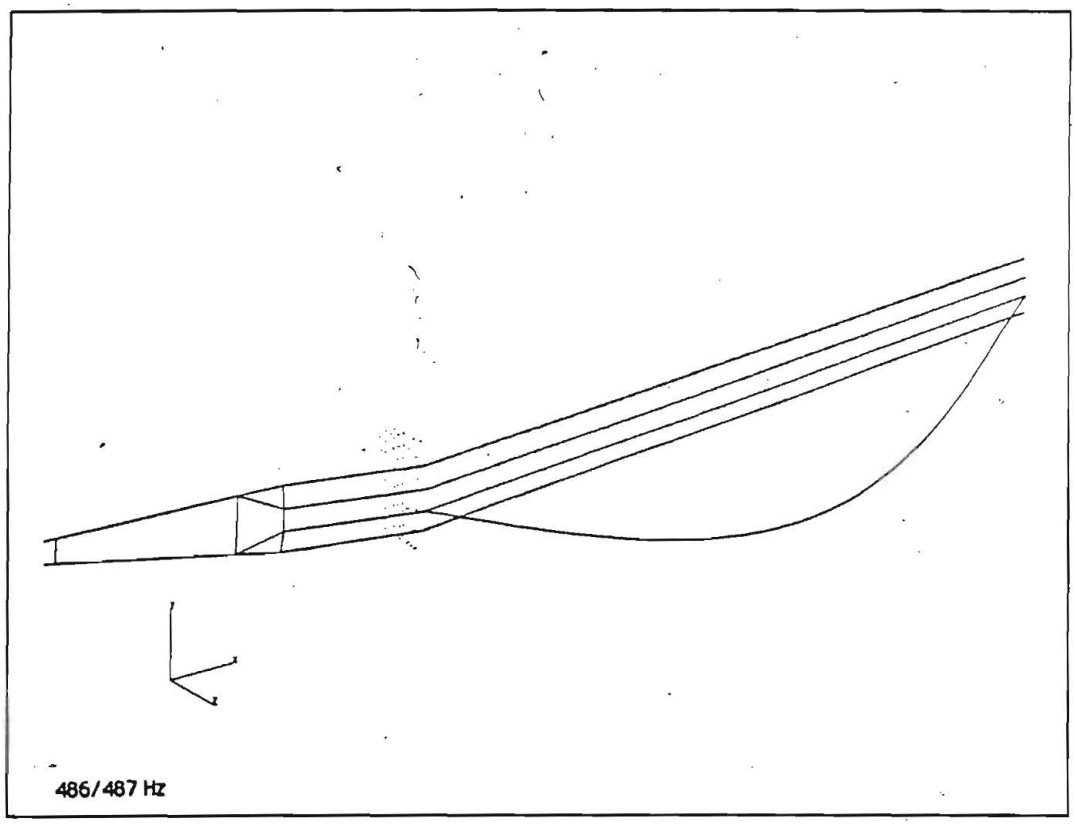

Figure D17. Modes 12/13

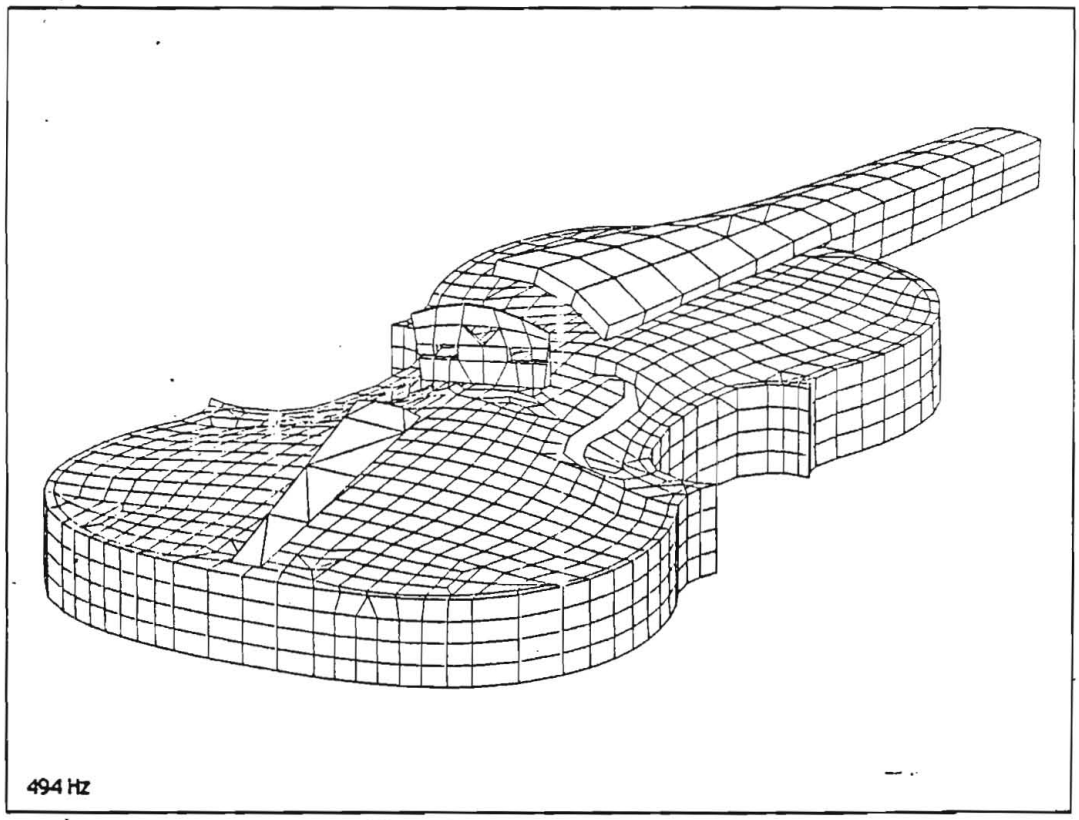

Figure D18. Mode 14

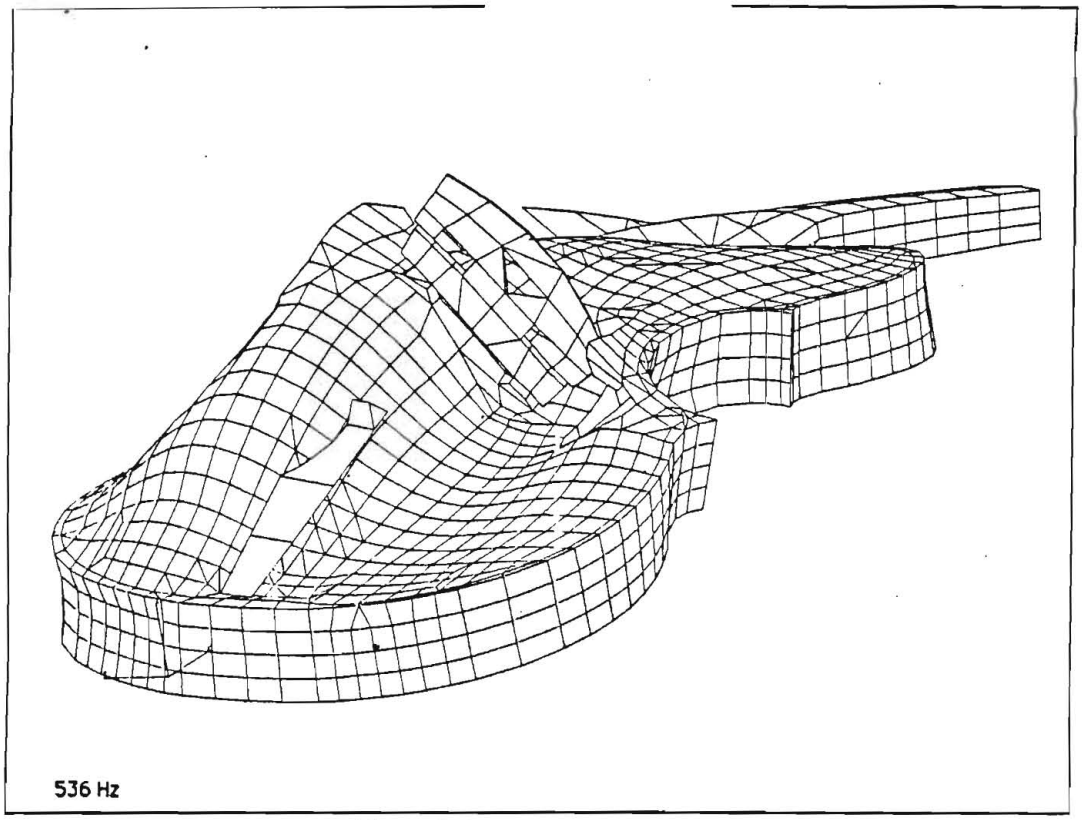

Figure D19. Mode 15

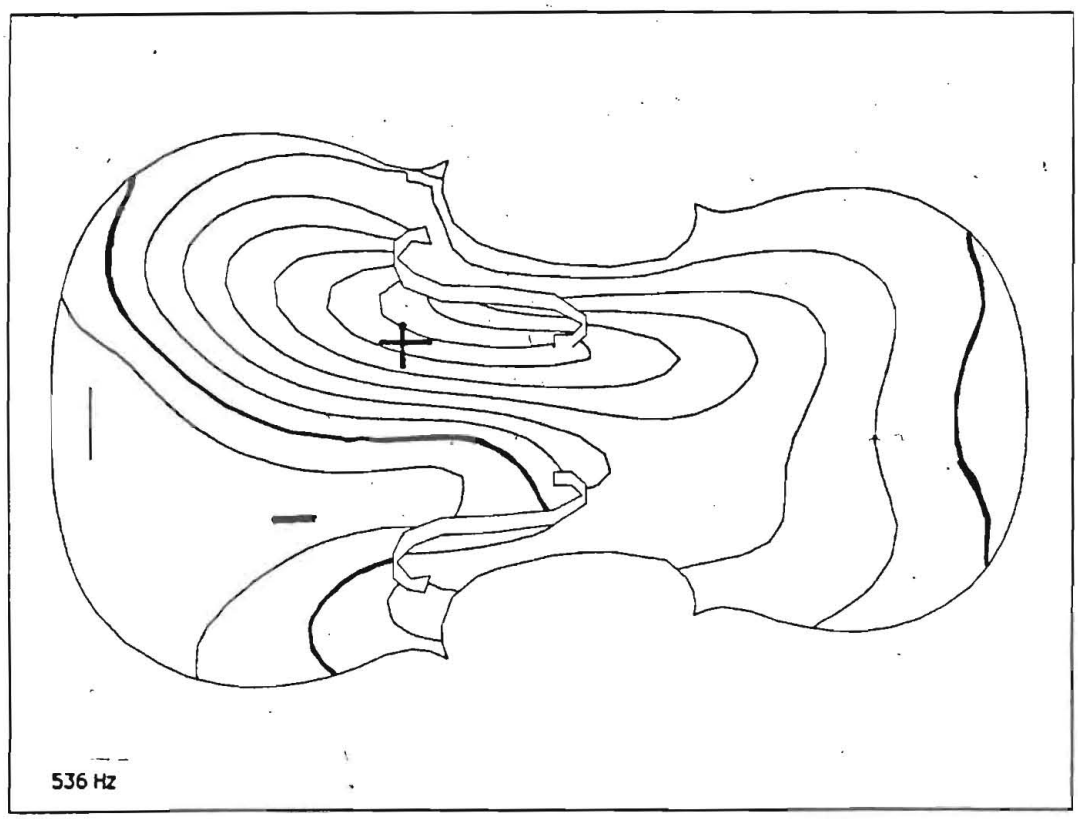

Figure D20. Mode 15 - top

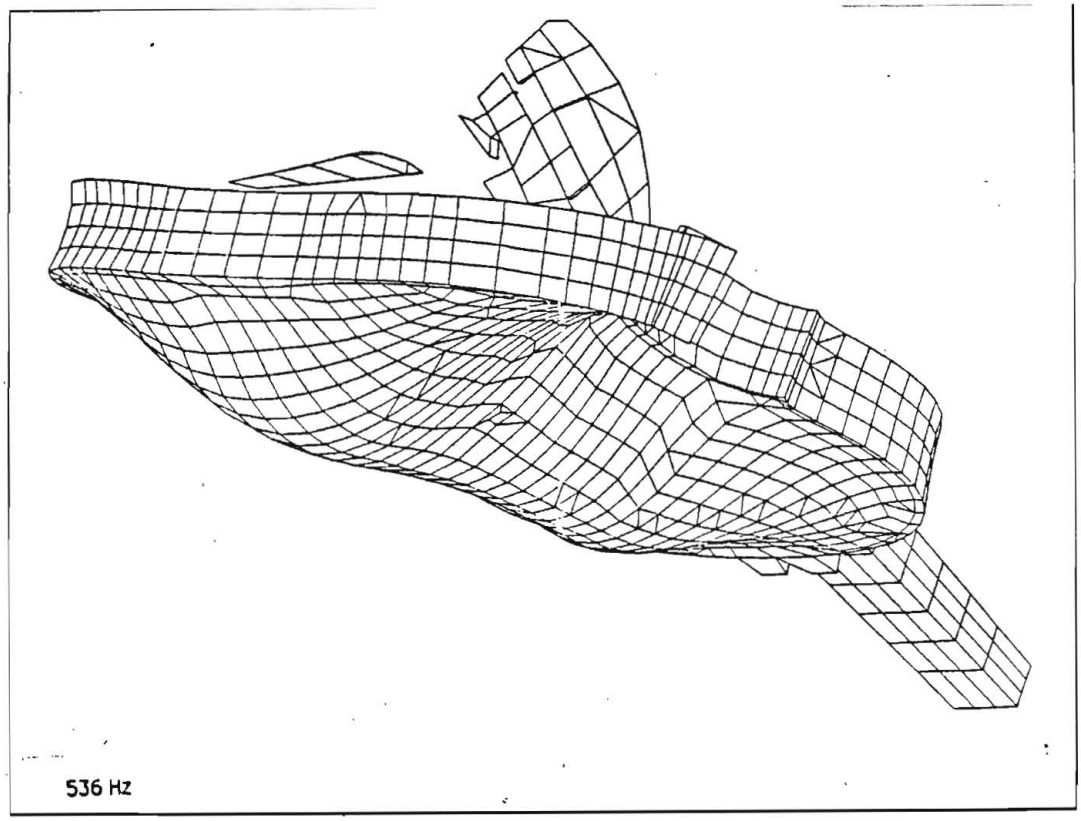

Figure D21. Mode 15

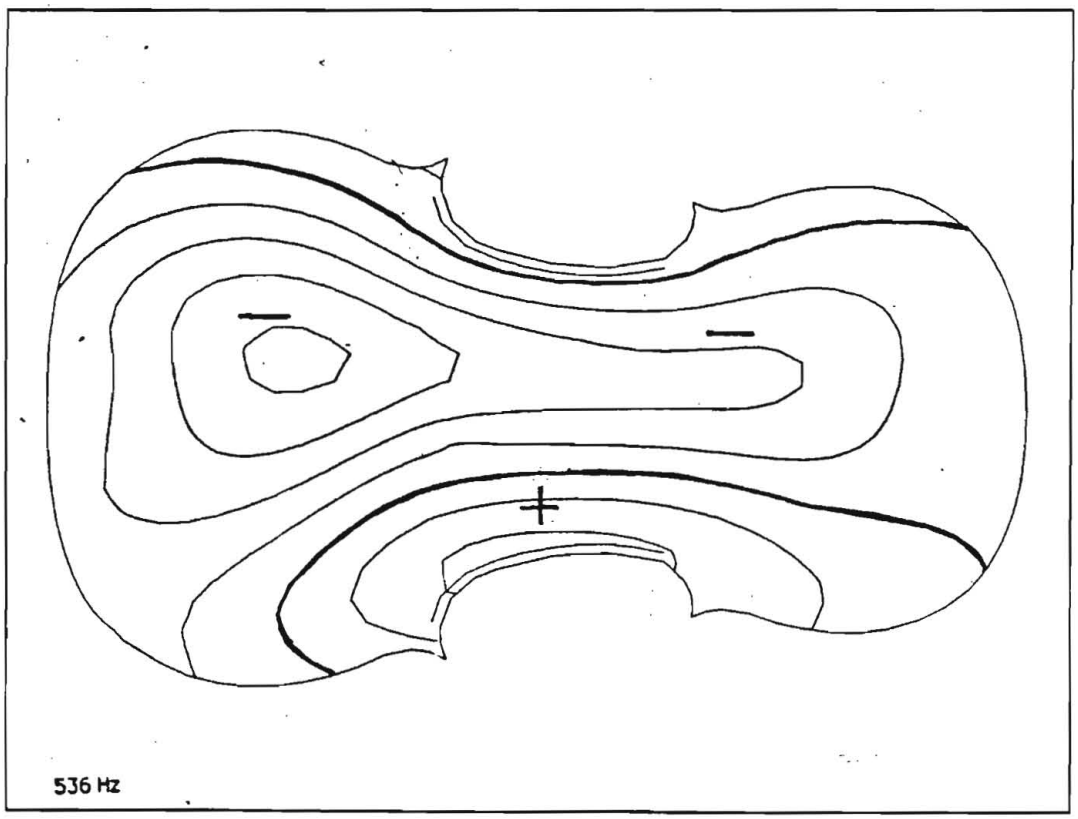

Figure D22. Mode 15 - back

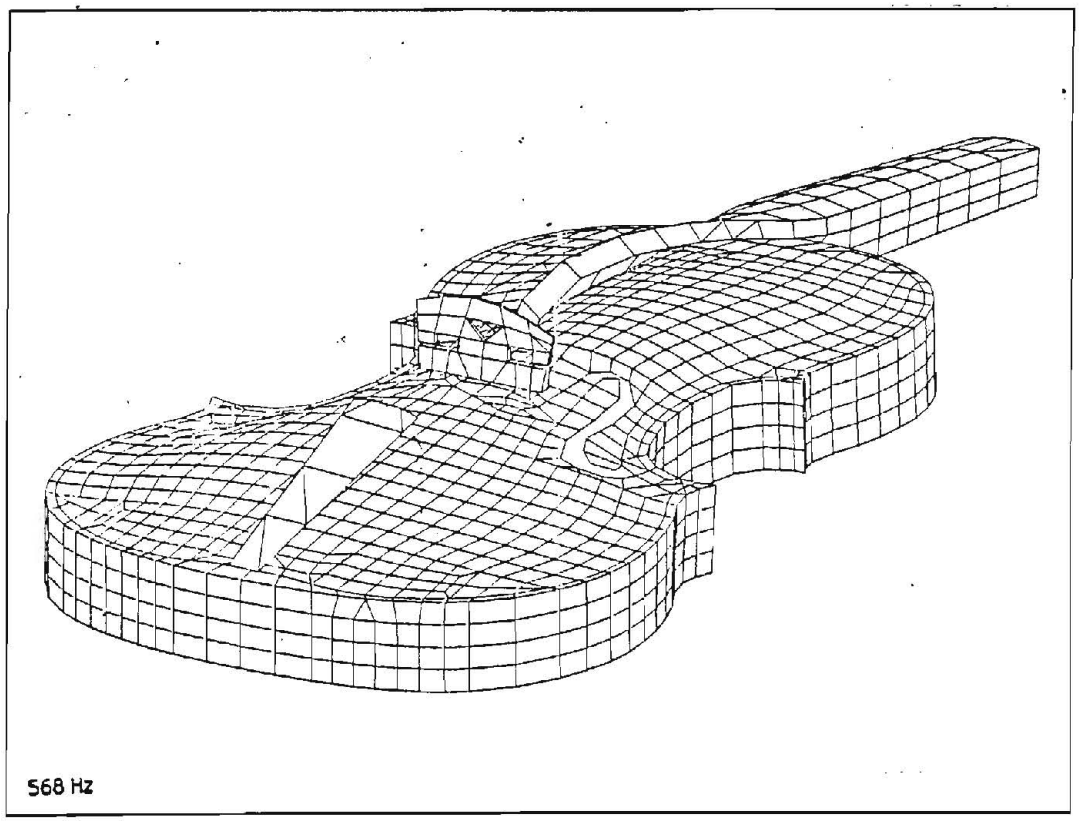

Figure D23. Mode 16

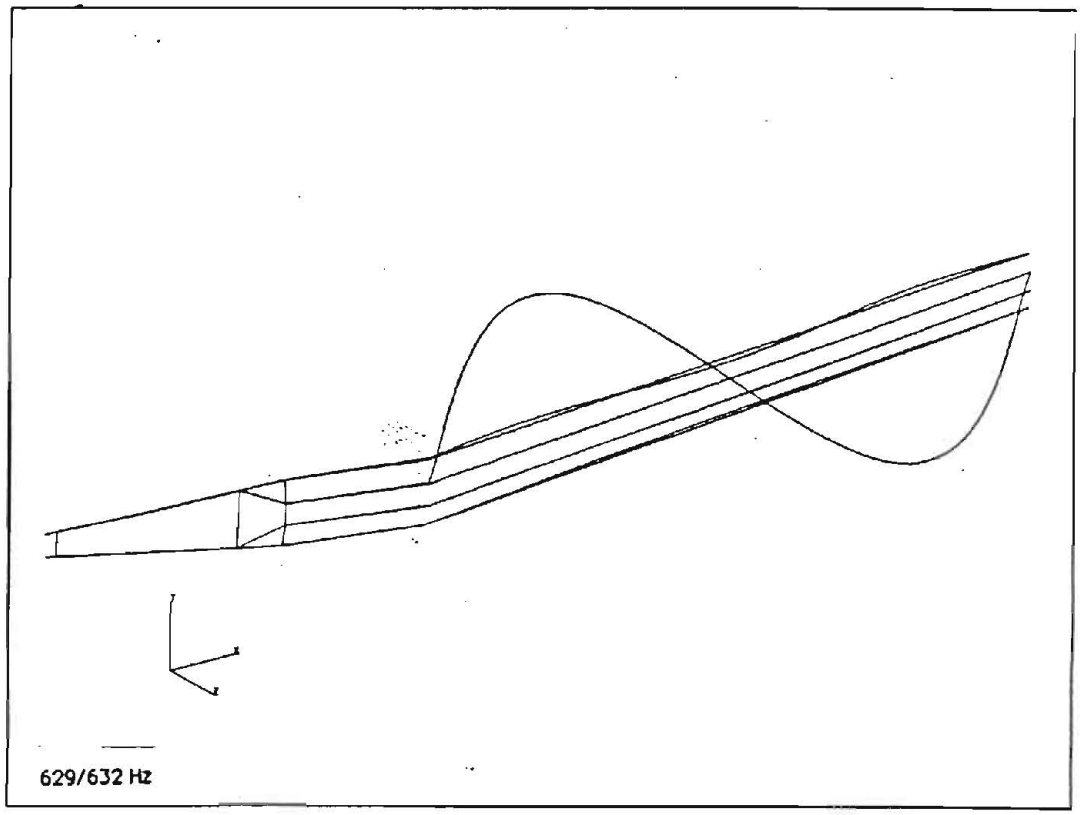

Figure D24. Modes 18/19

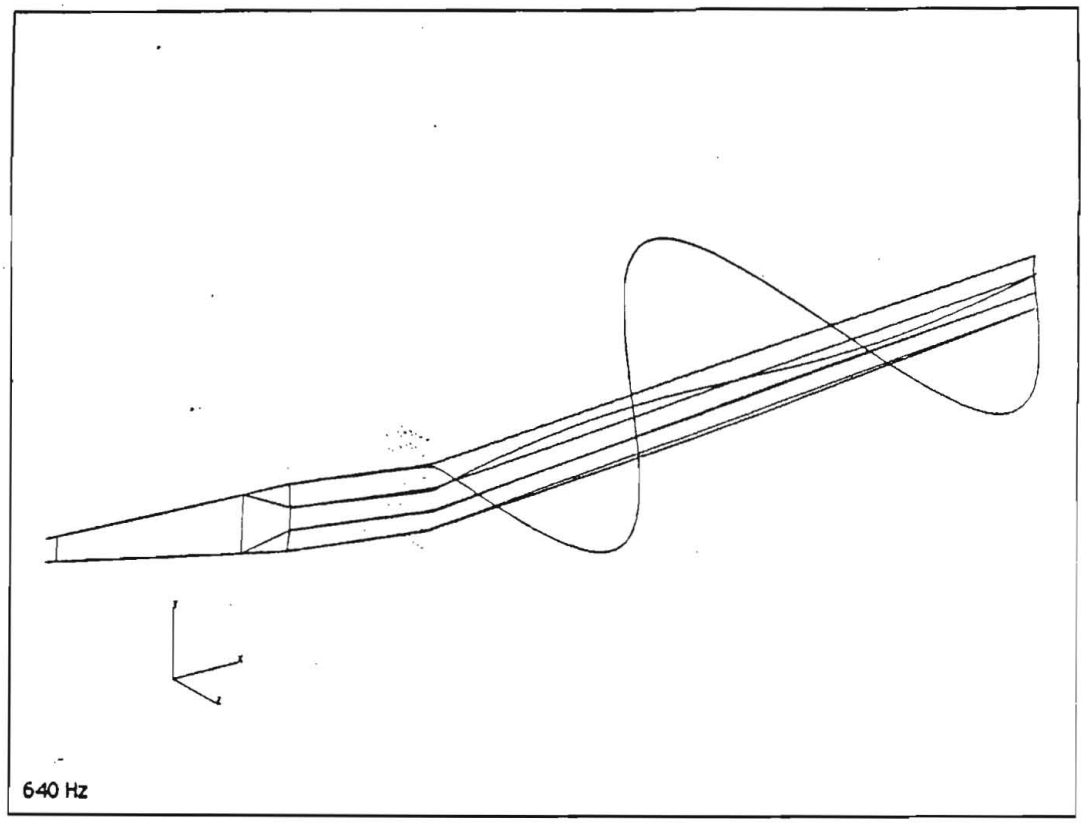

Figure D25. Mode 20

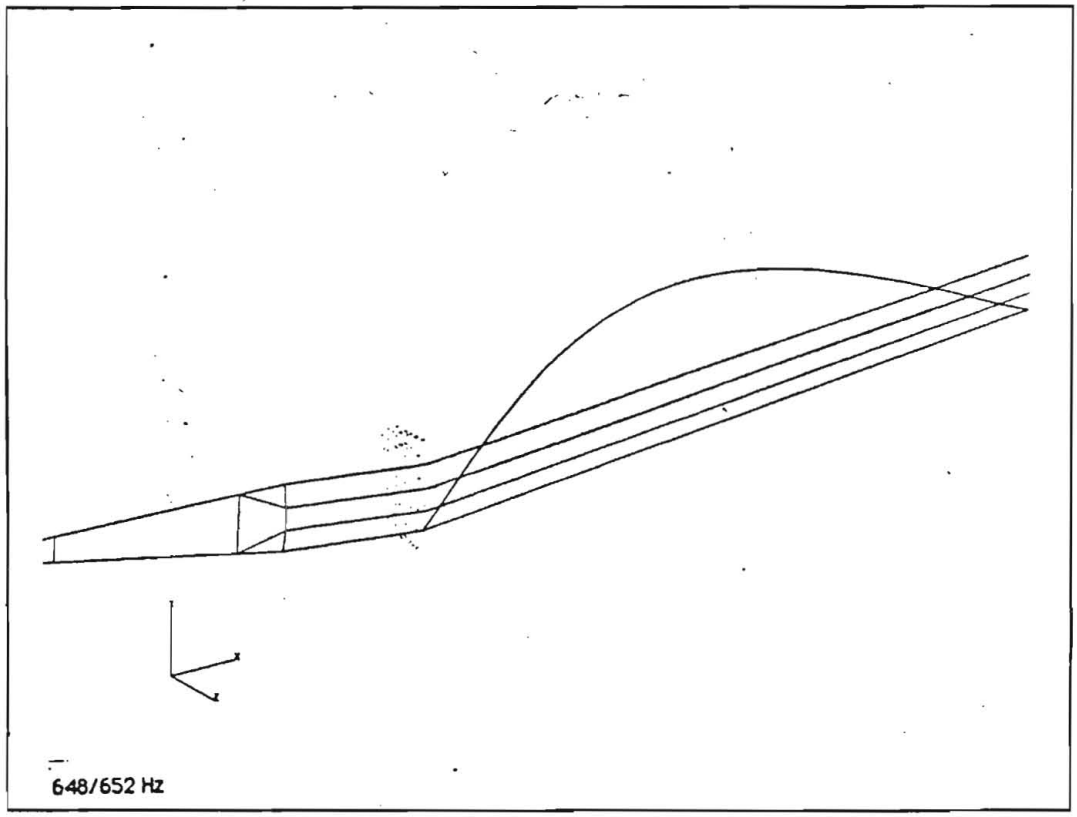

Figure D26. Mode 21/22

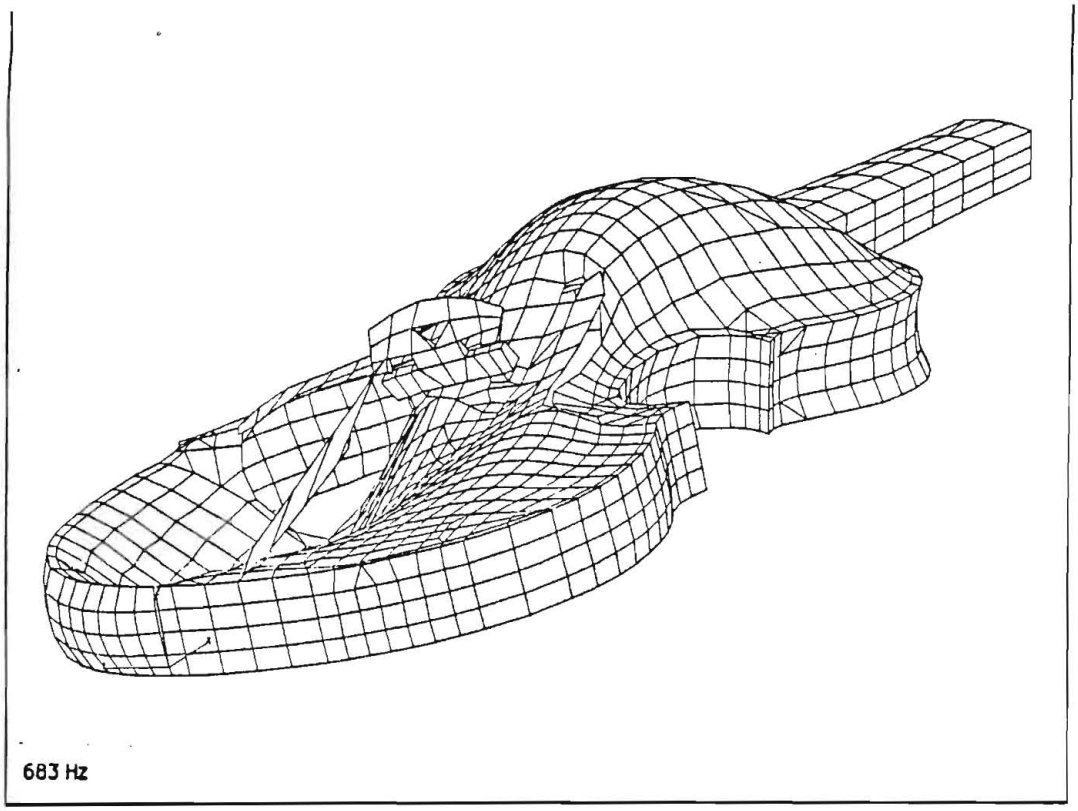

Figure D27. Mode 24

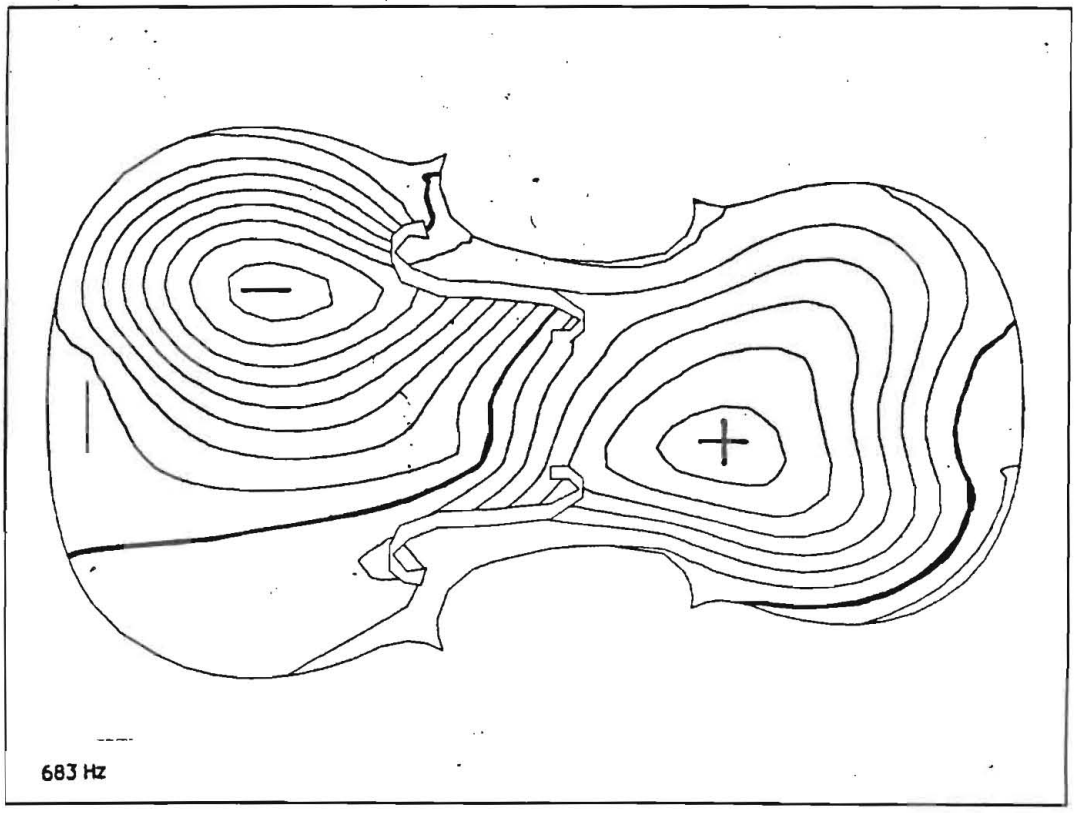

Figure D28. Mode 24 - top

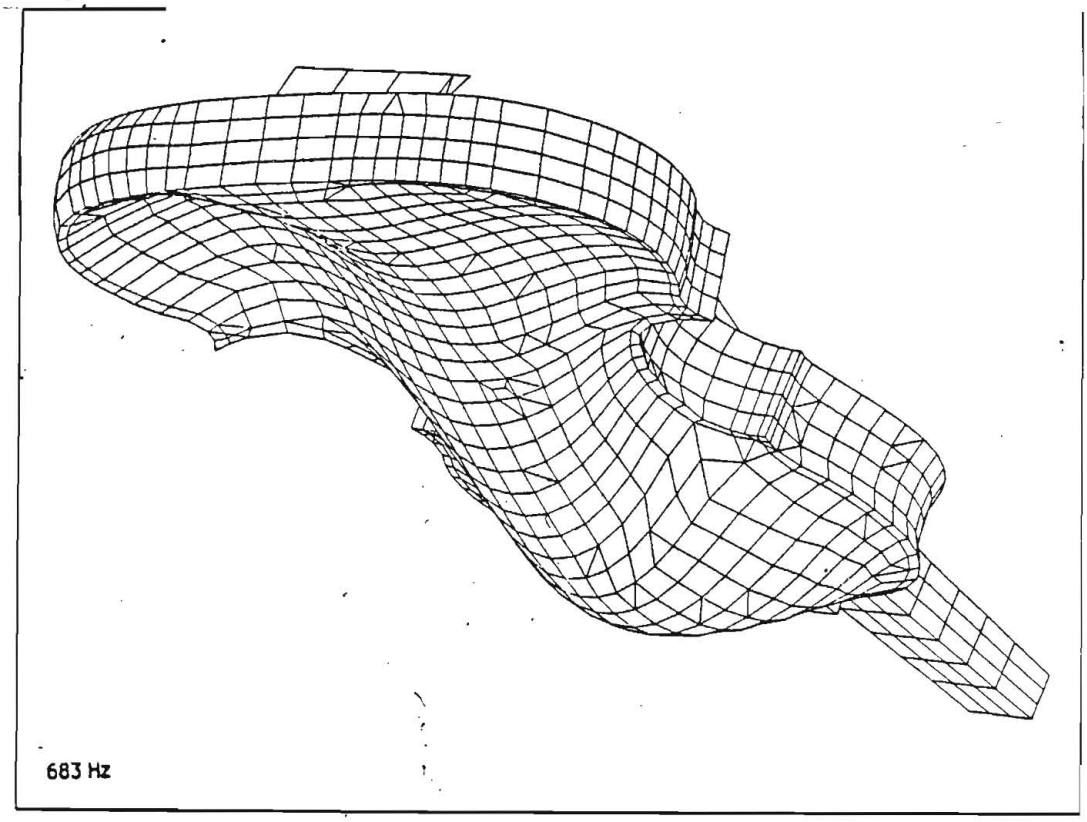

Figure D29. Mode 24

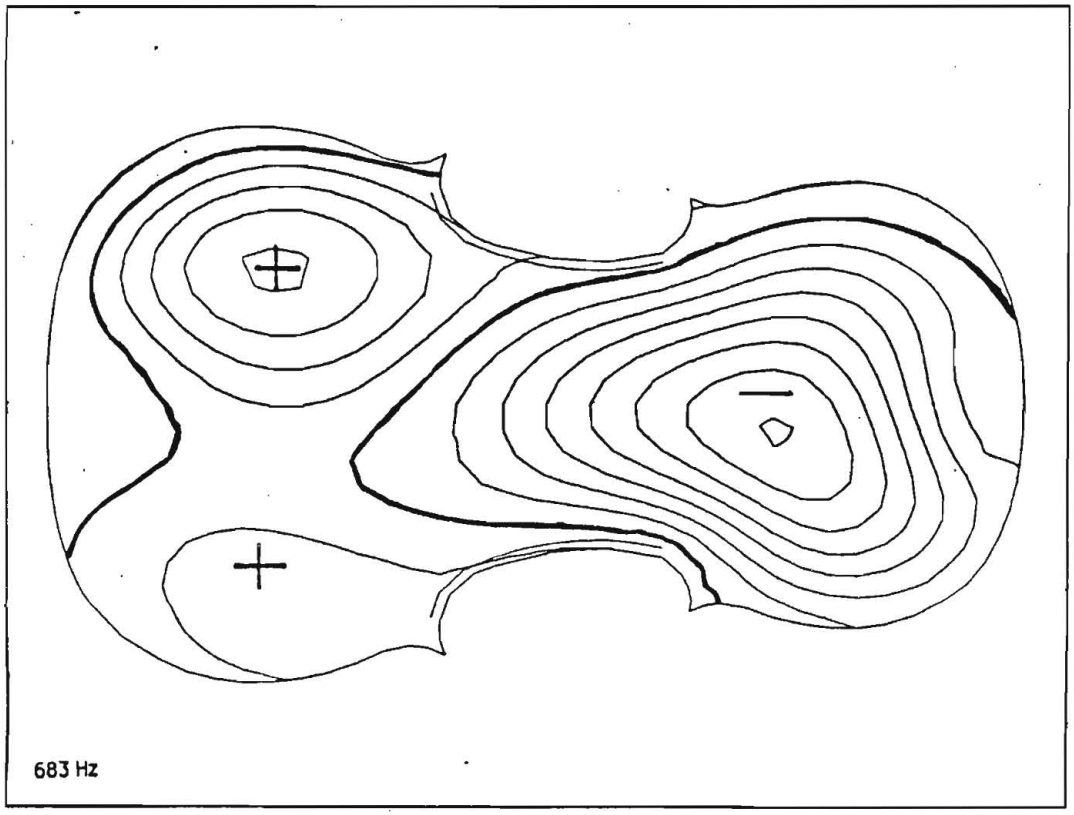

Figure D30. Mode 24 - back

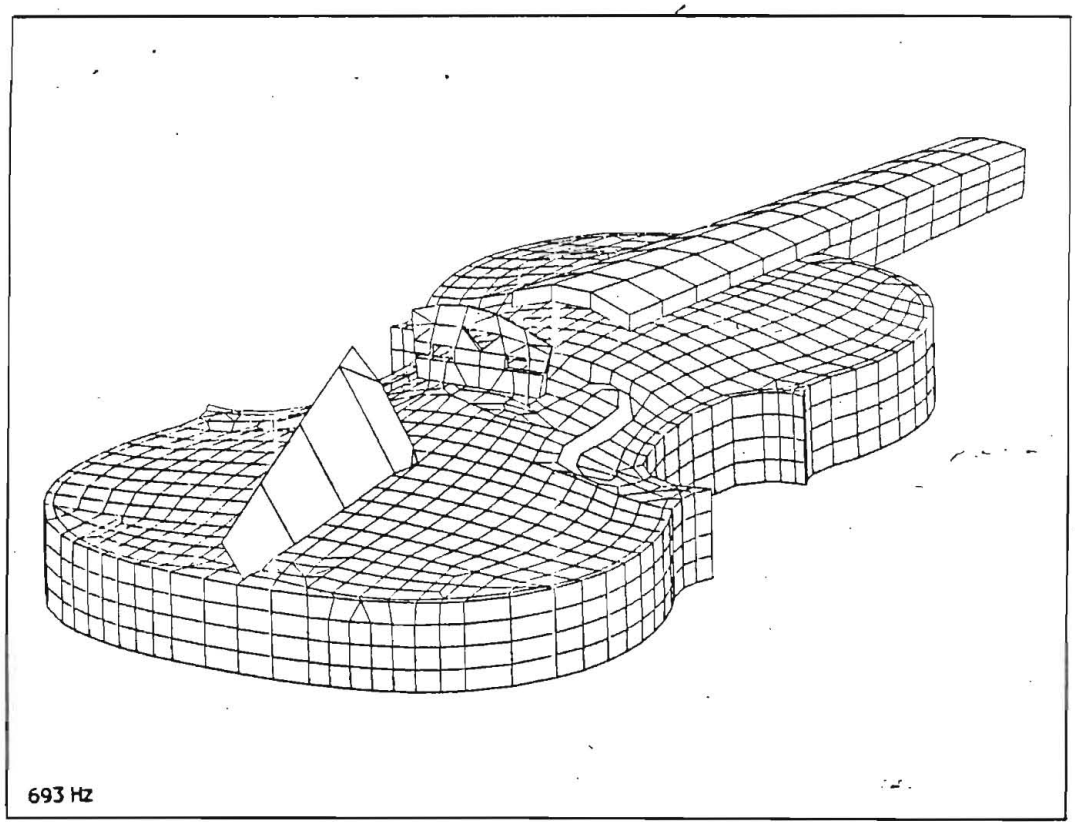

Figure D31. Mode 25

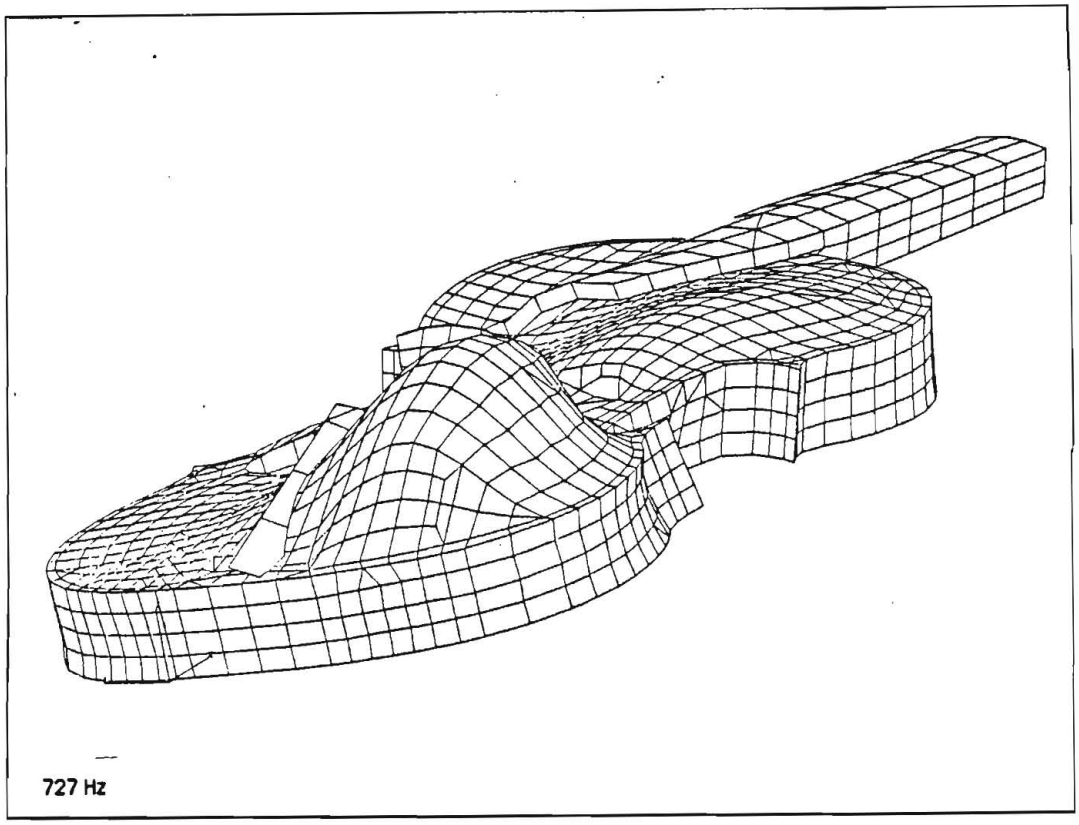

Figure D32. Mode 26

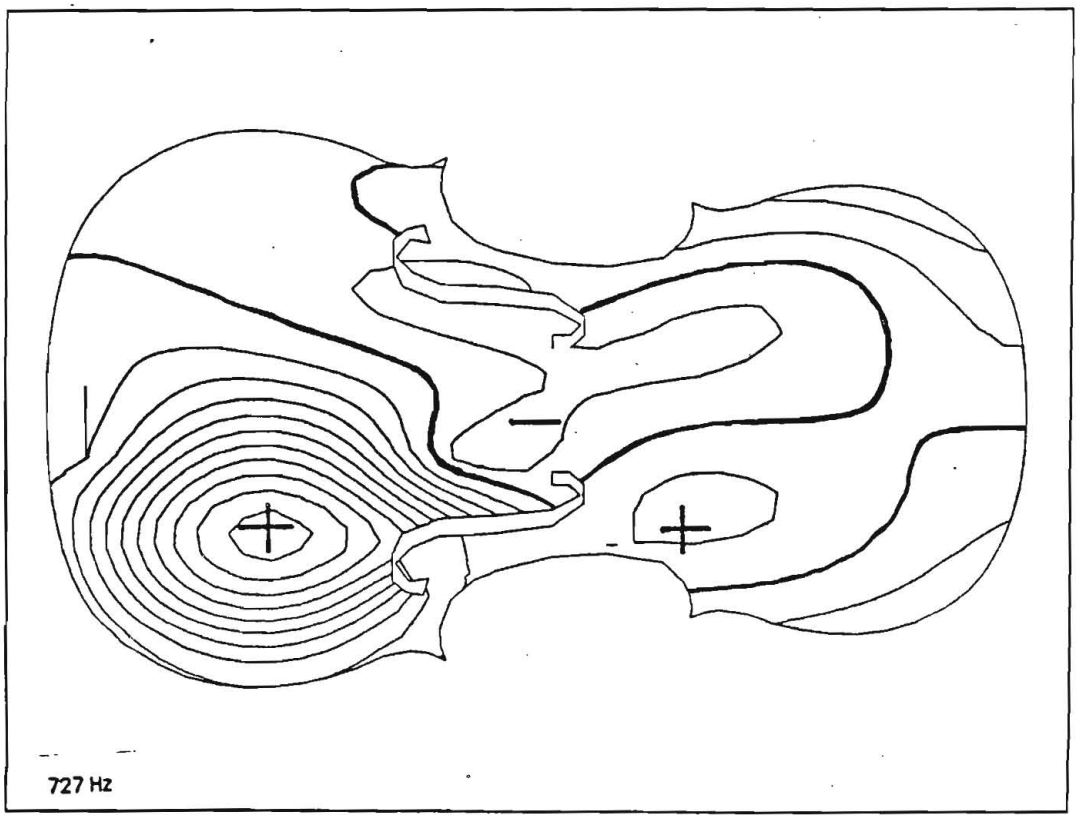

Figure D33. Mode 26 -top

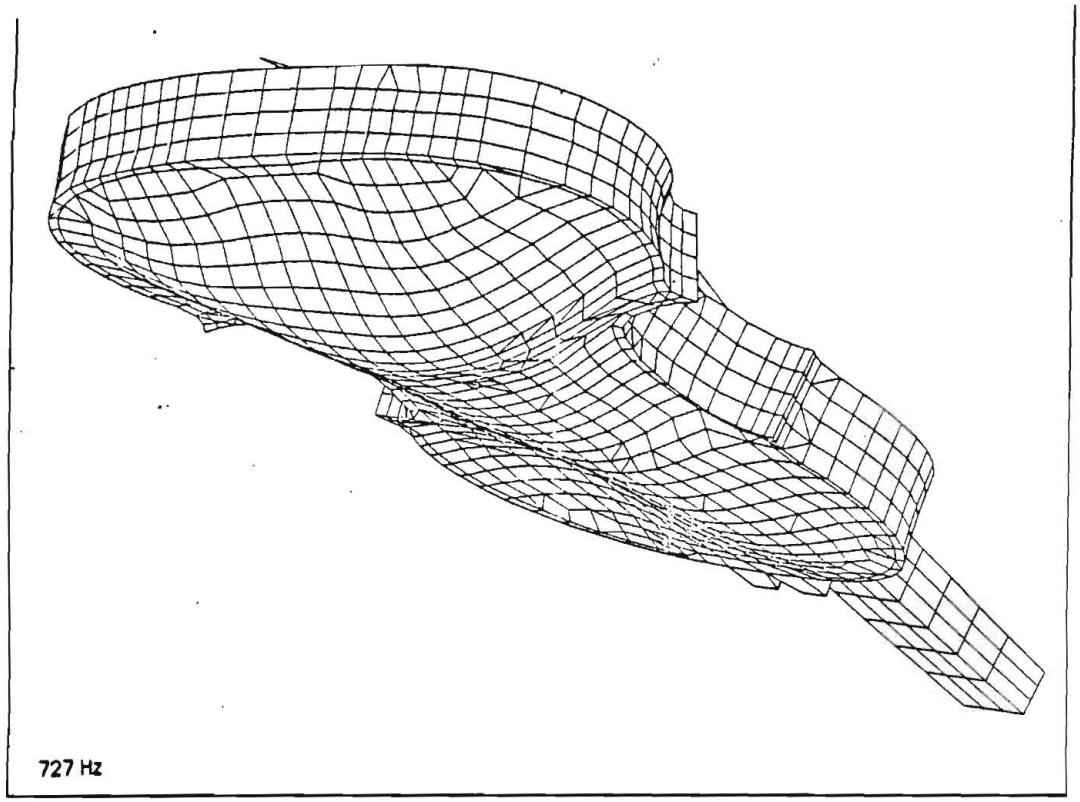

Figure D34. Mode 26

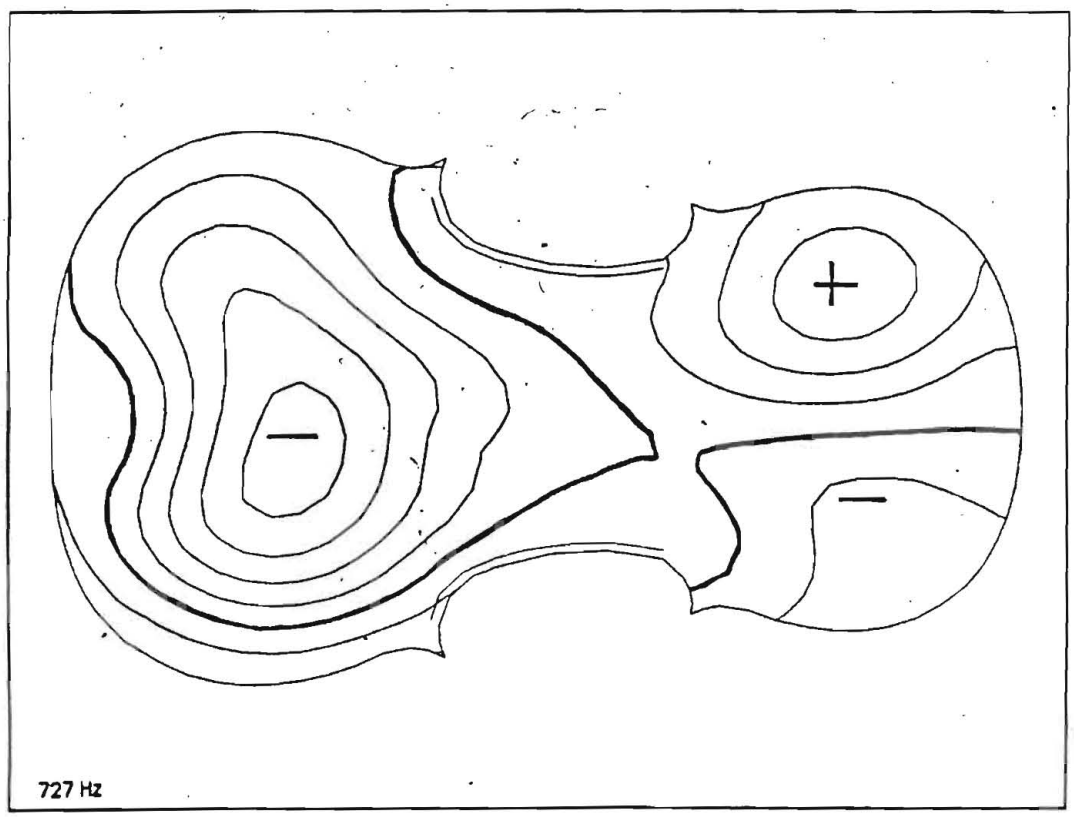

Figure D35. Mode 26 - back

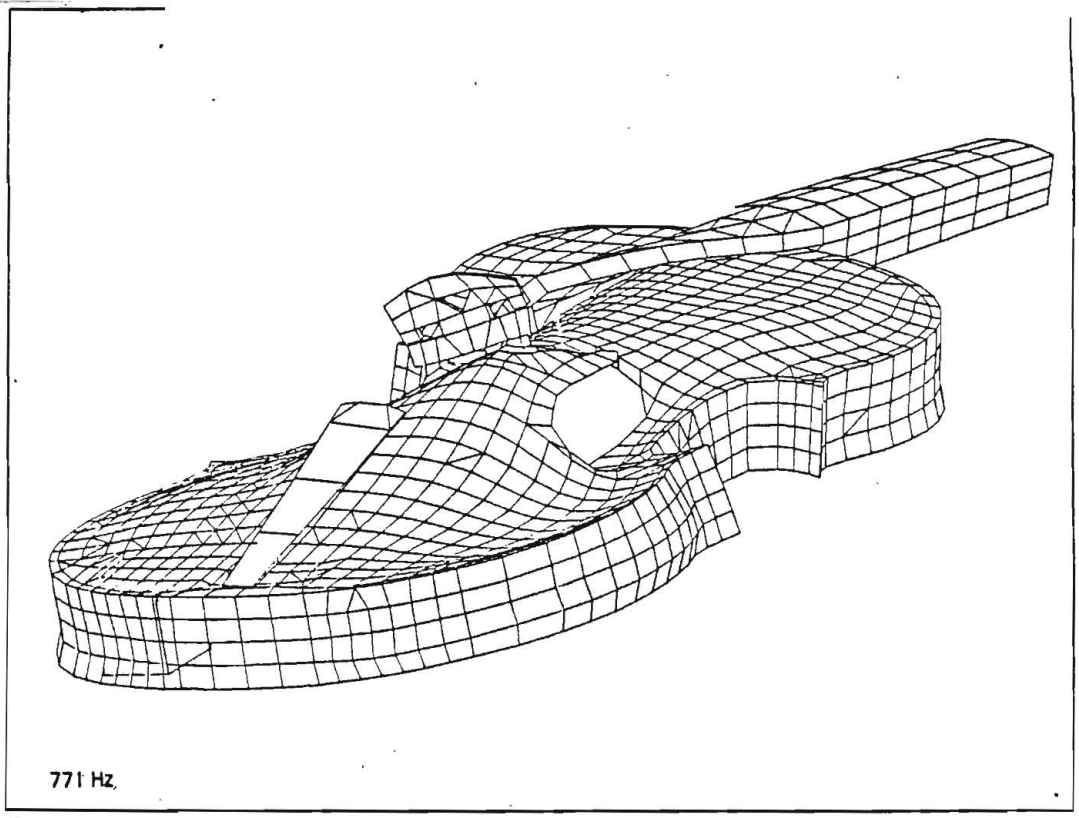

Figure D36. Mode 27

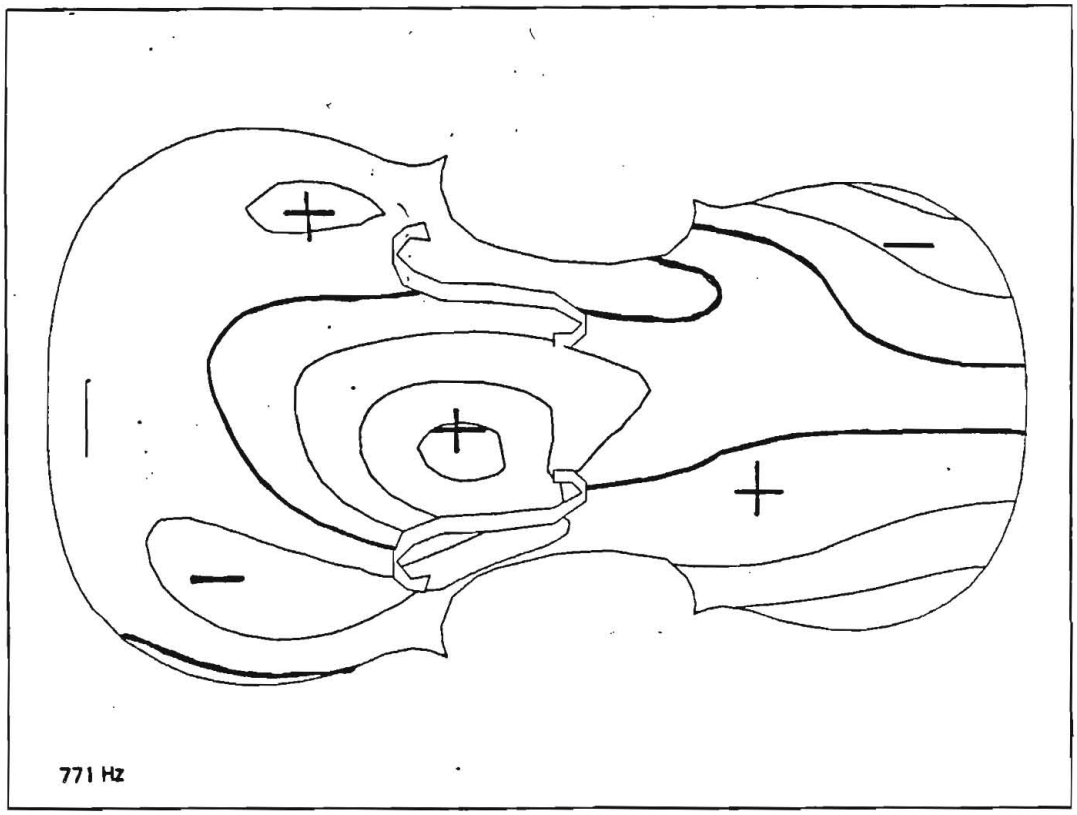

Figure D37. Mode 27 - top

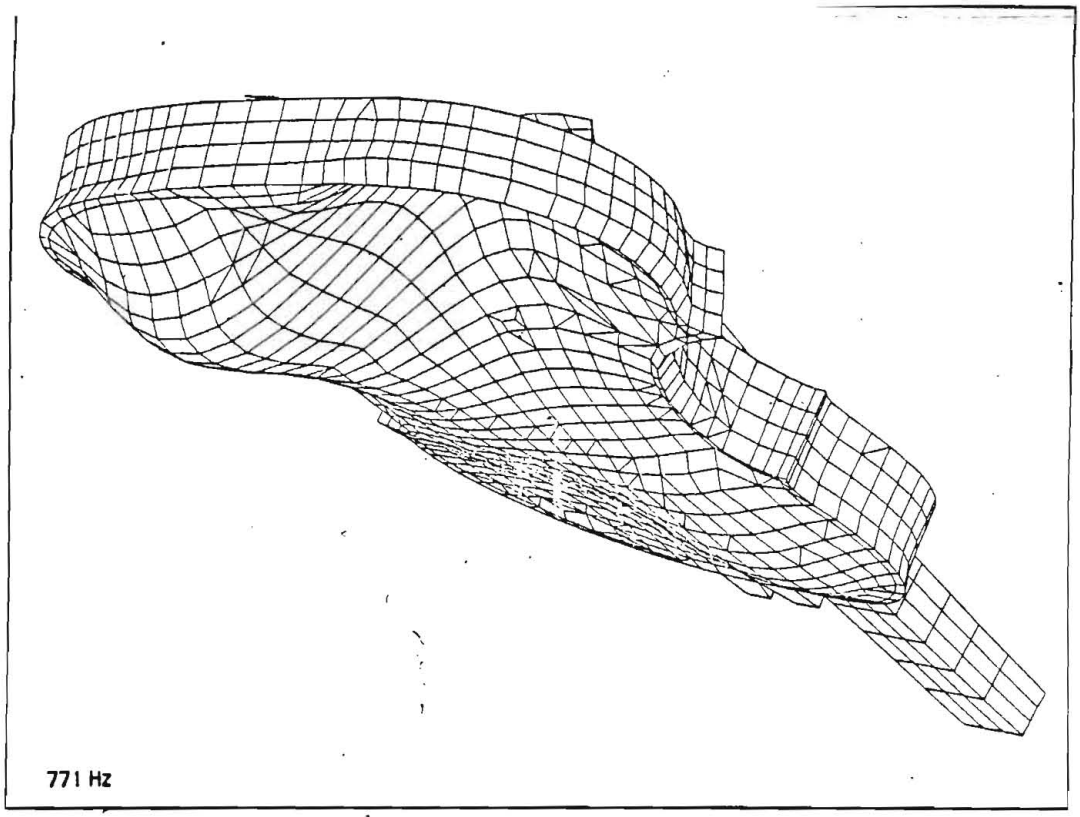

Figure D38. Mode 27

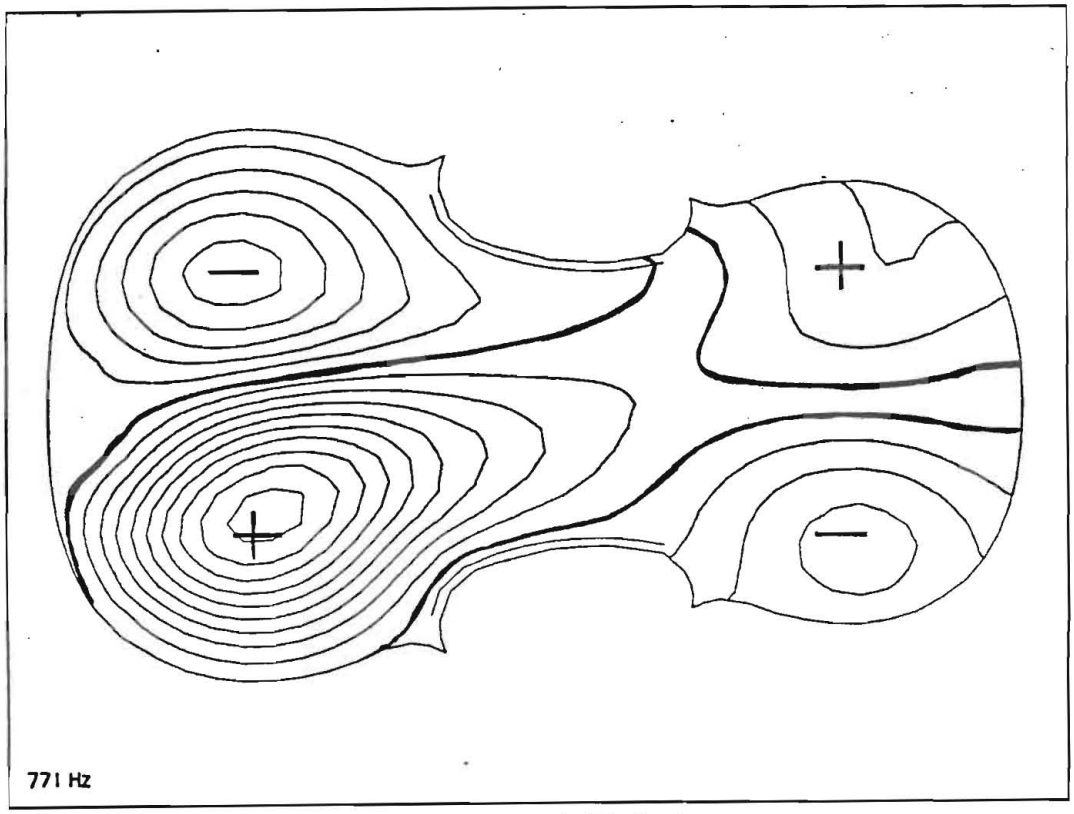

Figure D39. Mode 27 - back

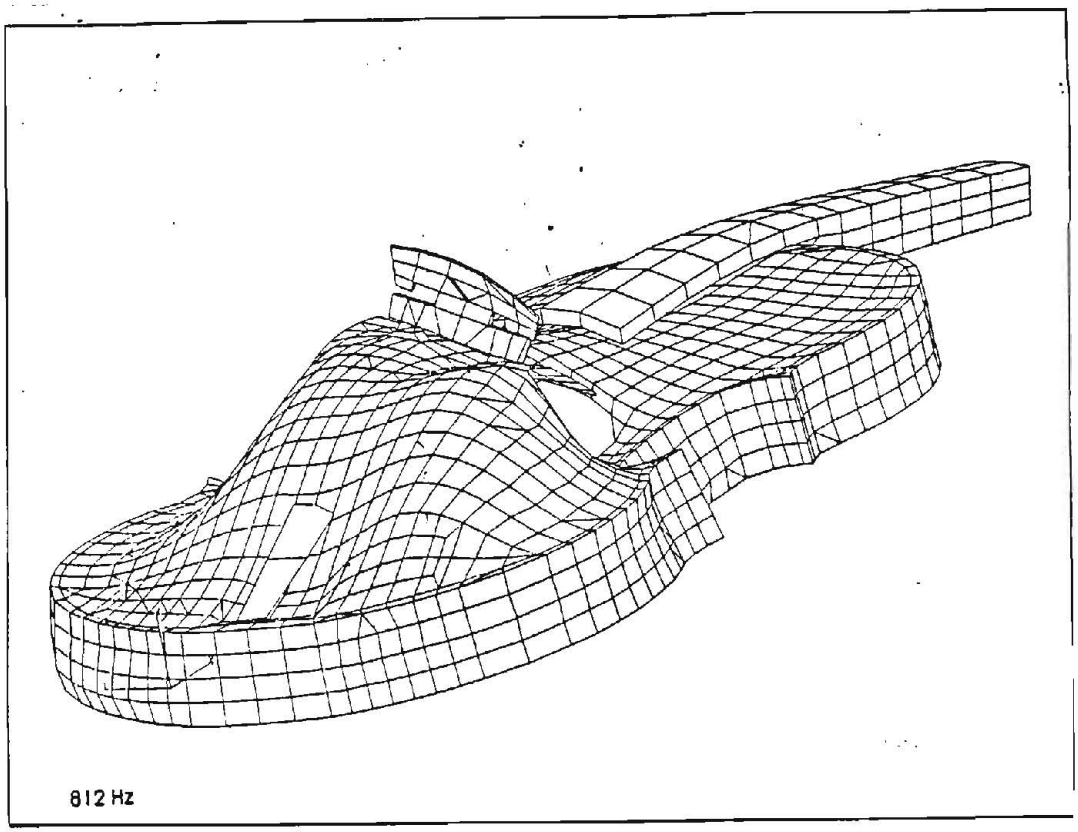

Figure D40. Mode 28

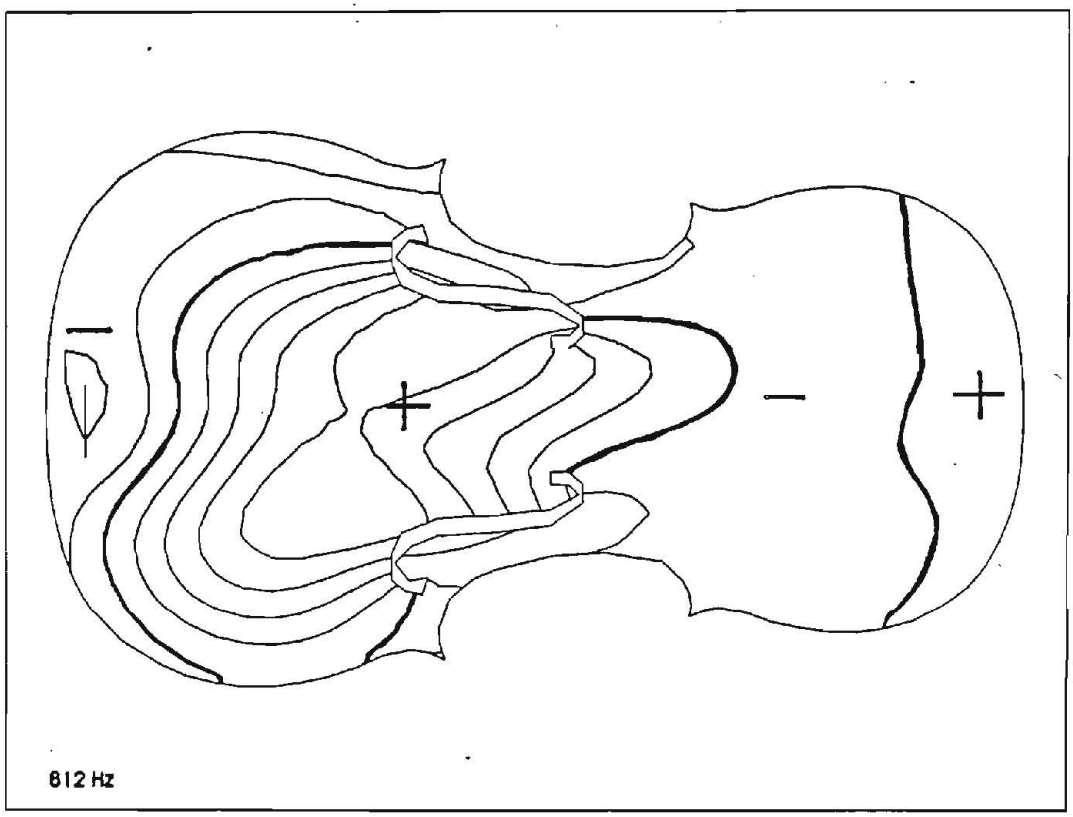

Figure D41. Mode 28 - top

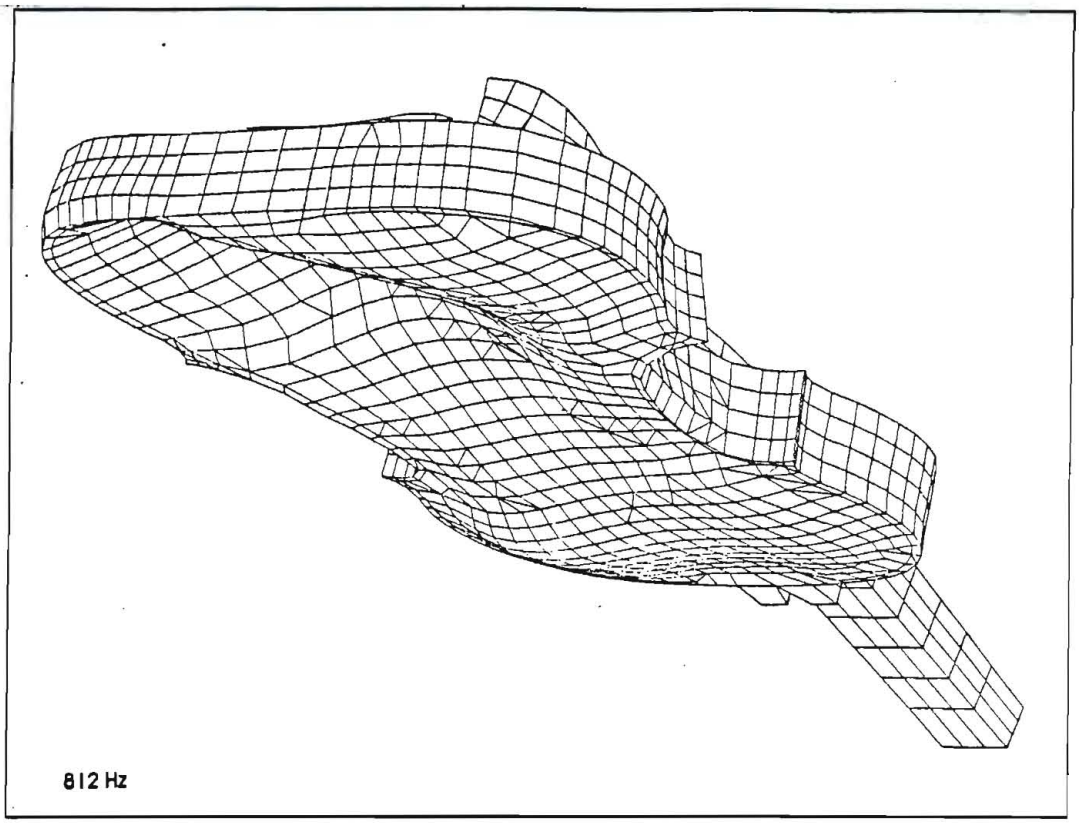

Figure D42. Mode 28

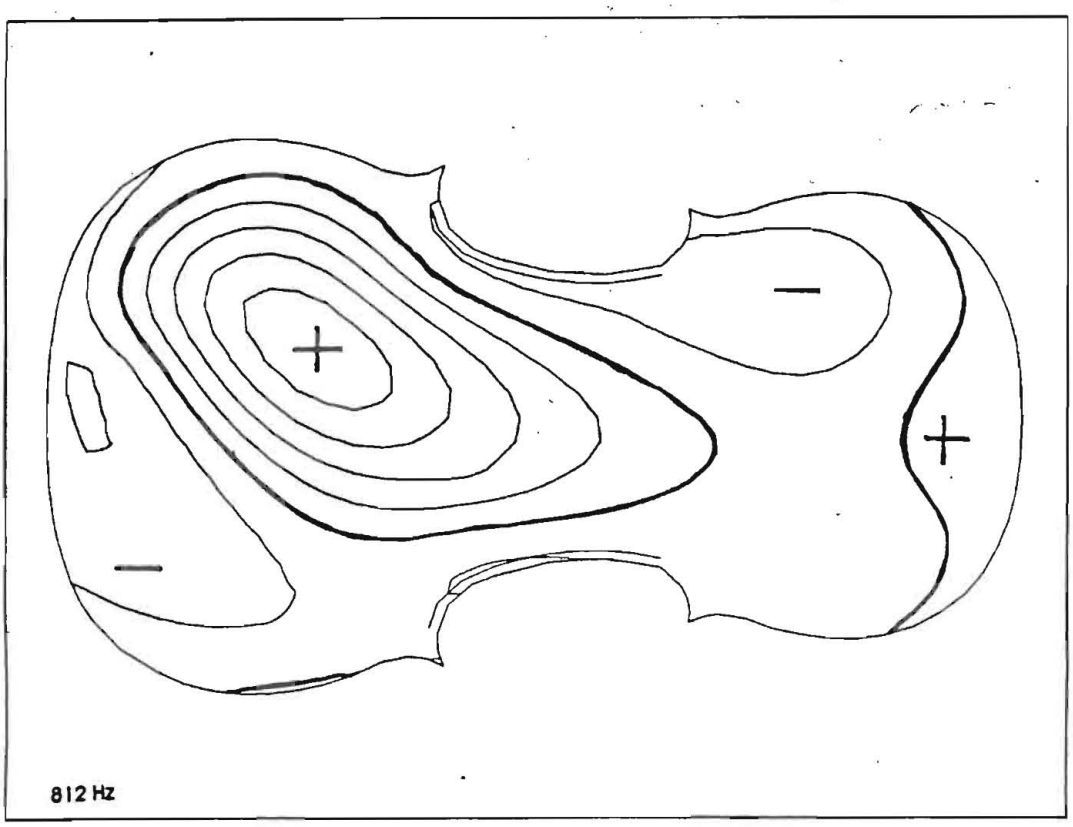

Figure D43. Mode 28 - back

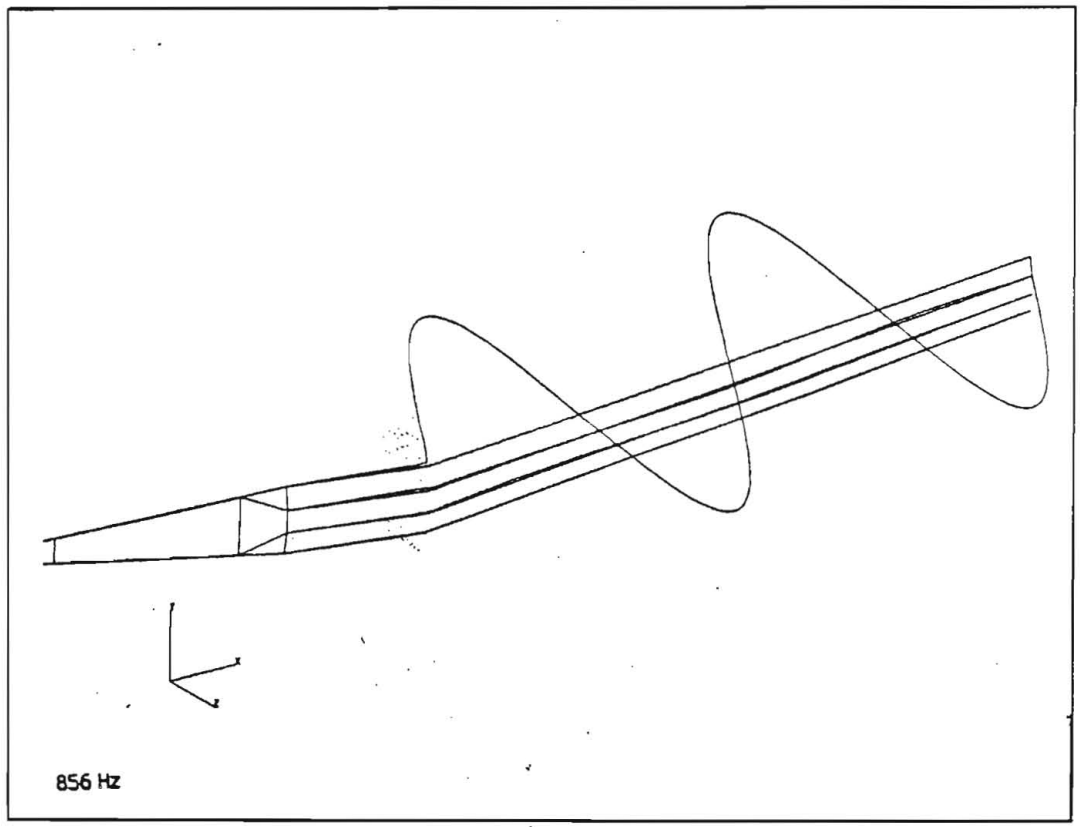

Figure D44. Mode 29

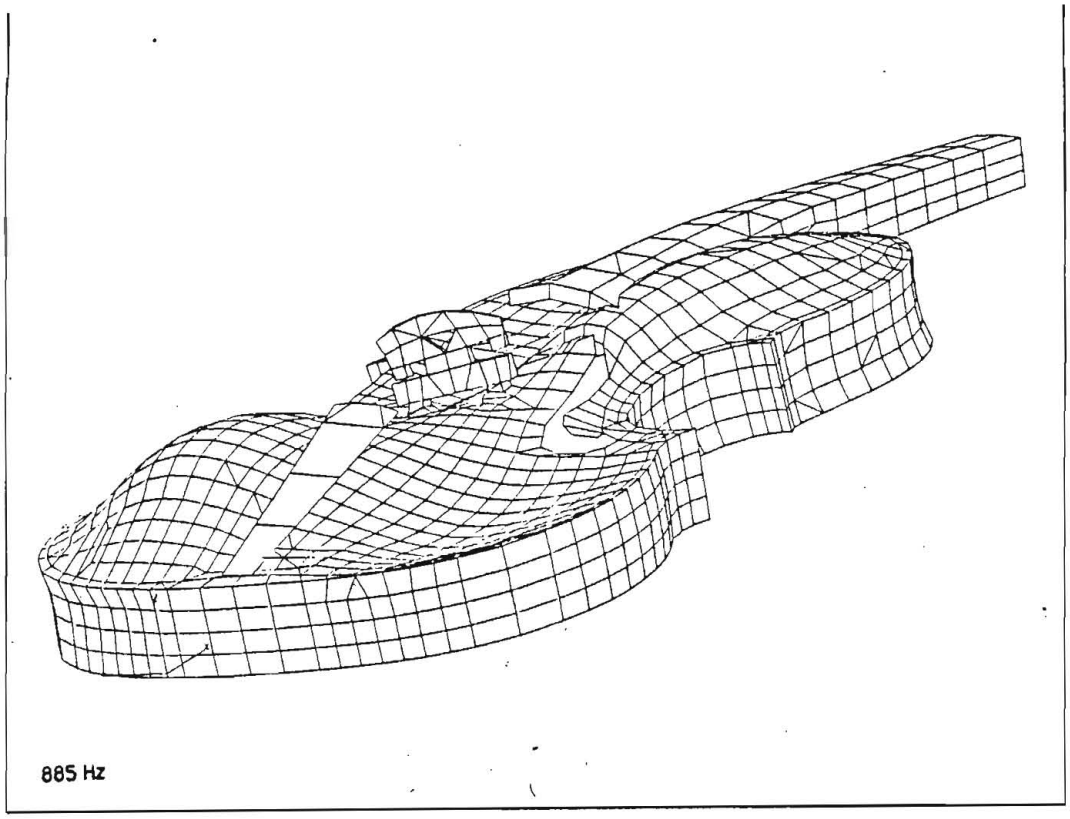

Figure D45. Mode 30

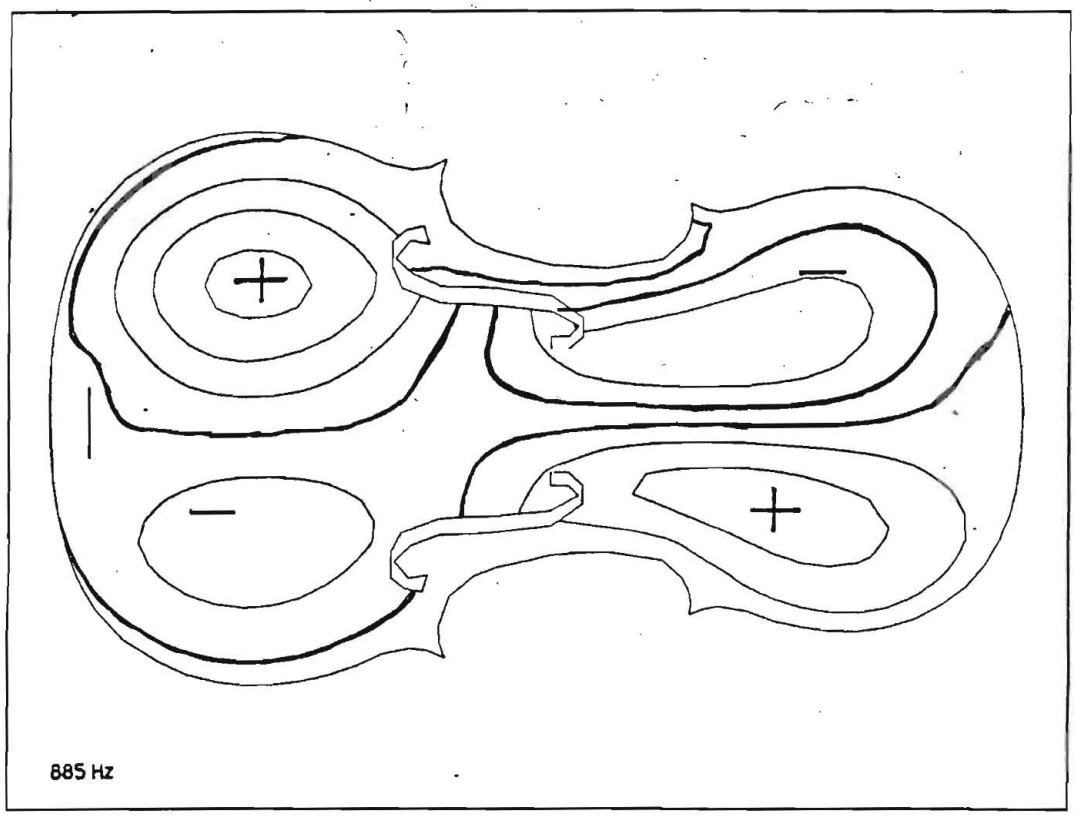

Figure D46. Mode 30 - top

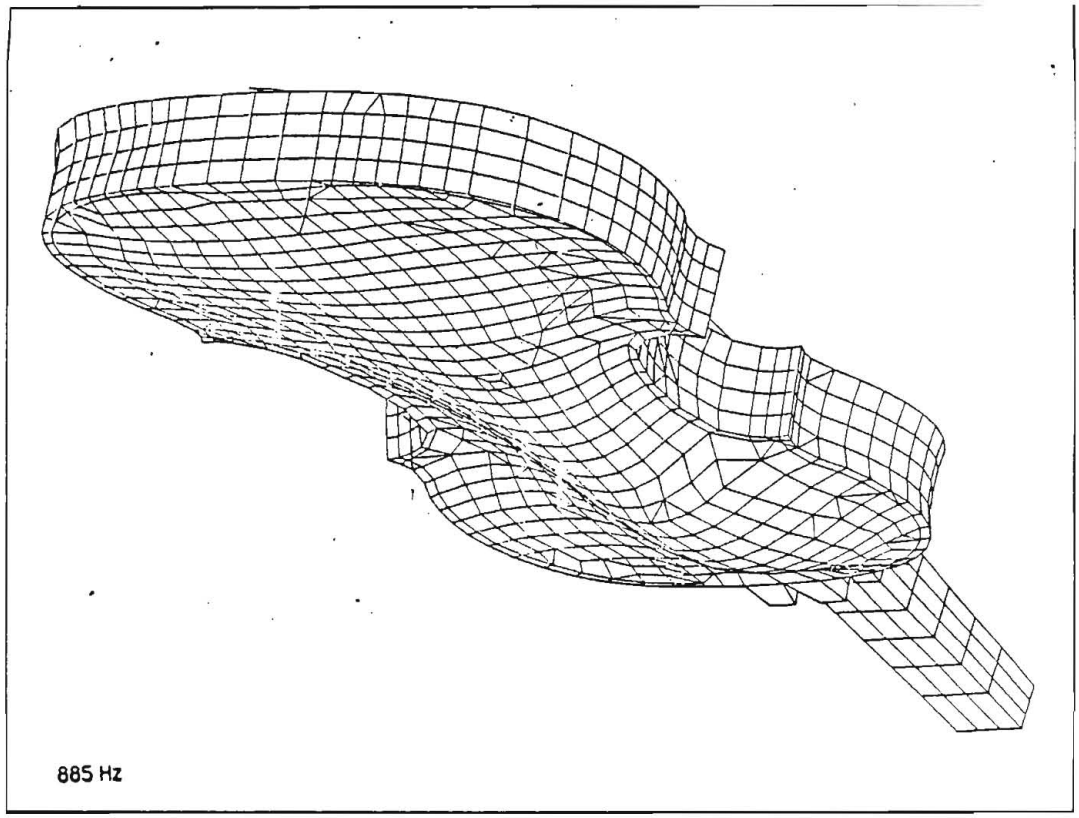

Figure D47. Mode 30

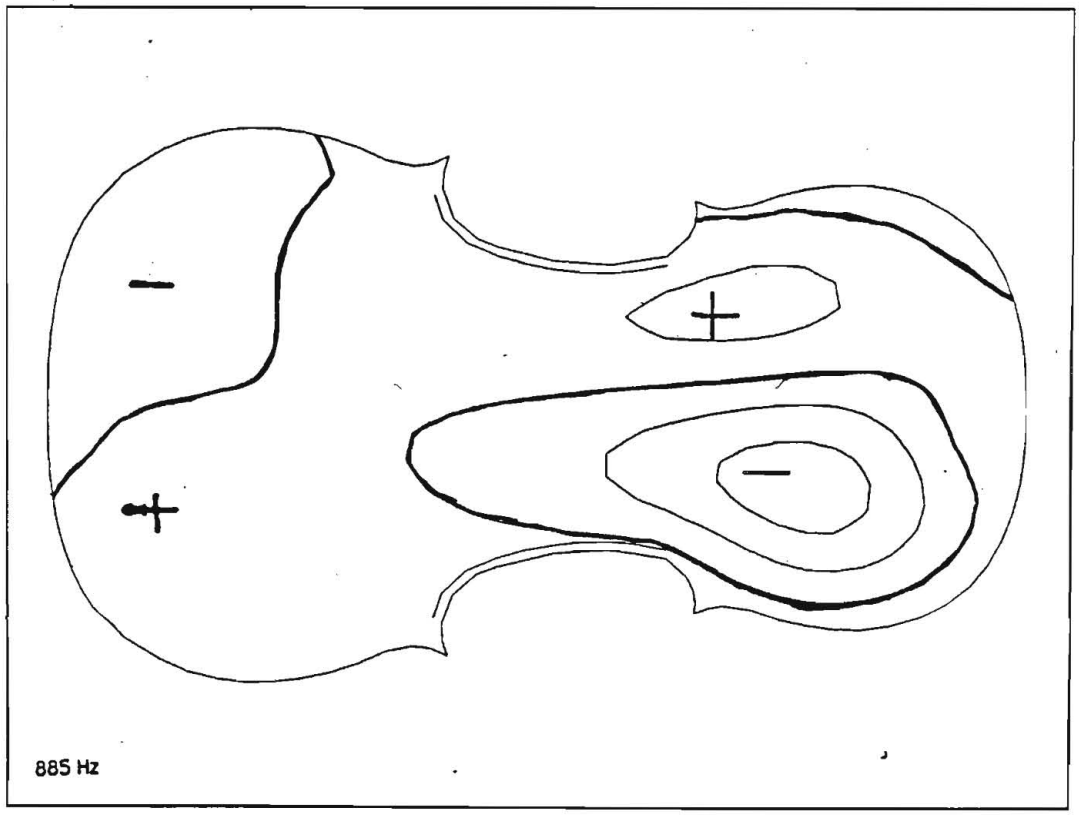

Figure D48. Mode 30 - back

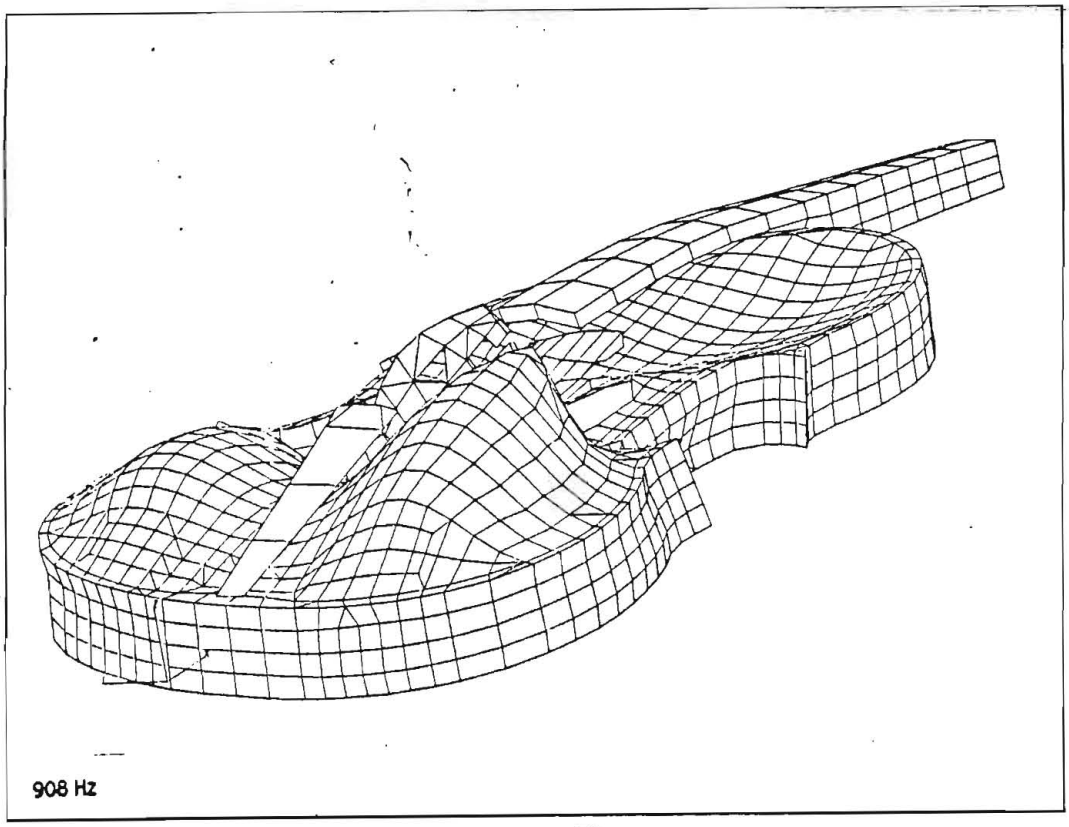

Figure D49. Mode 32

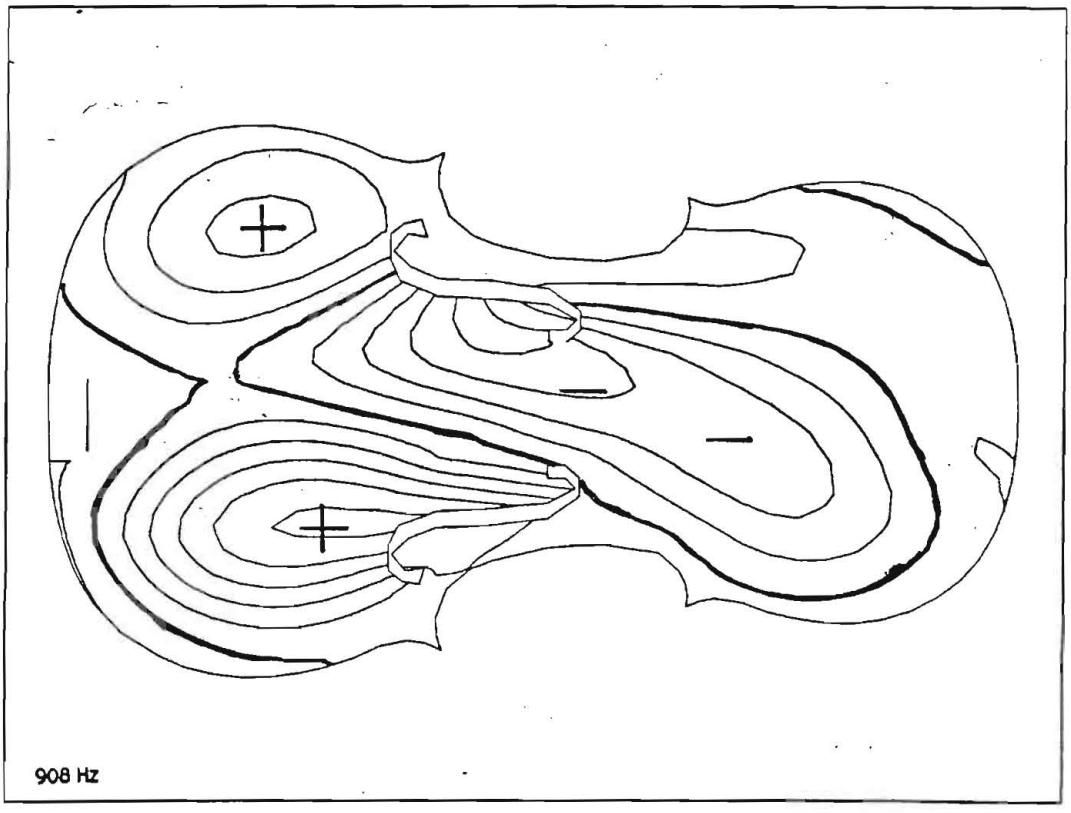

Figure D50. Mode 32 - top

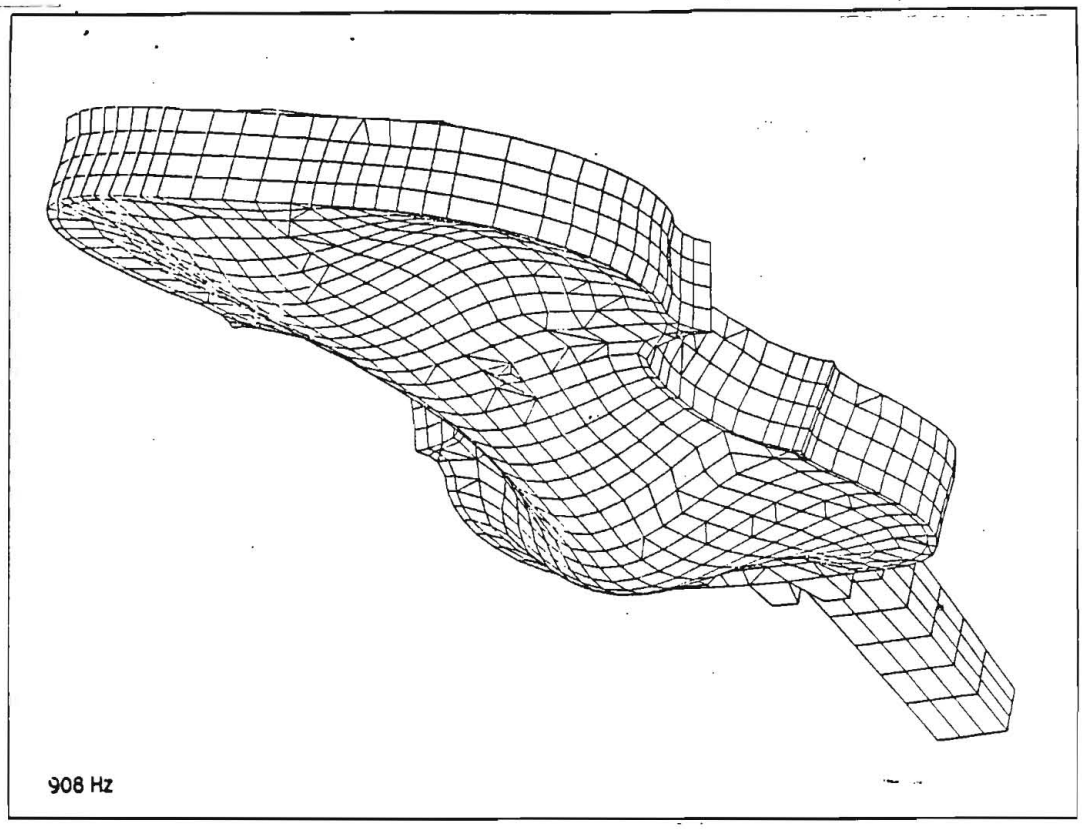

Figure D51. Mode 32

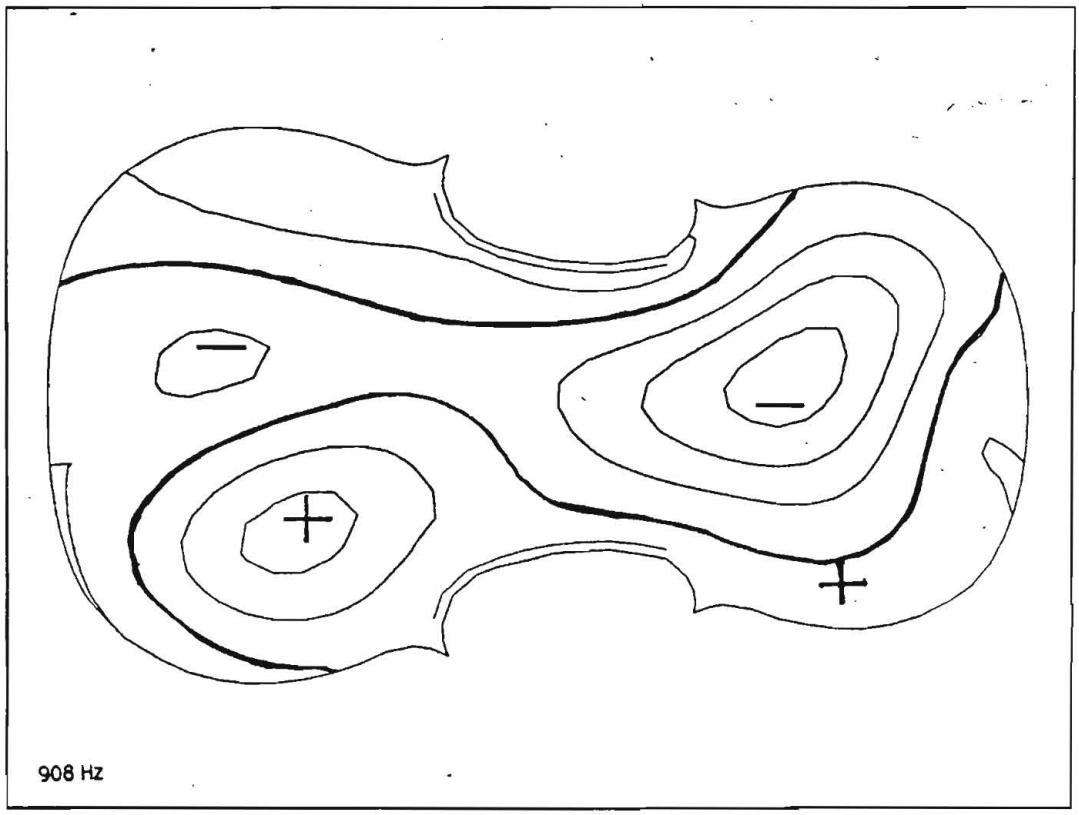

Figure D52. Mode 32 - back

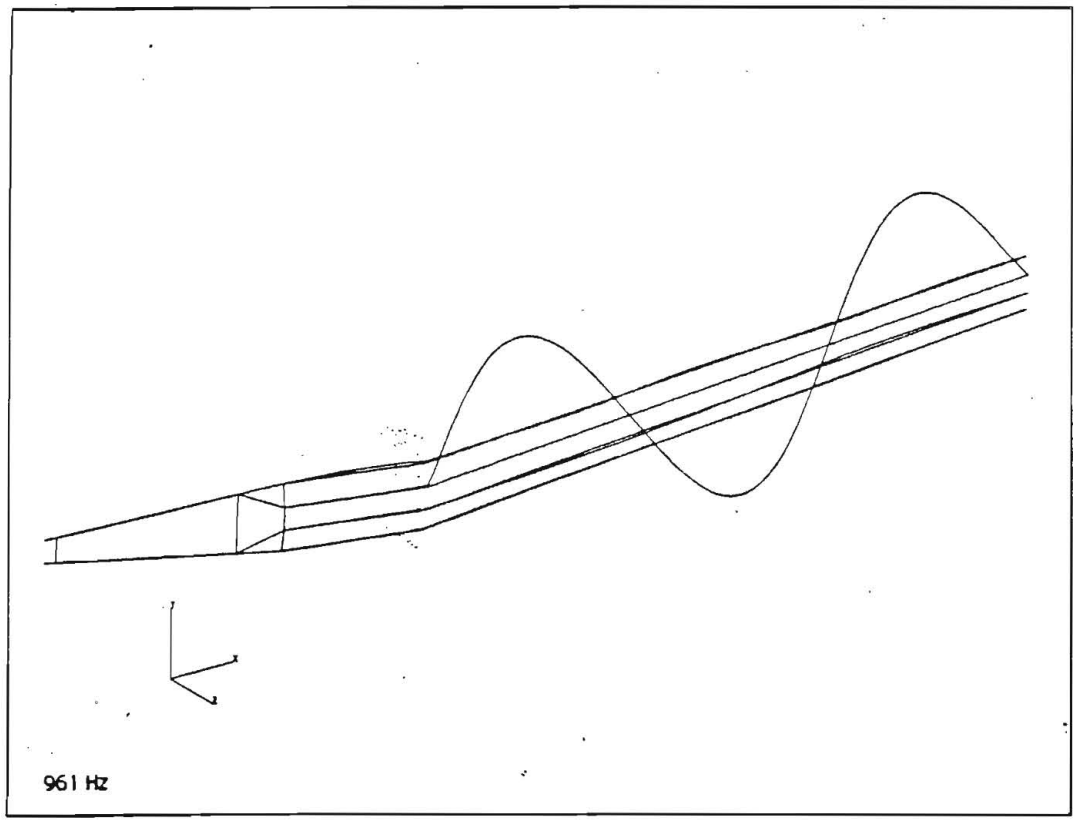

Figure D53. Mode 33

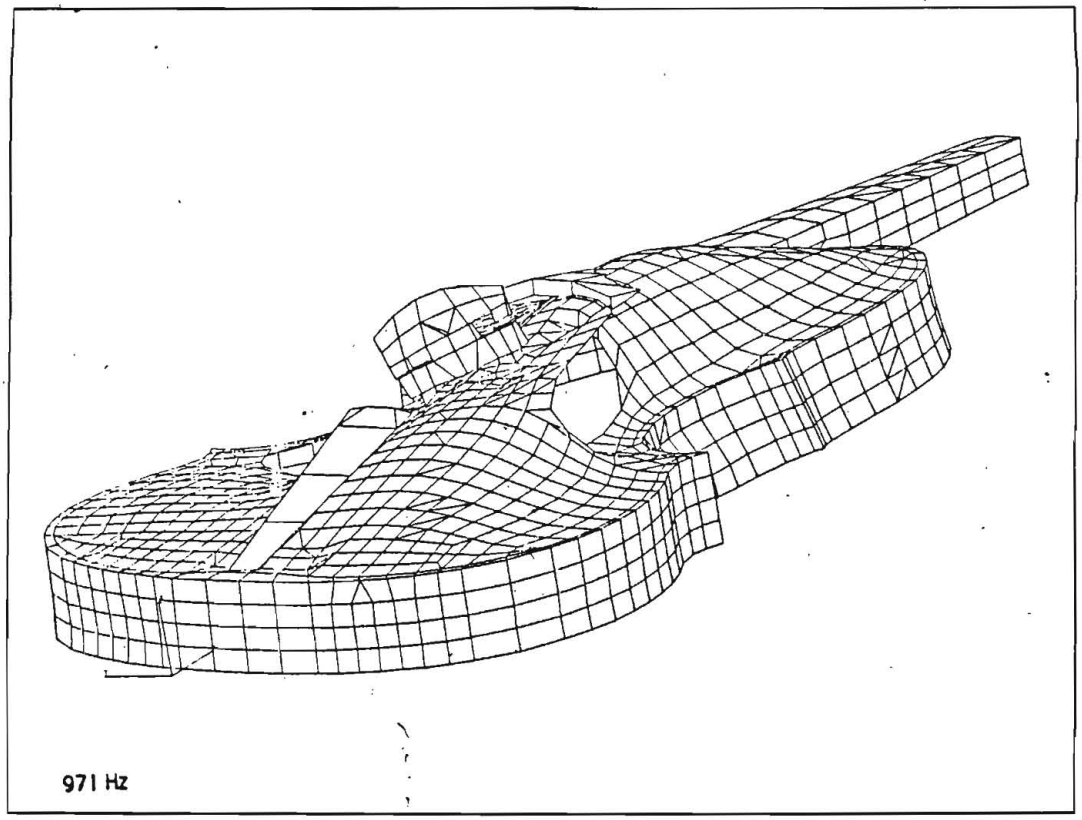

Figure D54. Mode 34

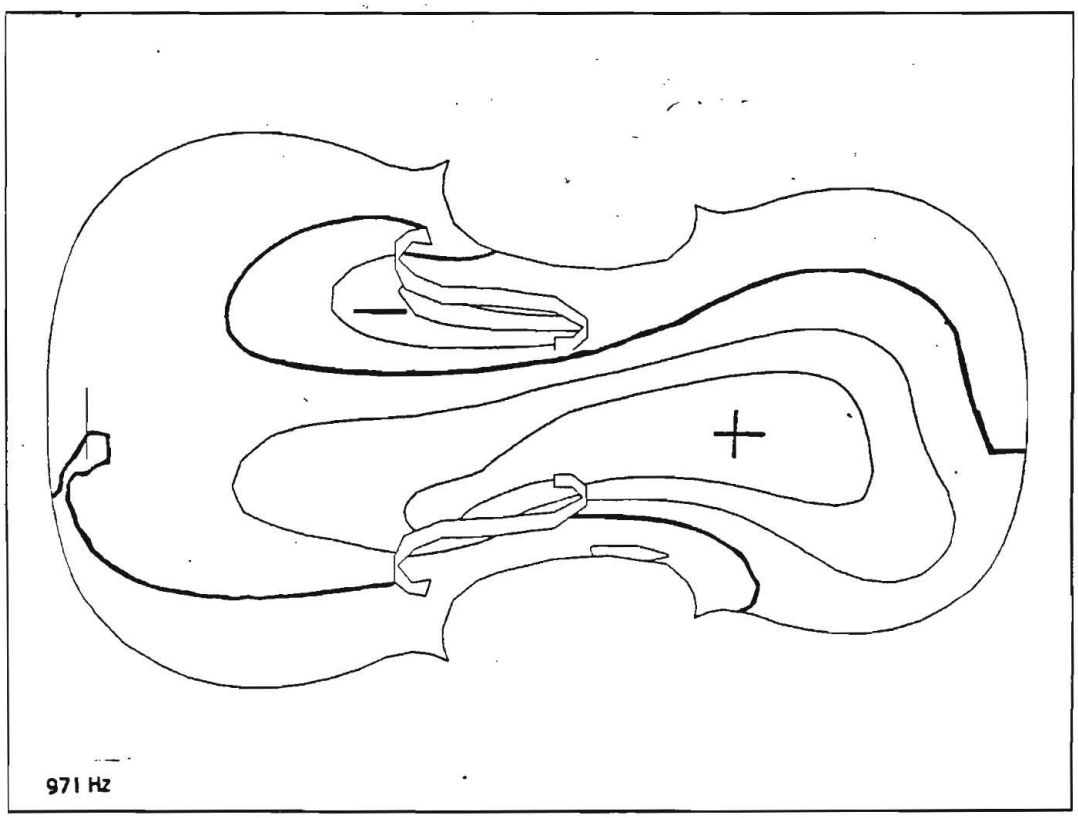

Figure D55. Mode 34 - top

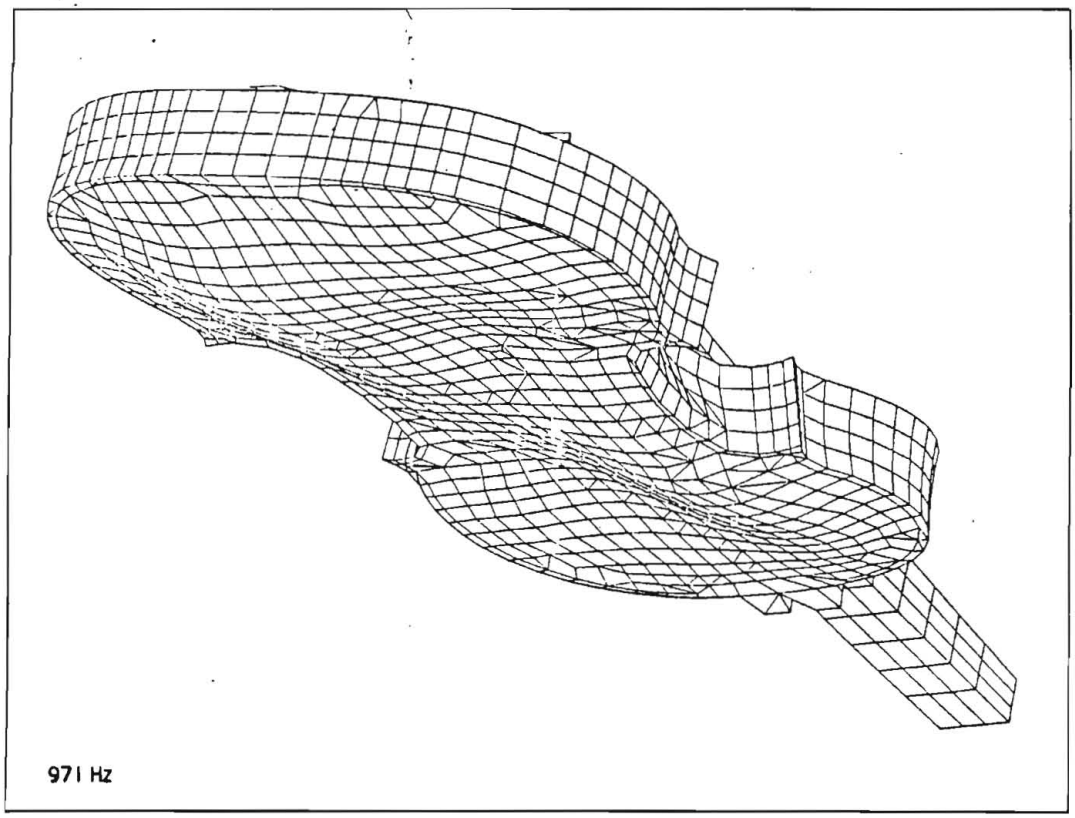

Figure D56. Mode 34

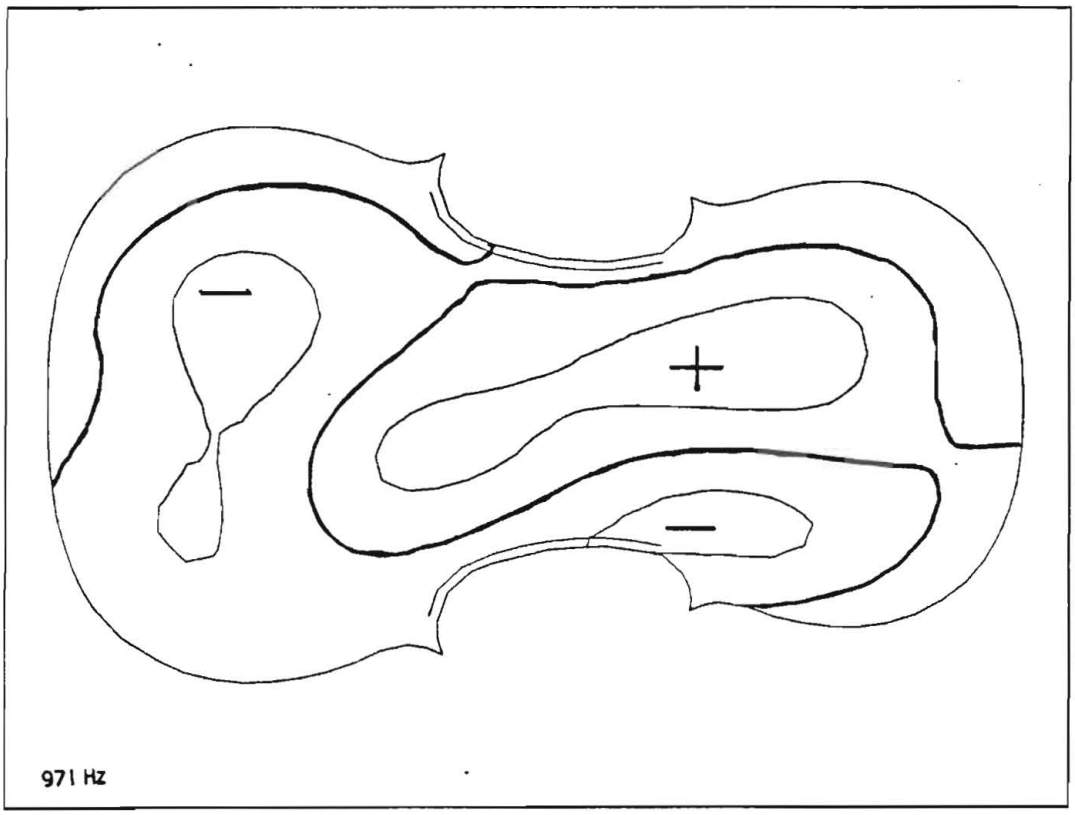

Figure D57. Mode 34 - back

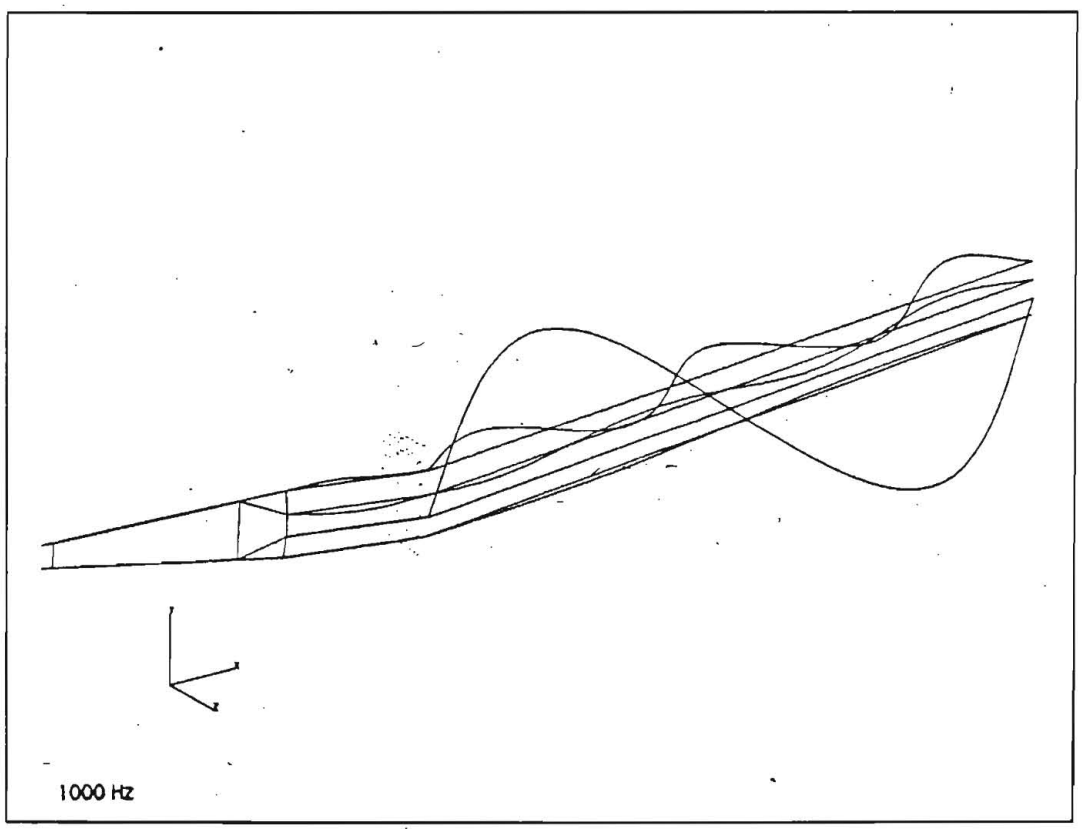

Figure D58. Mode 35

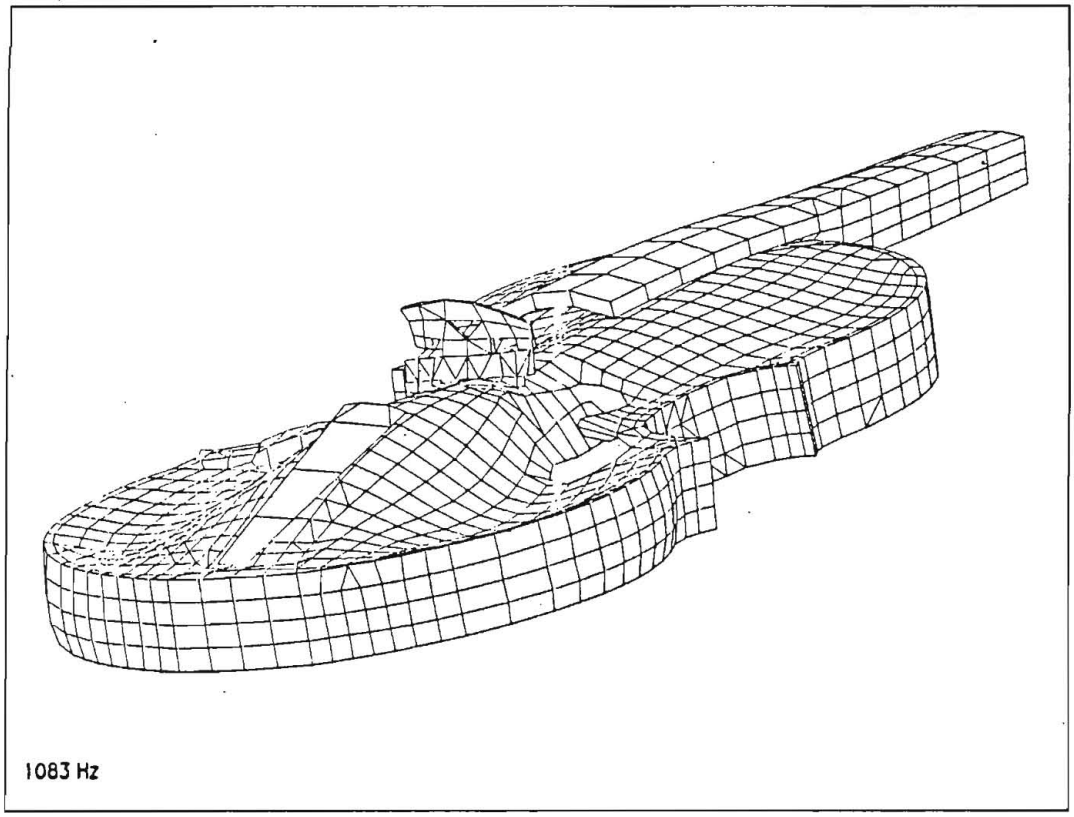

Figure D59. Mode 36

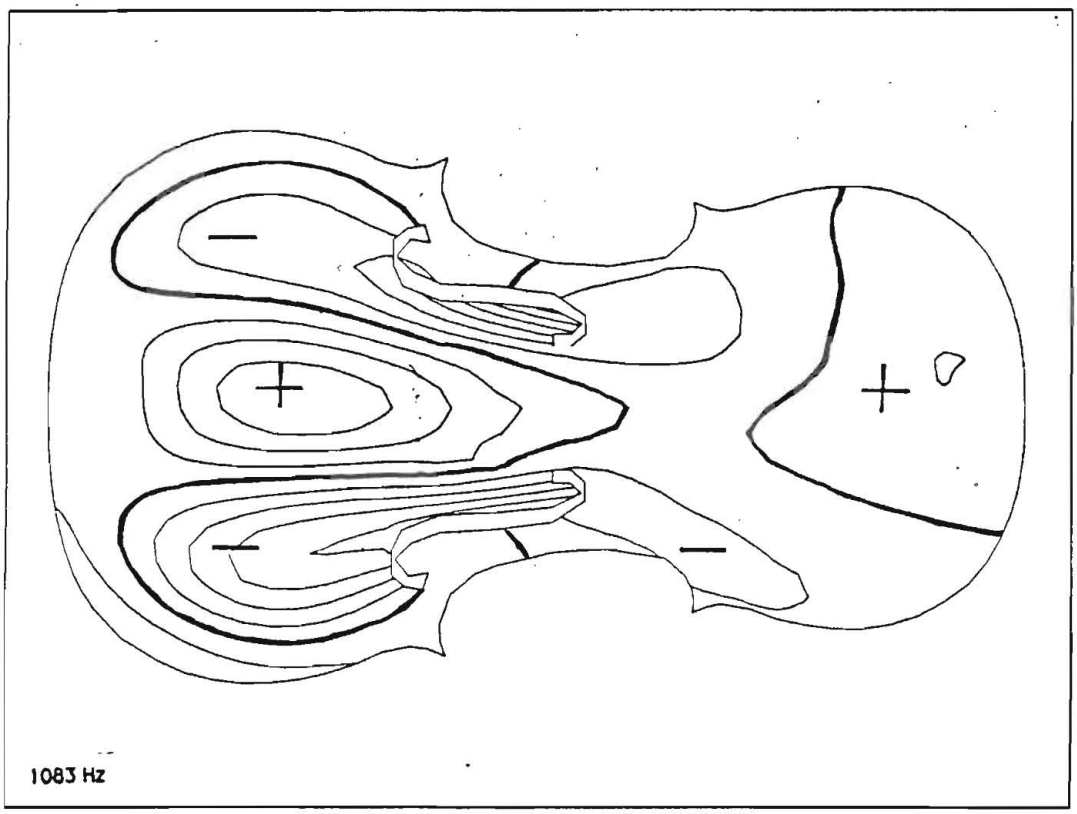

Figure D60. Mode 36 - top

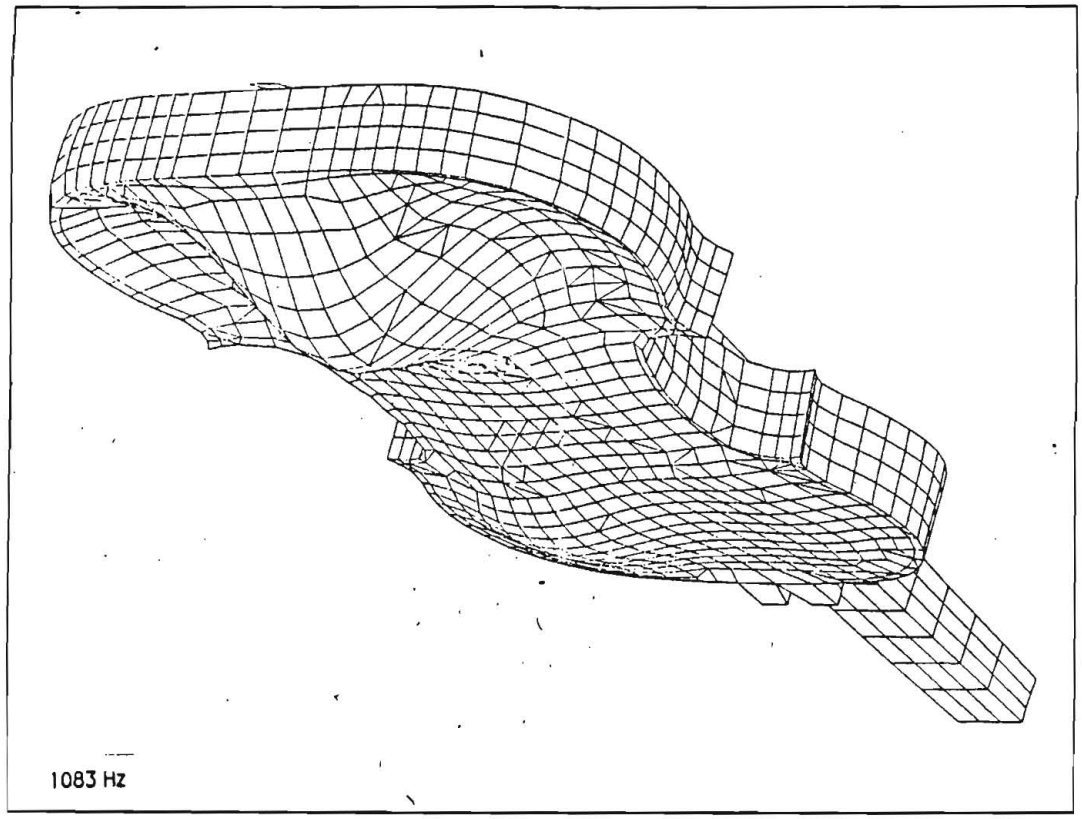

Figure D61. Mode 36

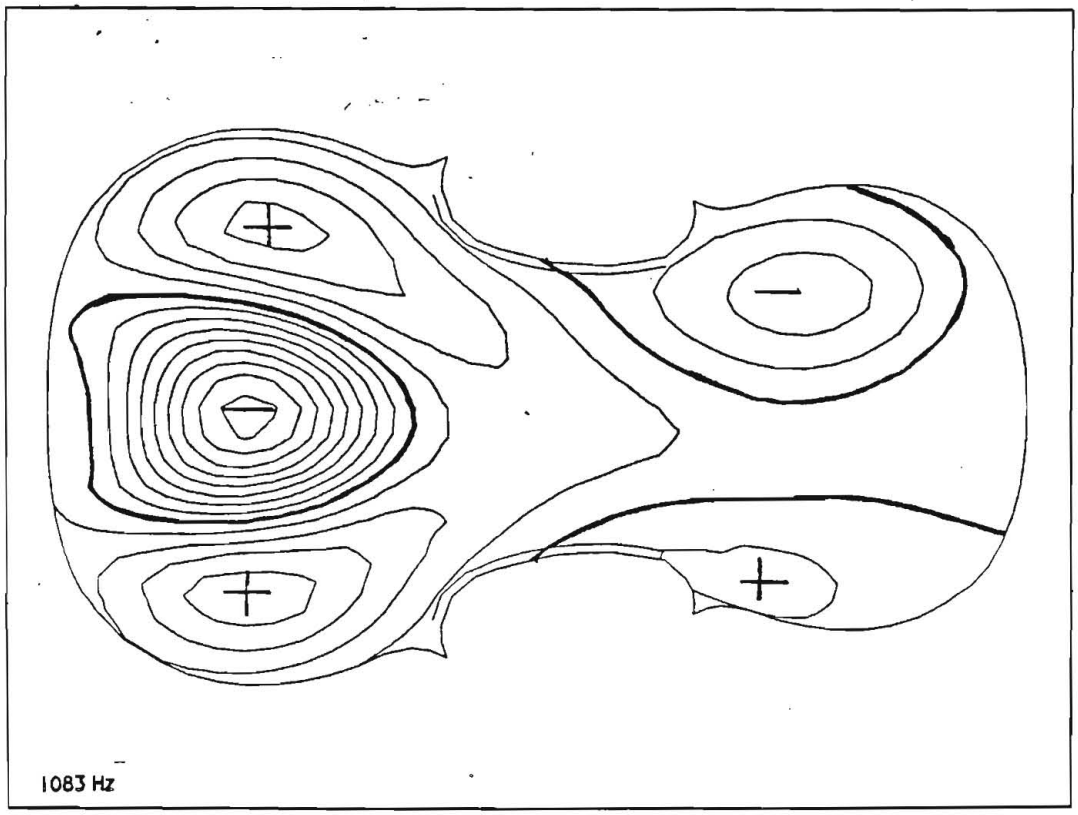

Figure D62. Mode 36 - back

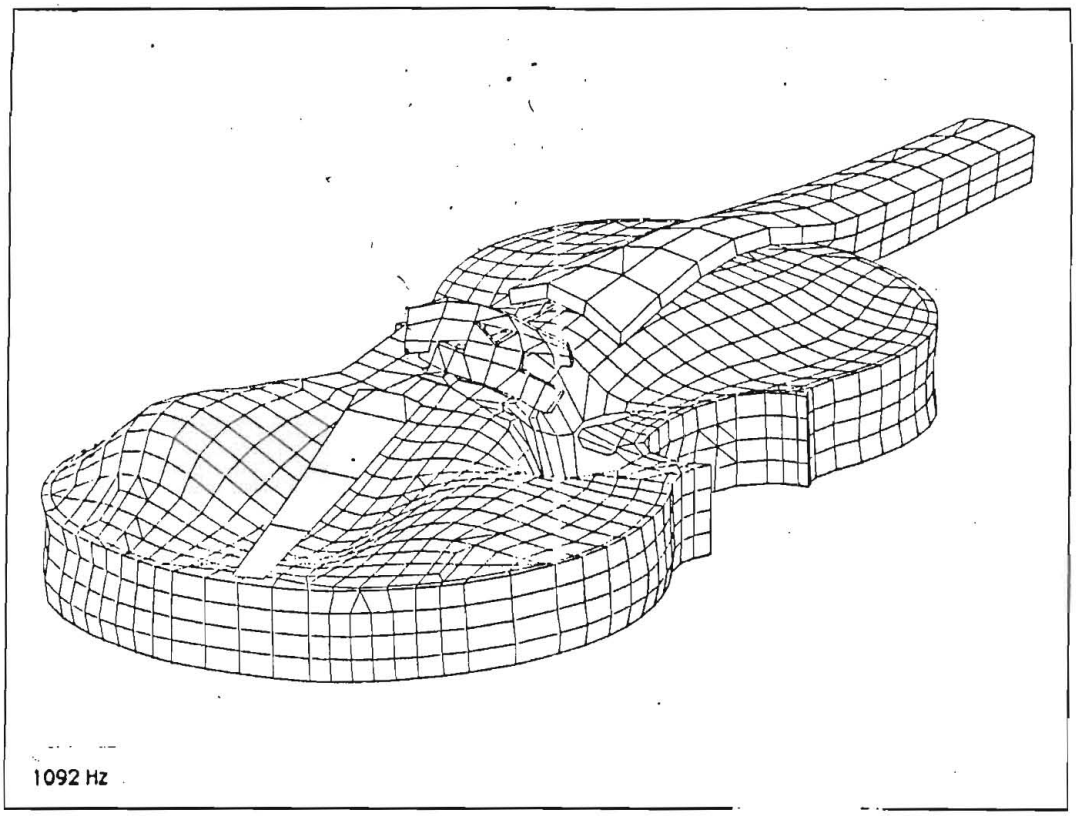

Figure D63. Mode 37

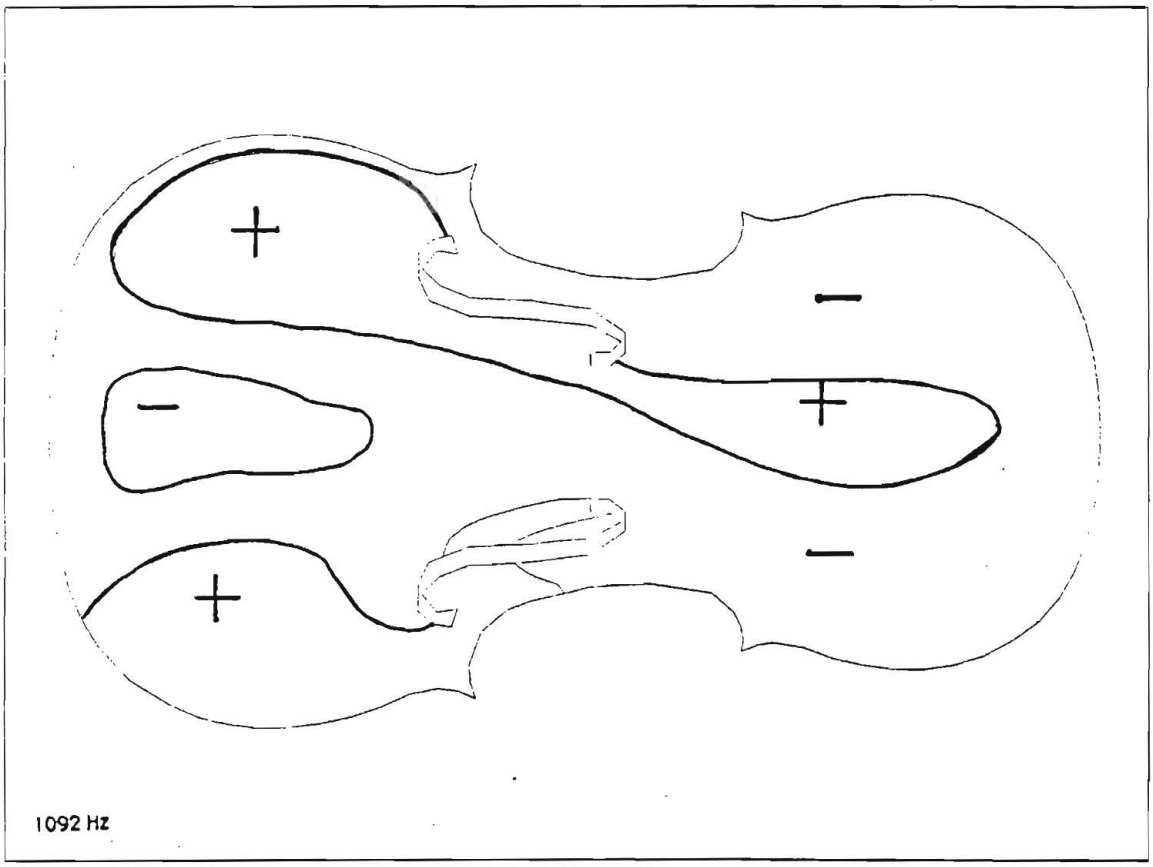

Figure D64. Mode 37 - top

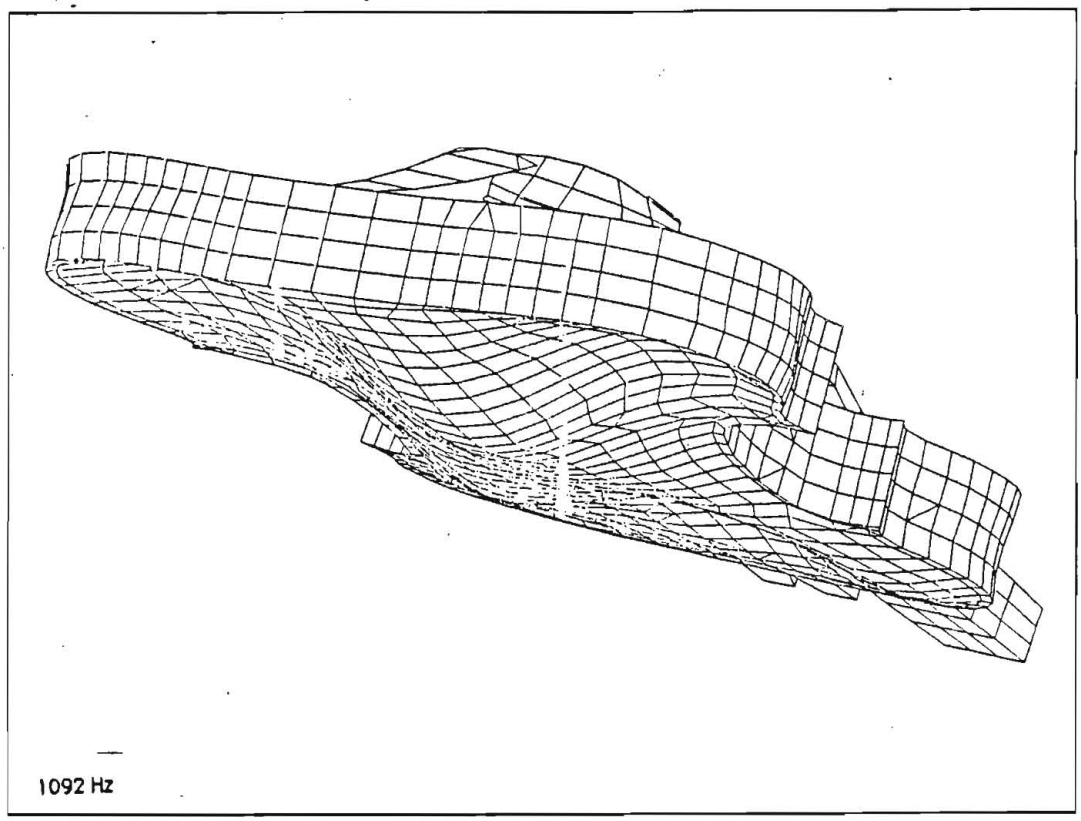

Figure D65. Mode 37

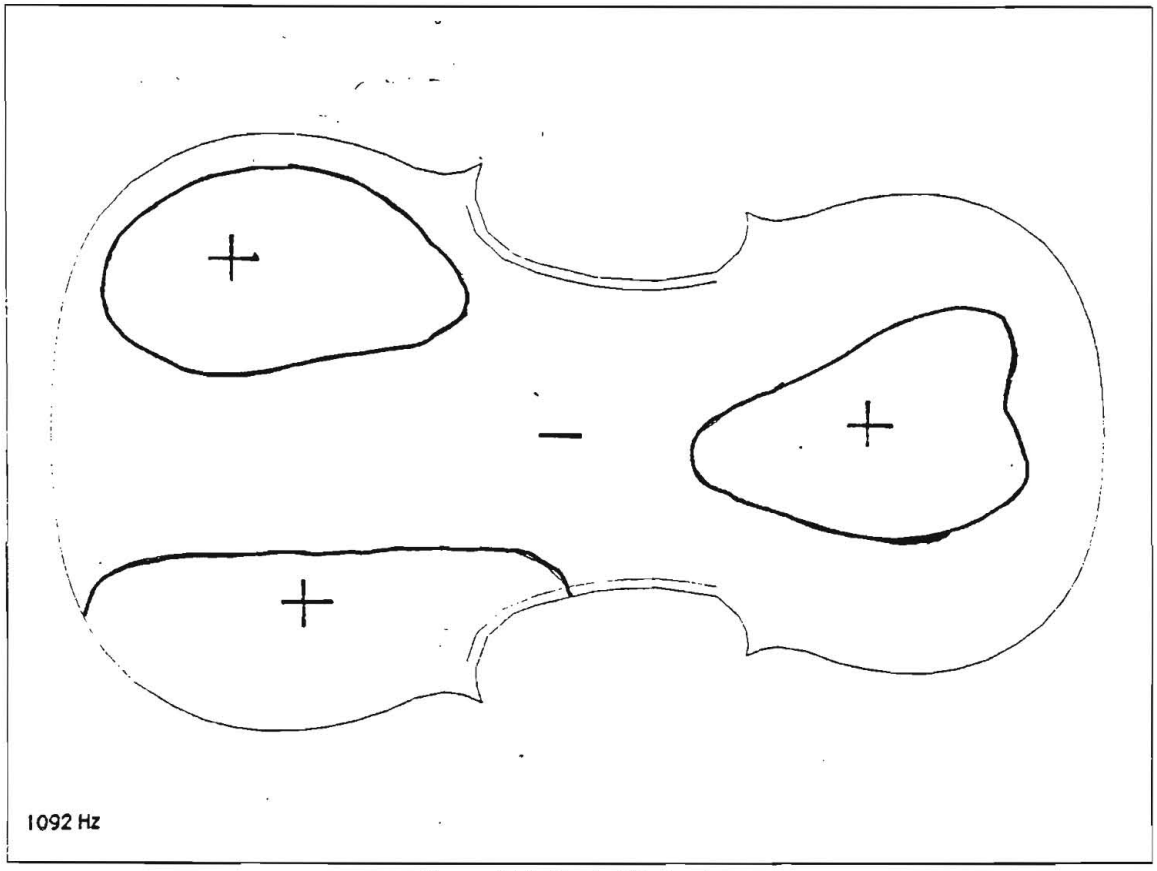

Figure D66. Mode 37 - back

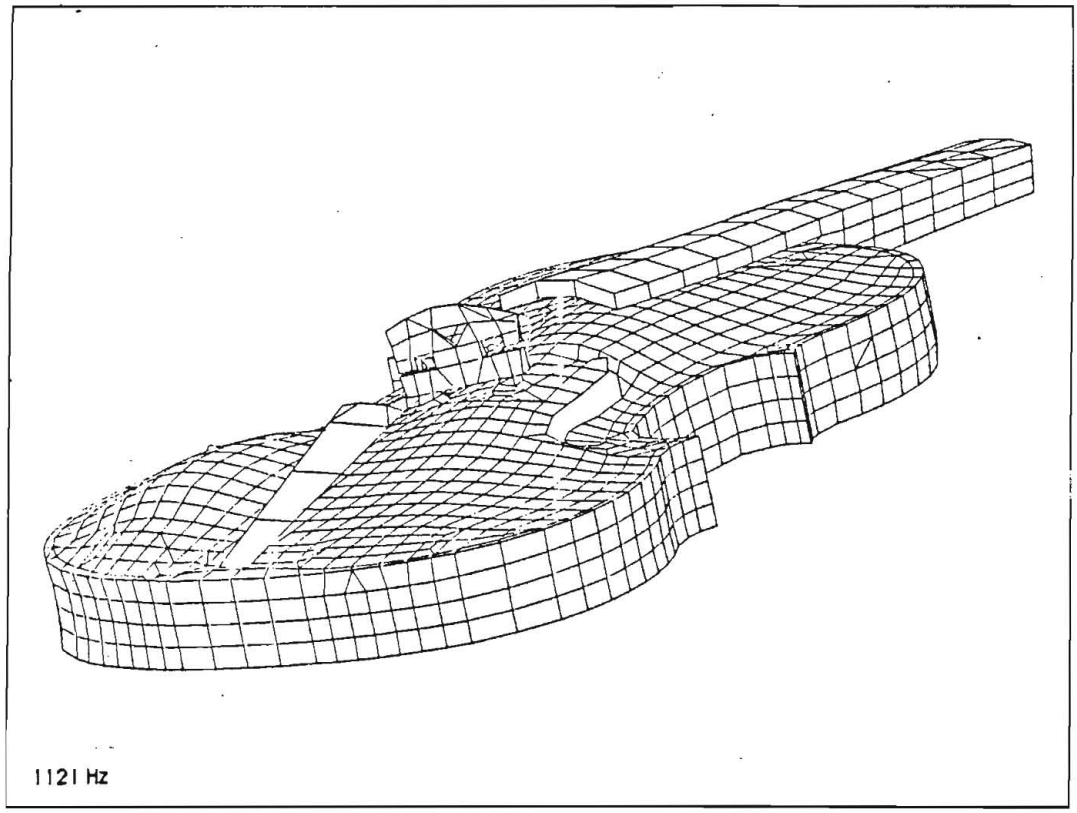

Figure D67. Mode 38

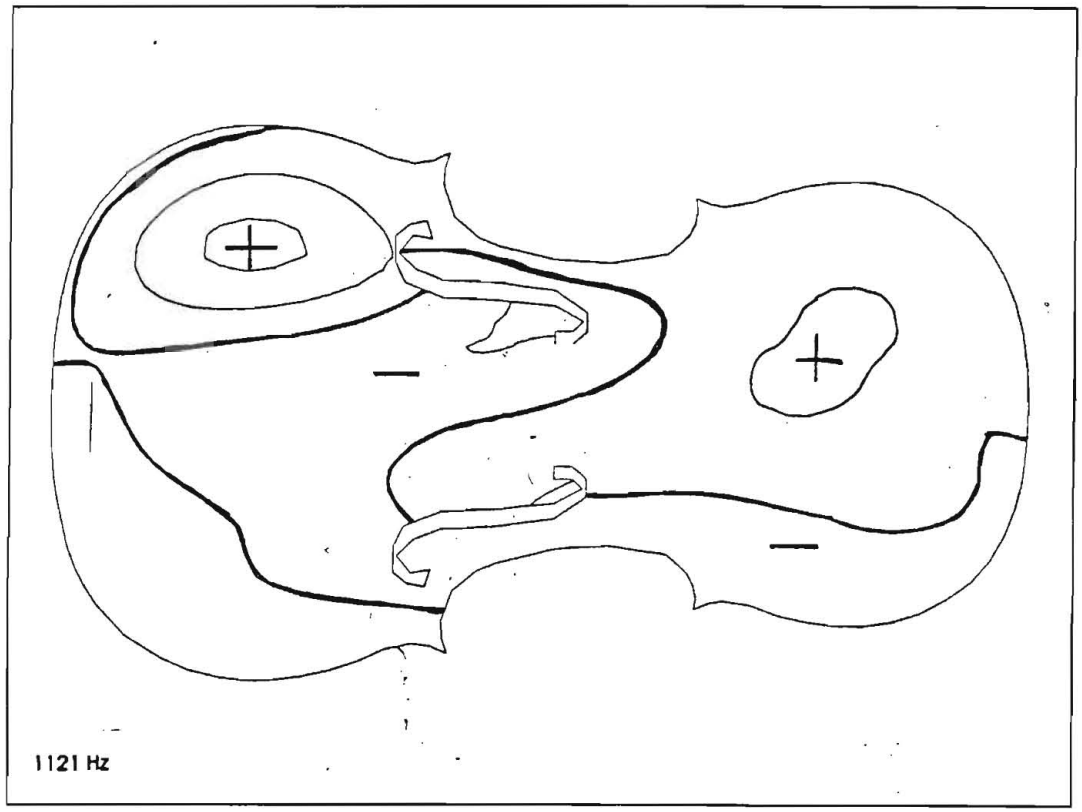

Figure D68. Mode 38 - top

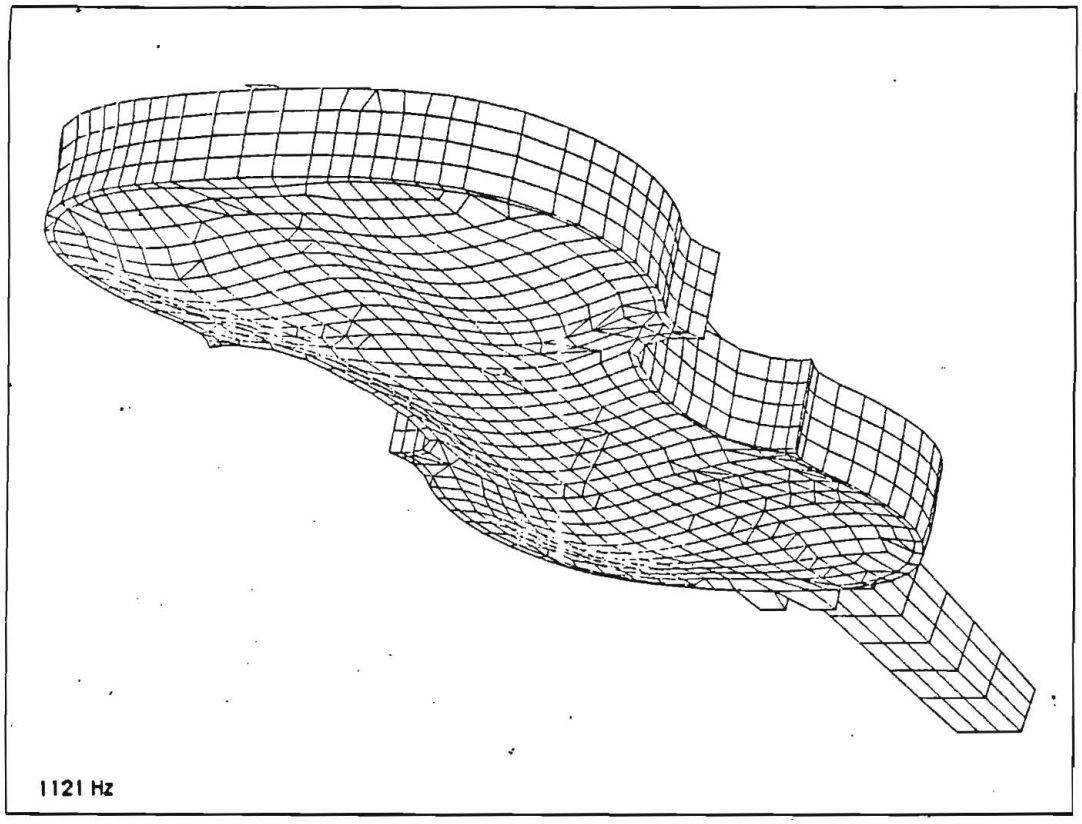

Figure D69. Mode 38

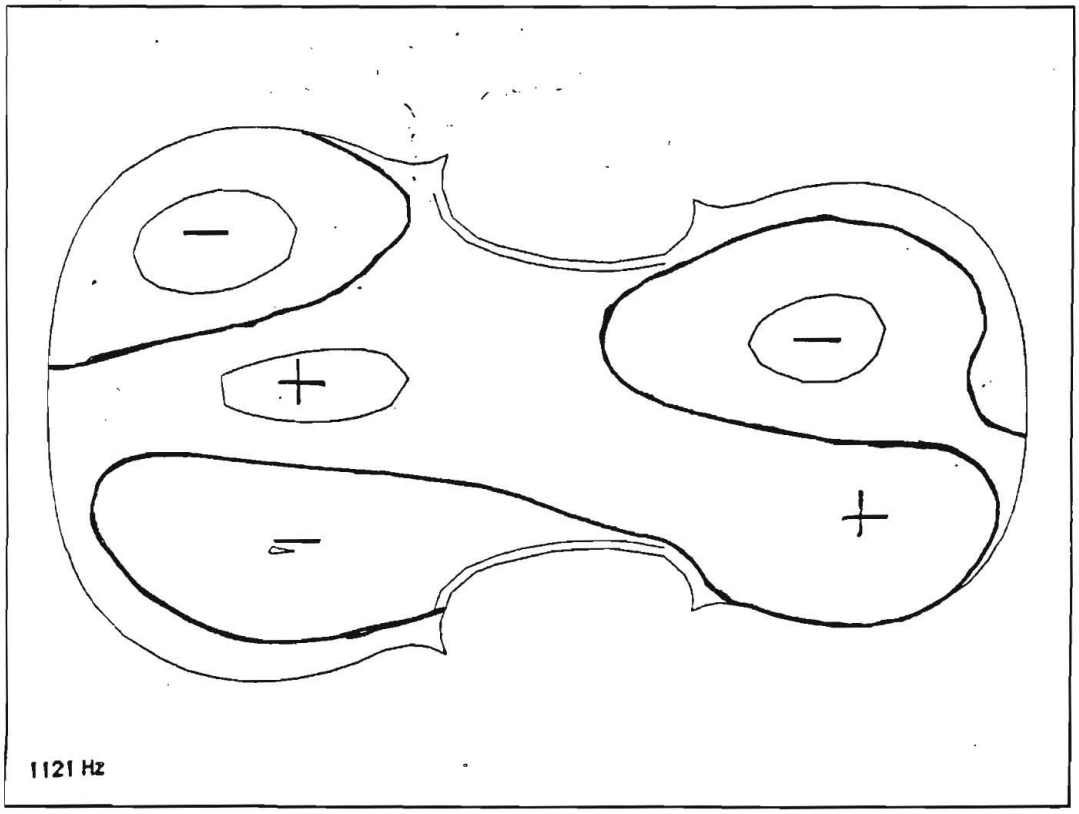

Figure D70. Mode 38 - back

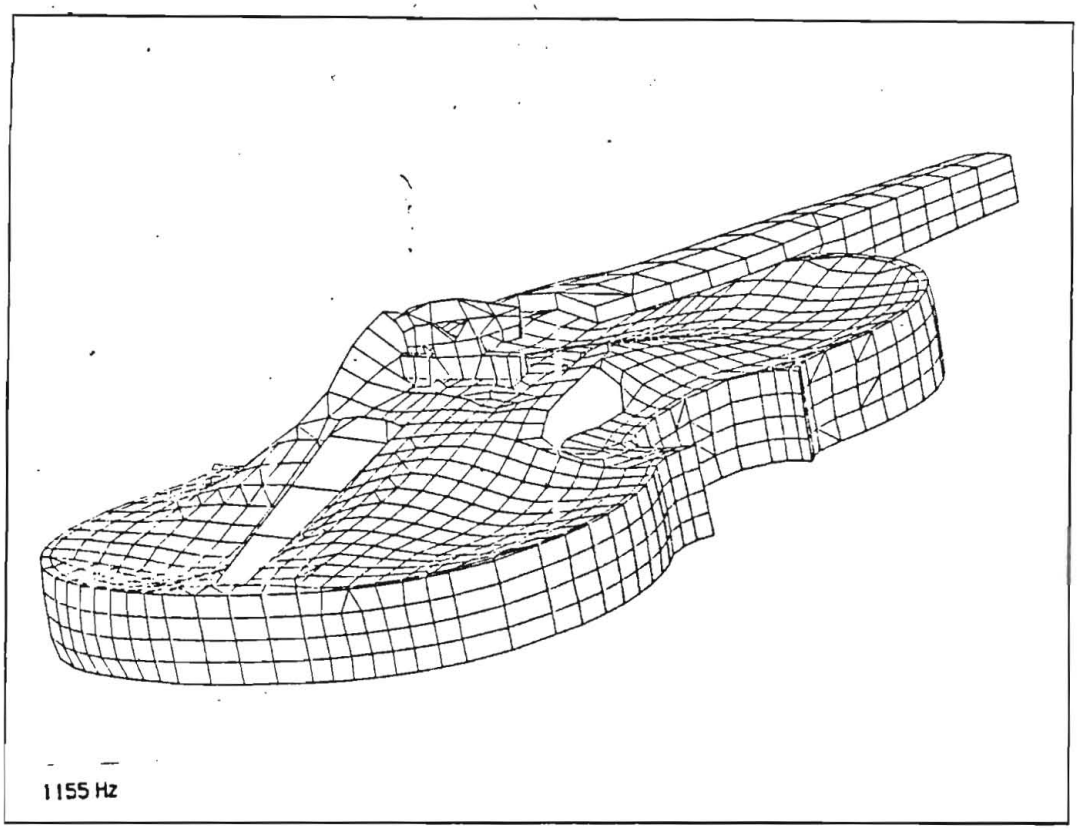

Figure D71. Mode 39

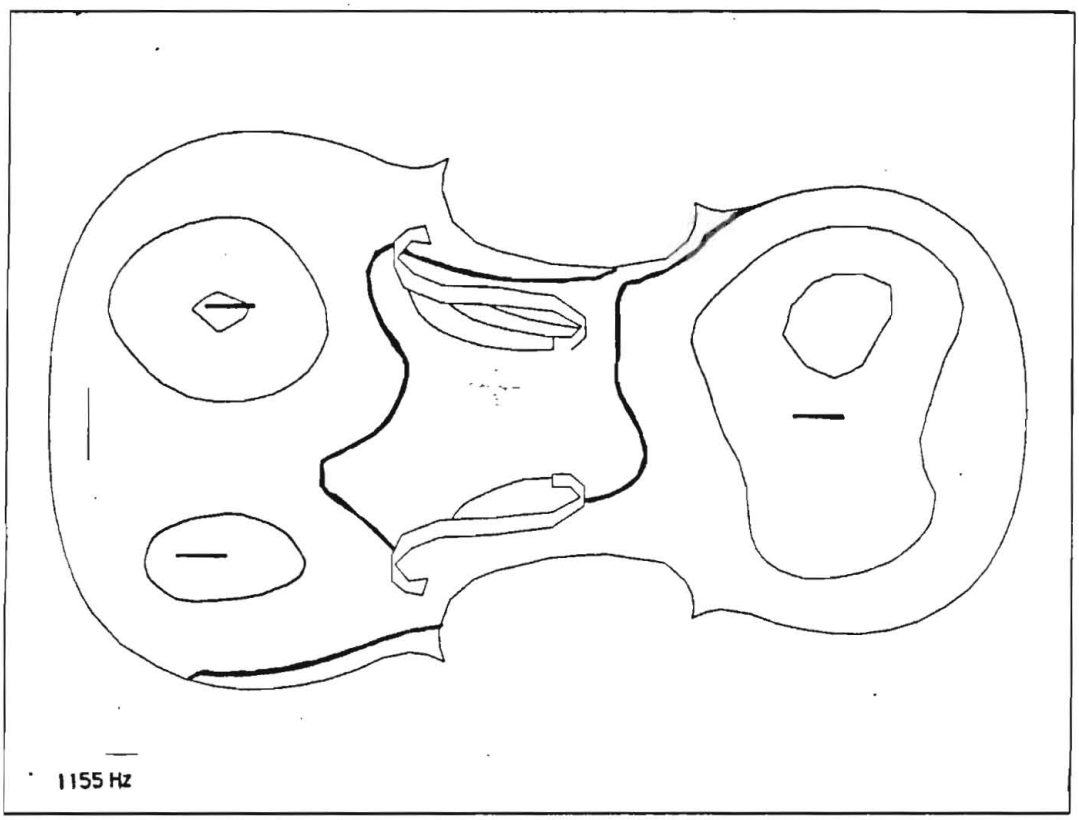

Figure D72. Mode 39 - top

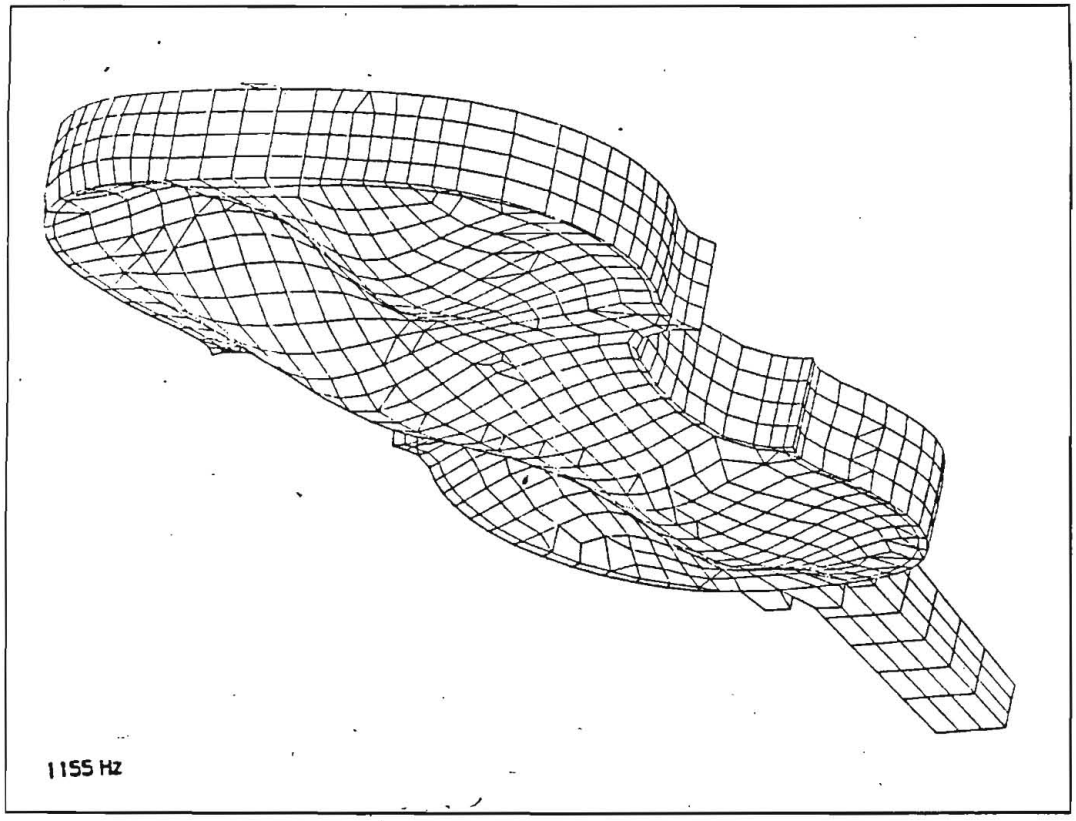

Figure D73. Mode 39

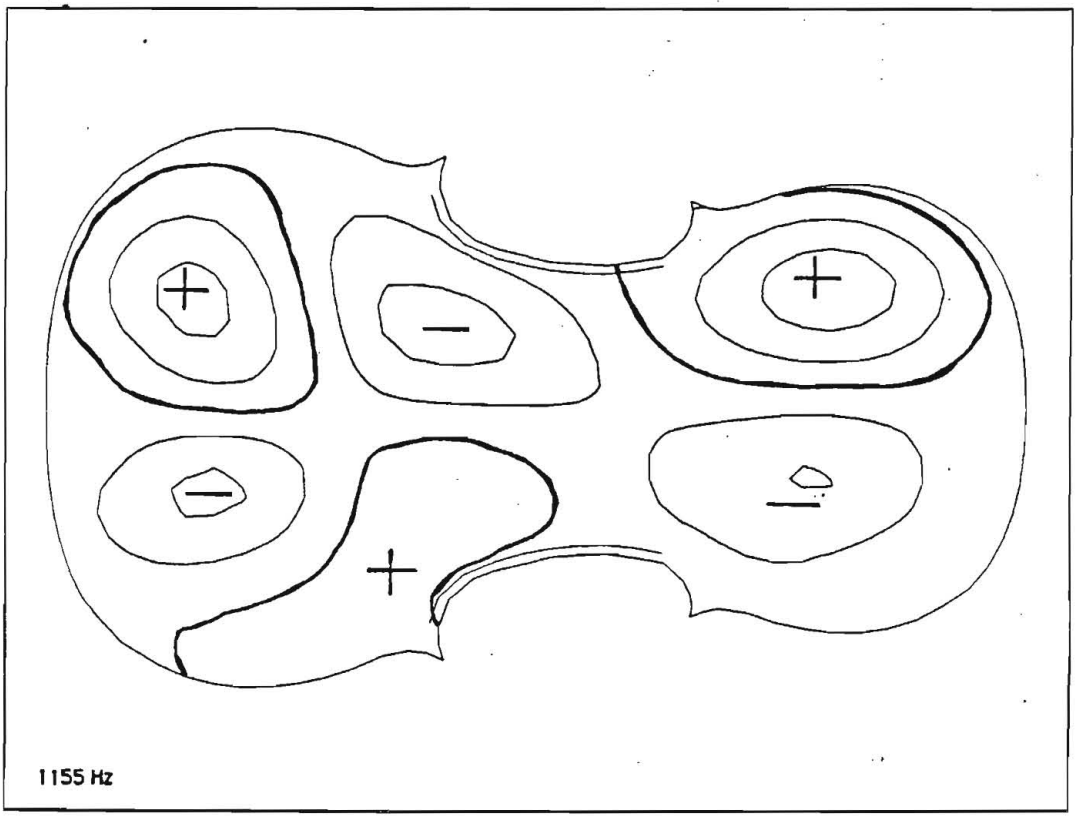

Figure D74. Mode 39 - back

APPENDIX E

NASTRAN PROGRAM LISTINGS

The following program listings are of the NASTRAN case control, executive routine, and partial bulk data decks for the violin model.

For the top and back plates a rigid format solution sequence was used. Figure E1 is a partial listing of the executive, case control, and bulk data decks. Comments are shown in light face type.

```
SOL 3                    Rigid format for normal modes analysis.
CEND                     Designates the end of the executive deck.
METHOD = 1               Set ID directive. Refers to EIGR, 1 below.
SET 1 = ALL              All grid points (nodes) are in set one.
BEGIN BULK
EIGR, 1, MGIV, 0.0, 200.0,22,,,1.-8,+E1
+E1,MASS                 Set ID 1 real eigenvalue extraction using
                         the modified Givens method. Roots from
                         0 to 200 Hz with eigenvectors mass
                         normalized. 22 roots estimated.
GRID,1,,0.,0.,0.         Node number and x, y, z coordinates.
    •
GRID,1000,,20.,30.,15.
CTRIA3,1,1,6,13,7                Element type.
    •
CTRIA3,1900,1,258,259,260
PSHELL,1,1,0.3,1,,1              Property card.
MAT8,1,13.+10,8.+9,.375,3.+9,9.+9,.7+9,.46      Material
                                                property card.
ENDDATA
```

Figure E1. Normal modes analysis example data deck

It should be emphasized that Figure E1 is a partial listing of the executive and case control decks. Refer to the Finite Element Primer [Ref.15] for the detailed information needed to assemble the data deck.

```
SOL 61
TIME 50.
ALTER 365
PARAM     //ME/V,N,NOADD/SEID/0 $
COND      NOADD1,NOADD $
MATGEN    EQEXINS/INTEXT/9/0/LUSETS $
MPYAD     INTEXT,KGG,/KGGM $
MPYAD     KGGE,INTEXT,/KGGM////6 $
MATMOD    KGGM,EQEXINS,,,,/MATP1,/16/1 $
EXIT $
LABEL     NOADD1 $
ECHO
TITLE = BOX AND NECK ONLY
SUBTITLE = CREMONESE 1715
LABEL = CALCULATE THE EQUIVALENT STIFFNESS MATRIX
ECHO = NONE
SEALL = ALL
SPC = 1
SUBCASE 1
   SUPER = 1
SUBCASE 2
BEGIN BULK
PARAM,PROPST,NO
SPC1,1,123456,431
SESET,1,1,THRU,393
SESET,1,565
SESET,1,567,THRU,569
SESET,1,572,573
SESET,1,575,THRU,579
SESET,1,581,THRU,2107
SESET,1,2112,THRU,2357
SESET,1,2359
SESET,1,2361,THRU,10000
PARAM,MAXRATIO,1.+20
$
```

Figure E2. Equivalent Stiffness Matrix Data Deck

```
$2-D SPRUCE FOR TOP PLATE
MAT3,1,1.3-3,9.3+8,  75,1.014+9,9.99+8,7.2+7,4.6-4,+MT1
+MT1,0.,0.
PSHELL,1,1,2.99,1,,1
$
$2-D MAPLE/POPLAR FOR BACK PLATE (PSHELL 9 IS FOR THE SIDES)
MAT3,2,17.+9,2.5+9,.318,1.275+9,1.173+9,1.870+8,8.-4,+MT2
+MT2,0.,0.,0.
PSHELL,2,2,3.3,2,,2
PSHELL,3,2,2.5,2,,2
PSHELL,4,2,2.6,2,,2
PSHELL,5,2,3.8,2,,2
PSHELL,6,2,2.9,2,,2
PSHELL,9,2,0.999,2,,2
$
$3-D MAPLE FOR NECK (PSOLID,12)
MAT9,3,17.5+9,991.2+6,660.0+6,,,,2.0376+9,+M256
+M256,704.67+6,,,,978.66+6,,,,+M257
+M257,1.275+9,,,,.187+9,,1.173+9,8.0-4,,+MT3
+MT3,,,,,,0.
PSOLID,12,5,13
$
$3-D ISOTROPIC MAPLE-LIKE MATERIAL FOR NECK TETRA ELEMENTS
MAT1,6,17.5+9,,.318,8.0-4,0.,0.
PSOLID,15,6
$
$ISOTROPIC STEEL FOR E STRING
MAT1,7,19.5+10,,0.28,7.7-3,6.-6,0.
$
$STEEL FOR TAIL PIECE
MAT1,9,19.5+10,,0.28,1.86-3
PSHELL,14,9,4.,9,,9
$CUT CORE FOR G, D, AND A STRINGS(PBEAM16-G, 17-D, 18-A, 20-TAIL)
MAT1,8,3+10,,,4,1.2-3,6.-6,0.
PBEAM,19,7,57.3-3,261.3-6,261.3-6,,522.6-6
PBEAM,16,8,282.0-3,6.328-3,6.328-3,,12.656-3,2.692-3
PBEAM,17,8,166.0-3,2.193-3,2.193-3,,4.386-3,1.352-3
PBEAM,18,8,85.5-3,581.7-6,581.7-6,,1163.-6,0.557-3
PBEAM,20,8,3.2,434.5-3,484.5-3,,969.-3

$
$IR FOR BASSBAR
MAT9,3,12.897+9,408.65+6,396.63+6,,,,963.59+6,+M100
+M100,285.56+6,,,,711.87+6,,,,+M200
+M200,.794+9,,,,.868+9,,.907+9,5.06-4,,+MT4
+MT4,,,,,,0.
PSOLID,7,3,6
$
$SPRUCE FOR BLOCKS (PSOLID,8), LININGS (PSOLID,10), POST (PSOLID,11)
$AND BRIDGE (PSOLID,13)
MAT9,4,13.455+9,674.24+6,493.2+6,,,,1.0321+9,+M500
+M500,267.03+6,,,,751.35+6,,,,+M600
+M600,.910+9,,,,.884+9,,.572+9,4.6-4,,+MT5
+MT5,,,,,,0.
PSOLID,8,4,2
PSOLID,10,4,6
PSOLID,11,4,2
PSOLID,13,4,6
$
```

Figure E2(Cont.) Equivalent Stifness Matrix Data Deck

```
ID STRING ANALYSIS
SOL 66
TIME 30.
ALTER 1
OUTPUT2   ,,,,,//-1/11 $
ALTER 4
FILE      KGGW=SAVE $
ALTER 66
MATRIX    ,,MATP ODL,GEOEXINS,CSILS,/KGGW,,/V,N,LUSET/S,N,NOKGGW $
EMA       GPECT,KDICT1,KELM1,CBGPDT,CSILS,CCSTMS/KGG2,/ $
ADD       KGG2,KGGW/KGG1 $
ALTER     183,183
EMA       HSPECT,KDICT,KELM,CBGPDT,CSILS,CCSTMS/KJJX,/-1 $
ADD       KGGW,KJJX/KJJ $
ALTER     231,231
MPYAD     KGGW,HJGV,/FGX $
ADD       FGX,FG/FT $
ADD       HPG,FT/PG1//(-1.,0.) $
ALTER     321
DBFETCH   /KGG1,,KJJ,,,/MODEL/0/1 $
ADD       XKJJ,XKGG1/XKJJ//(-1.,0.) $
MATGEN    FXSEXINS/INTEXT/ /0/LUSET $
MPYAD     INTEXT,XKJJ,/KGGX/1 $
MPYAD     KGGF,INTEXT,/KGGZ/////6 $
MATMOD    KGGZ,FXSEXINS,,,,/MATP1,/10/1 $
ALTER 285
VECPLOT   FOGV,PSGPDT,PEQEXINS,PGSTMS,CASEXX,/UGVB/0/0/5 $
SDR2      CASEXX,,,,PXSEXINS,,,,,,,UGVB,,
          /,,OUGVX,,,/APP/0 $
OUTPUT2   OUGVX//0/11 $
SALTER 295
SDCMP      CUSET,CSILS,JEQEXINS,KAA/LAA,/1/0/-1/     V,Y,MAXR=1.E20/C,N,A/
$          1.E-20/////////S,N,ZSING/  S,N,ZRBRCHC/S,N,ZNP $
CEND
TITLE = STRINGS AND BRIDGE
SUBTITLE = ORIENTESE 1715
LABEL = NON-LINEAR ANALYSIS - DMIG INPUT FOR BODY
ECHO = NONE
SEALL = ALL
SPC = 1
TEMP(LOAD) = 101
SET 666 = 2730,2378,2971,3024
ELFORCE = 66
SUBCASE 1
SUBCASE 2
SUBCASE 3
SUBCASE 4
SUBCASE 5
SUBCASE 6

SUBCASE 7
SUBCASE 8
SUBCASE 9
SUBCASE 10
SUBCASE 11
SUBCASE 12
SUBCASE 13
SUBCASE 14
SUBCASE 15
  DISP = ALL
  ELFORCE = ALL
BEGIN BULK
PARAM,MAXRATIO,1.+20
$
$ SPC FOR STRING ENDS
$
$
$ SPC FOR GRID POINTS
$
SPC1,1,456,2187,2190,2206
SPC1,1,456,2268,2276,2277
```

Figure E3. String Analysis Data Deck

```
$
MAT1,[illegible].0+[illegible],,0.28,0.0
PBEAM,100,100,252.0-3,6.328-3,6.328-3
$
TEMPD,100,0.
$ C STRING ENFORCED DISP(2.2MM)
TEMPRB,100,2740,-1.,-1.,0.,0.,0.,0.,+XB11
+XB11,,,,,,,,,+XB12
+XB12,2741,THRU,2868
TEMPRB,100,2869,-1.,-1.,0.,0.,0.,0.,+XB101
+XB101,,,,,,,,,+XB102
+XB102,2870,THRU,2877
$
$ D STRING ENFORCED DISP(4.2MM)
TEMPRB,100,2878,-1.,-1.,0.,0.,0.,0.,+XB13
+XB13,,,,,,,,,+XB14
+XB14,2879,THRU,2961
TEMPRB,100,2962,-1.,-1.,0.,0.,0.,0.,+XB103
+XB103,,,,,,,,,+XB104
+XB104,2963,THRU,2970
$
$ A STRING ENFORCED DISP(3.3MM)
TEMPRB,100,2971,-1.,-1.,0.,0.,0.,0.,+XB15
+XB15,,,,,,,,,+XB16
+XB16,2972,THRU,3014
TEMPRB,100,3015,-1.,-1.,0.,0.,0.,0.,+XB105
+XB105,,,,,,,,,+XB106
+XB106,3015,THRU,3023
$
$ E STRING ENFORCED DISP(2.3MM)
TEMPRB,100,3024,-1.,-1.,0.,0.,0.,0.,+XB17
+XB17,,,,,,,,,+XB18
+XB18,3025,THRU,3057
TEMPRB,100,3058,-1.,-1.,0.,0.,0.,0.,+XB107
+XB107,,,,,,,,,+XB108
+XB108,3059,THRU,3066
$
TEMPD,101,0.
$ C STRING ENFORCED DISP(2.2MM)
TEMPRB,101,2740,-1274.,-1274.,0.,0.,0.,0.,+TB11
+TB11,,,,,,,,,+TB12
+TB12,2741,THRU,2868
TEMPRB,101,2869,-1248.,-1248.,0.,0.,0.,0.,+TB101
+TB101,,,,,,,,,+TB102

+TB[illegible],2870,THRU,2877
$
$ D STRING ENFORCED DISP(4.2MM)
TEMPRB,101,2878,-2305.,-2305.,0.,0.,0.,0.,+TB13
+TB13,,,,,,,,,+TB14
+TB14,2879,THRU,2961
TEMPRB,101,2962,-2299.,-2299.,0.,0.,0.,0.,+TB103
+TB103,,,,,,,,,+TB104
+TB104,2963,THRU,2970
$
$ A STRING ENFORCED DISP(3.3MM)
TEMPRB,101,2971,-4473.,-4473.,0.,0.,0.,0.,+TB15
+TB15,,,,,,,,,+TB16
+TB16,2972,THRU,3014
TEMPRB,101,3015,-4378.,-4378.,0.,0.,0.,0.,+TB105
+TB105,,,,,,,,,+TB106
+TB106,3015,THRU,3023
$
$ E STRING ENFORCED DISP(2.3MM)
TEMPRB,101,3024,-1312.,-1312.,0.,0.,0.,0.,+TB17
+TB17,,,,,,,,,+TB18
+TB18,3025,THRU,3057
TEMPRB,101,3058,-1256.,-1256.,0.,0.,0.,0.,+TB107
+TB107,,,,,,,,,+TB108
+TB108,3059,THRU,3066
```

Figure E3(Cont.) String Analysis Data Deck

```
SOL 63
TIME 120.
CEND
TITLE =
SUBTITLE = CREMONESE 1715
LABEL = RESTART WITH STRING DIFFERENTIAL STIFFNESS
ECHO = NONE
SEALL = ALL
SPC = 1
DYNRED = 1
METHOD = 1
BEGIN BULK
PARAM,MAXRATIO,1.+20
SPC1,1,0,99001,THRU,99150
SPOINT,99001,THRU,99150
ASET1,0,99001,THRU,99150
QSET1,0,99001,THRU,99150
DYNRED,1,1200.
EIGR,1,GIV,0.,1200.,,,,,1.-8,+E1
+E1,MAX
$

*READ DMIG
```

Figure E4. Restart With Differential Stiffness

REFERENCES

1. H. L. Schwab, "Finite Element Analysis of a Guitar Soundboard," Catgut Acoust. Soc. Newslett. **24** & **25**, (1974).

2. B. E. Richardson and G. W. Roberts, "The Adjustment of Mode Frequencies in Guitars: A Study by Means of Holographic Interferometry and Finite Element Analysis", Proceedings of the SMAC 1983 Conference. (1983).

3. G. Jenner, personal correspondence, (July 1985).

4. B. E. Richardson and G. W. Roberts, "Predictions of the Behaivior of Violin Plates by the Finite Element Method", Proceedings of the Institute of Acoustics. (1985). (IN PRESS).

5. C. Rubin and D. F. Farrar, "Computer Analysis of the Vibrations of a Violin Back", Department of Mechanical and Materials Engineering, Vanderbuilt University, Nashville, Tennessee, 37235. (1984).

6. B. E. Richardson and G. W. Roberts, Lecture given at the Acoustical Society of America meeting in Austin, Texas. (1985).

7. G. A. Knott, Lecture given at the Acoustical Society of America meeting in Austin, Texas. (1985).

8. O. Rodgers, personal correspondence, (July 1985).

9. K. D. Marshall, "Modal Analysis of a Violin", J. Acoust. Soc. Am. **77**, pp. 695-709 (1985).

10. A. Ekwall, "A Study of the Stradivari-Sacconi Violin Arching for Getting a Computerizable Arching of the Same Type", Catgut Acoust. Soc. Newslett. **35**, pp. 33-36 (1981).

11. S. F. Sacconi, "Die Geheimnisse Stradivaris", Verlag Das Musicinstrument, Frankfurt/M. (1976).

12. D. W. Haines, "On Musical Instrument Wood", Catgut Acoust. Soc. Newslett. **31**, pp. 23-32 (1979).

13. "Wood Products Handbook", U.S. Forest Products Lab, Madison, Wisconsin, p. 79 (1955).

14. C. M. Hutchens, "The Acoustics of Violin Plates", Sci. Am. **245**, pp. 171-186 (October 1981).

15. H. G. Schaeffer, "MSC/NASTRAN Primer", Schaeffer Analysis, Inc., Mont Vernon, New Hampshire (1984).

16. C. M. Hutchens, K. A. Stetson and P. A. Taylor, "Clarification of Free plate tap tones by Hologram Interferometry", Catgut Acoust. Soc. Newslett. **16**, pp.15 - 23 (1971).

17. J. H. Wilkinson, "The Algebraic Eigenvalue Problem", Oxford Press, London (1965).

INITIAL DISTRIBUTION LIST

		No. Copies
1.	Defence Technical Information Center Cameron Station Alexandria, Virginia 22304-6145	2
2.	Library, Code 0142 Naval Postgraduate School Monterey, California 93943-5002	2
3.	Carol Rubin Department of Mechanical and Materials Engineering Vanderbuilt University Nashville, Tennessee 37235	1
4.	B. E. Richardson and G. W. Roberts Department of Physics University College P. O. Box 78 Cardiff CF 1XL Wales, UNITED KINGDOM	2
5.	Mladdin Chargin Research Engineer Ames Research Center Moffett Field, California	2
6.	Carleen M. Hutchins 112 Essex Avenue Montclair, New Jersey 07042	2

7. Thomas D. Rossing — 1
Department of Physics
Northern Illinois University
Dekalb, Illinois 60115-2854

8. Kenshi Kishi — 1
Department of Communication Engineering
The University of Electro-Communications
Chofugaoka, Chofu, TOKYO
182 JAPAN

9. George Jenner — 1
38/10 Carr Street
Waverton, N.S.W. 2060.
AUSTRALIA

10. Kenneth D. Marshall — 1
BFGoodrich Research and Development Center
9921 Brecksville Road
Brecksville, Ohio 44141

11. Young S. Shin, Code 69 SG — 3
Department of Mechanical Engineering
Naval Postgraduate School
Monterey, California 93943

12. Steven L. Garrett, Code 61 GX — 3
Department of Physics
Naval Postgraduate School
Monterey, California 93943

13. John Strawn — 1
P. O. Box CS-8180
San Rafael, California 94912

14. Uwe J. Hansen — 1
Department of Physics
Indiana State University
Terre Haute, Indiana 47809

15. Jean N. Decarpigny — 1
Department of Physics
Institut Superieur d'Electronique du Nord
3 rue Francois Baes
59046. LILLE Cedex
FRANCE

16. Tim Johnson — 1
Rt 5 Box 267
Santa Fe, New Mexico 87501

17. George A. Knott — 2
6560 Bose Lane
San Jose, California 95120

18. George L. Knott — 1
1262 Willowhaven Drive
San Jose, California 95126

19. Steven E. Knott — 1
1020 Aoloa Place #105 B
Kailua, Hawaii 96734

20. Martine A. Shelley — 1
566 35th Avenue
San Francisco, California 94121

21. A. H. Benade — 1
Case Western University
Cleavland, Ohio 44106

22. R. W. Young — 1
1696 Los Altos Road
San Diego, California 92109

23. James A. Woods — 1
3740 25th Street #602
San Francisco, California 94110

24. Richard Boudreault
Canadian Astronautics LTD
1050 Morrison Drive
Ottawa, Ontario K2H 8K7
CANADA
1

25. Oliver E. Rodgers
507 South Providence Road
Wallingford, Pennsylvania 19086
1

26. Tom R. Bushbach
4600 Silver Hill Road
Washington, D.C. 20389
1

27. Lothar Cremer
8160 Miesbach
Immanuel Kant Strasse 12
Germany
1

28. Daniel W. Haines
CIBA-GEIGY Corporation
Ardsley, New York 10502
1